Title
Southern California Climate and Vegetation Over the Past 125,000 Years from Lake Sequences in the San Bernardino Mountains

Author
Glover, Katherine

Publication Date
2016

Peer reviewed|Thesis/dissertation

UNIVERSITY OF CALIFORNIA

Los Angeles

Southern California Climate and Vegetation Over the Past 125,000 Years from Lake Sequences in the San Bernardino Mountains

A dissertation submitted in partial satisfaction of the requirements for the degree of Doctor of Philosophy in Geography

by

Katherine Colby Glover

2016

ABSTRACT OF THE DISSERTATION

Southern California Climate and Vegetation

Over the Past 125,000 Years

from Lake Sequences in the San Bernardino Mountains

by

Katherine Colby Glover

Doctor of Philosophy in Geography

University of California, Los Angeles, 2016

Professor Glen Michael MacDonald, Chair

Long sediment records from offshore and terrestrial basins in California show a history of vegetation and climatic change since the last interglacial (130,000 years BP). Vegetation sensitive to temperature and hydroclimatic change tended to be basin-specific, though the expansion of shrubs and herbs universally signalled arid conditions, and landscpe conversion to steppe. Multi-proxy analyses were conducted on two cores from the Big Bear Valley in the San Bernardino Mountains to reconstruct a 125,000-year history for alpine southern California, at the transition between mediterranean alpine forest and Mojave desert. Age control was based upon radiocarbon and luminescence dating. Loss-on-ignition, magnetic susceptibility, grain size, x-ray fluorescence, pollen, biogenic silica, and charcoal analyses showed that the paleoclimate of the San Bernardino Mountains was highly subject to globally pervasive forcing mechanisms that register in northern hemispheric oceans. Primary productivity in Baldwin Lake during most of its

history showed a strong correlation to historic fluctuations in local summer solar radiation values. Rapid organic perturbations in the Baldwin Lake core were coeval with Dansgaard-Oeschger (D-O) events from the North Atlantic, which were evident in records from the Santa Barbara Basin. The predominant vegetation signal at Baldwin Lake was one of temperate conifer forest expansion during moist conditions, and contraction during dry conditions. This expansion and contraction was paced with summer insolation fluctuations during Marine Isotope Stage 5 (110,000 – 71,000 years BP), before a regime change towards more rapid, shorter-lived hydroclimate extremes. Wildfire is an important agent of landscape change throughout the Valley's history, with two hiatuses during cold and moist conditions from 25,000 – 14,000 years BP, and arid conditions 7,000 – 3,000 years BP. Taken together, this multi-proxy dataset suggests that paleoclimatic changes in alpine southern California have been highly sensitive to three climate drivers: 1) shifts in local summer insolation, 2) rapid warming in the North Atlantic, and 3) changes in the strength of the California Current. The record also showed a wide range of possible moisture states in southern California's past that vary from present conditions, including multi-millennial states of long-term aridity and pre-glacial deep lake conditions.

The dissertation of Katherine Colby Glover is approved.

Thomas Welch Gillespie

Matthew E. Kirby

Marilyn Raphael

Glen Michael MacDonald, Committee Chair

University of California, Los Angeles

2016

For my family — John, Mom, Dad, Andrew, Olivia, and Athena.

Table of Contents

List of Figures and Tables

Acknowledgements

UCLA is a world-class research and teaching institution, and it has been my privilege to engage in both over the past five years. I could have never imagined the number of opportunities I'd have here when I decided to leave high school teaching, and such widespread financial support for my re-entry to paleoclimate research. This work was supported by: UCLA's Institute of the Environment and Sustainability Presidential Fund, the John Muir Memorial Chair Endowment, the U.S. Department of the Interior's Southwest Climate Science Center, the Geological Society of America, Society of Woman Geographers, UCLA La Kretz Center for California Conservation Science, and the Limnological Research Center. I thank UCLA Graduate Division, the Society of Woman Geographers, and the American Association of Stratigraphic Palynologists for discretionary fellowship and travel funds that supplemented graduate income, and allowed for valuable conference attendance.

Taking the new Baldwin Lake core in August 2012 would not have been possible without the help of Katie Nelson, Scott Eliason, and Gina Riggins of the San Bernardino National Forest Service. Gregg Drilling, L.L.C. provided incredible service and a talented drilling team: Jeff Keithley, Sam Gutierrez, and Daniel Del Castillo. Larry Winslow of the Baldwin Lake Fire Dept helped immensely on-site with a route of access via his property, water and supplies to the drilling team, and contact with Big Bear Lake's local press.

Since my prospective visit to the Geography Department, I've been impressed by the collegiality among graduate students and professors. I thank those peers and colleagues I met in the pursuit of this degree, and their support and friendship: Mike Antos, Cameran Ashraf, Clare Beer, KT Bender, Nick Burkhart, Vena Chu, Dylan Connor, Abigail Cooke, Ashley Fent, Andrew Fricker, Colin Gleason, Andrew Grant, Sarah Halterman, Ali Hamdan, Timur

Hammond, Tyler Harlan, Sara Hughes, Shenyue Jia, Hana Kahn, Mahmood Kahn, Tuyen Le, Evan Lyons, Taylor McCleary, Tom Narins, Amanda Pearson, Chelsea Robinson, Corey Rovzar, Scott Stephenson, Jida Wang, Diane Ward, and Kate Willis. Thanks for the many dinners, beers, hikes and fun we had around Los Angeles, and at AAG, AGU, and CGS. I also thank my officemates Luis Alverez-Leon, Emma Colven, Nerve Macaspac, Sam Nowak, Clark Taylor and Diane Ward, whose camaraderie, encouragement, and studiousness helped propel me to the final stages. For all the conversation and help needed on 4th-floor Botany, I thank Rachel Clausing, Peggy Fong, Ranjan Muthukishnan, and Stacie Smith. I'm grateful for Jennifer Schneiderman Pressburg's friendship so consistently throughout my five-year residence in L.A., and I thank the members of the Sierra Club Wilderness Adventure Chapter, especially leaders Bob Cody, Mary Forgione, and Mandy Horak, for all the hikes and miles we shared. Always enthusiastic to hear of my research findings, climbing so many SoCal mountains together informed my knowledge of the alpine wilderness around the L.A. Basin.

I also thank the Geography Department staff who helped with the degree and financial requirements of the program, including Student Affair Officers Nayla Huq, Lisa Lee, Kristina Magpayo, and Irina Tauber. The persistence and good humor of Vanessa de la Rosa, Tanja Hrast, and Jenée Misrai were instrumental to the nuts and bolts of research and travel. Shahara Ben-Iesau and Karen Lefkowitz of the Institute of the Environment and Sustainability were also key to project planning, and I thank them for their help navigating university procedures that could only be described as labyrinthian. Matt Zebrowski helped amplify my research presentations with his design skills, and Brian Won offered his tech savvy more times than I can count. Huge thanks goes to Kasi MacMurray, who helped on the "front lines" of operations and funding on every level of the university, department, and laboratory. I'm indebted to the

consistent empathy, sense of humor, and listening ear she provided during my time at UCLA.

I've been fortunate to have colleagues like my labmates: Rémi Bardou, Lauren Brown, Elly Fard, Jessie George, James Holmquist, Julie Loisel, Scott Lydon, Simona Katav, Setareh Najet, Jordan Rosencranz, Marcus Thomson, Sophie Webber, and Kate Willis. You provided friendship and more, with support and help for lab and field tasks, and never hesitated to help work through ideas and the snarls of research. Many undergraduate and visiting students assisted with this project, convincing me that UCLA students are world-class for their collective enthusiasm and inquisitiveness. Thank you to April Chaney, Elaine Chang, Tamryn Kong, Alec Lautanen, Alex Pakalniskis, Sargam Saraf, Nicole Tachiki, Sam Trumbly, Alexis Whitaker, Alice Wong, and Renée Yun for all your subsampling and data collection. At collaborating institutions, Christine Hiner and Alex Woodward at CSU-Fullerton, and Jennifer Leidelmeijer at CSU-Long Beach, provided their enthusiasm and help.

Lab managers that made collaboration run smoothly and swiftly include Wendy Barrera of the UCLA Luminescence Laboratory, Kristina Brady and Jessica Rodysill at the University of Minnesota's Limnological Research Center, Katherine Whitacre of Northern Arizona University's Amino Acid Geochronology Lab, and Beau Campbell and Aisling Farrell at the Page Museum at the La Brea Tar Pits. I thank the broader community of Quaternary paleoclimatologists who offered their words of advice, suggestions, humor, feedback and encouragement over the years, in many mediums: at conferences, over emails, and social media. I thank Linda Heusser especially for advice and data on West Coast pollen, and her many emails and conversation at conferences. Her ongoing and wise advice was indispensable as I navigated a rather complicated and time-consuming proxy that was new to me at the start of the PhD.

The members of my committee have been strong supporters of this work from its

inception, and offered valuable feedback and criticism. I thank Marilyn Raphael for her steadfast support, and Tom Gillespie for his consistent enthusiasm and expertise on California vegetation. Matt Kirby of CSU-Fullerton went above and beyond the requirements of an external member, offering advice on research design, collaboration opportunities with his lab, and accepted changes to his prior interpretations of Big Bear Valley paleoclimate with good grace and humor. I could have asked for no better committee head and advisor than Glen MacDonald, who lives so many qualities integral to doing good science: remarkable vision for project conception, and diligent lab technique and safety. His leadership and care for others have created a powerfully collegial, inclusive, productive lab group. Thanks for the all the times you "pulled me out of the weeds" to remember broader aims and impacts of my work.

My extended and immediate family has always provided their love and support for my academic pursuits. My father, who has taken me out to the woods and trails from a young age, instilled a lifelong curiosity and love of nature that has become a vocational calling for me in education, conservation, and scientific research. Mom's organizational skills, work ethic, artistry and creativity have always inspired me, and I am a better scientist for emulating these traits. My brother Andrew, the most selfless person I know, started his own academic journey while I was at UCLA, overcoming several obstacles. I'm humbled by your empathy and perseverance, which push me to be better, kinder, and more gracious.

Finally, my largest thanks of all go to John, who encouraged my pursuit of a PhD from its most inchoate conceptions back in Charlotte, NC. Coming from someone who left his own pursuit of a PhD degree — twice — his support, editorial advice, and love have moved me more times than I can count. I look forward to continuing our lives together as "Dr. and Mr."

VITA

Education

University of California – Los Angeles, Los Angeles, CA, USA
Ph.D. Candidate, Geography, expected December 2016

University of Cincinnati, Cincinnati, OH, USA
M.S., Geology, 2004

DePauw University, Greencastle, IN, USA
B.A., *cum laude*, Geology, 2001

Peer-Reviewed Publications

Glover, K. C., MacDonald, G. M., Kirby, M. K., Rhodes, E., Stevens, L., Silveira, E., Lydon, S., and Whittaker, A. *(in review)* Insolation and North Atlantic Climate Forcing in alpine Southern California since 125 ka. *Quaternary Science Reviews*

Glover, K. C., Lowell, T. V., Wiles, G., Pair, D., Applegate, P., Hajdas, I., 2011. Deglaciation, basin formation, and post-glacial climate change from a regional network of sediment core sites in Ohio and Eastern Indiana. *Quaternary Research* 76, 401-410.

Lowell, T. V., Fisher, T. G., Hajdas, I., **Glover, K.**, Loope H., Henry, T., 2009. Radiocarbon deglaciation chronology of the Thunder Bay, Ontario area and implications for ice sheet retreat patterns. *Quaternary Science Reviews* 28, 1597-1607.

Lowell, T. V., Fisher, T. G., Comer, G., Hajdas, I., Waterson, N., **Glover, K.**, Loope, H. M., Shaefer, J., Rinterknecht, V., Broecker, W., Denton, G., and Teller, J. T., 2005. Testing the Lake Agassiz Meltwater Trigger for the Younger Dryas. *Eos* 86 (40), 365-373.

Fellowships, Awards and Grants

2016: Geosystems Paper Award, California Geographical Society
Best Paper, Biogeography Specialty Group, American Association of Geographers
2015: Dissertation Year Fellowship, UCLA Graduate Division (2015-2016)
2014: Society of Woman Geographers National Fellow (2014-2015)
John Muir Memorial Chair Summer Fellowship
Tom McKnight 1st Place Paper Award, California Geographical Society
Limnological Research Center Graduate Student Travel Award
UCLA La Kretz Center for California Conservation Science student award
2013: Graduate Summer Research Mentorship, UCLA Graduate Division
Geological Society of America Graduate Student Grant
2012: Graduate Research Mentor Fellowship, UCLA Graduate Division (2012-2013)
Graduate Summer Research Mentorship, UCLA Graduate Division
2001: Fenneman Fellowship, Department of Geology, University of Cincinnati (2001-2002)

2000: Summer Research Fellowship, Faculty Development Committee, DePauw University
Rock Smith Scholarship, Department of Geology, DePauw University (2000-2001)
1999: Condit Science and Mathematics Scholarship Award, DePauw University (1999-2001)
1998: Summer Research Fellowship, Faculty Development Committee, DePauw University

Professional Service and Affiliations

Fossil Lab, La Brea Tar Pits, Los Angeles County Museums (2015-2016)
Organizing Committee, International Limnogeology Congress (ILIC6; 2013-2015)
Geography Graduate Curriculum Reform Committee, UCLA (2013-2014)
Faculty Welfare Committee, UCLA Academic Senate (2012-2013)

Member of: American Geophysical Union (2011-present), American Association of Geographers (2012-2013; 2015-2016), International Biogeography Society (2016-present), Earth Science Womens Network (2016-present), National Center for Faculty Diversity and Development (2016- present), American Association of Stratigraphic Palynologists (2014-present), Society of Woman Geographers (2013-present), California Geographical Society (2011-present), Geological Society of America (2001-present)

Selected Conference Presentations

Invited: "Insights into hydroclimatic variability of Southern California since 125 ka, from multi-proxy analyses of alpine lake records" (talk), American Geophysical Union Fall Meeting, San Francisco, CA, December 2016.

"Vegetation Change in the San Bernardino Mountains from 60,000 – 15,000 years BP" (talk), California Geographical Society Annual Meeting, San Jose, CA, May 2016.

"A 90,000-year fire history from the San Bernardino Mountains, Southern California" (talk), American Association of Geographers Annual Meeting, San Francisco, CA, April 2016.

"Southern California climate, hydrology and vegetation over the past c. 96 ka from Baldwin Lake, San Bernardino Mountains, California" (poster), American Geophysical Union Fall Meeting, San Francisco, CA, December 2015.

"Insight into Southern California paleoclimate since Marine Isotope Stage 5c (c. 96 ka) from Baldwin Lake, San Bernardino Mountains, CA" (talk), Geological Society of America Annual Meeting, Baltimore, MD, November 2015.

"Lake Sequences from Big Bear Valley, San Bernardino Mountains, CA Provide Insight into Western Paleoclimate over the Past 100 kyr" (talk), California Geographical Society, Annual Meeting, Los Angeles, CA, April 2014.

"A 9.2 ka paleoecological history of Lower Big Bear Lake, San Bernardino Mountains, CA, and implications for Holocene climate change in the U.S. Coastal Southwest" (talk). Geological Society of America Annual Meeting, Denver, CO, October 2013.

"Deglaciation, basin formation, and post-glacial climate change from a regional network of sediment core sites in Ohio and Eastern Indiana" (talk). American Geophysical Union Fall Meeting, San Francisco, CA, December 2011.

1. Introduction

Climate model projections for the rest of the 21st century suggest that increased radiative forcing will manifest as enhanced temperatures, and changes to the water cycle, throughout Earth. Improving and understanding these projections is especially important in Southern California and the U.S. Southwest, where population has expanded at some of the nation's highest rates in recent decades (Georgescu et al., 2012). This area lies on the boundary between projected precipitation increases in the north, and decreases in the south (IPCC, 2013), portending enhanced aridity and increased limits on valuable water resources for Southern California (MacDonald, 2010; MacDonald et al., 2008; Overpeck et al., 2013).

The effects of these projections have already become apparent in recent years. "California Drought" conditions are constantly being assessed statewide, and the topic is frequently in the news. The hottest years in California since instrumental record-keeping began (~150 years ago) were 2014 and 2015 (Hanak et al., 2015), and the last two decades anomalously hotter than the preceding century (Diffenbaugh et al., 2015). Lasting from 2012–2016, and at times designated as "exceptional drought," this has been a record-breaking event. While annual precipitation amounts have shown no discernible trend over instrumental record-keeping (Mann and Gleick, 2015), Diffenbaugh et al. (2015) find that, historically, 1) drier-than-average years co-occur with years of anomalously high temperatures, and 2) over the past century, drought years have been the most frequent during the years 1995–2015. Despite increased precipitation from El Niño in 2016, precipitation deficits can persist and have impacts years afterwards, and several central and southern California reservoirs remain below capacity (Hiltzik, 2016).

These projected temperature and water cycle changes have potential to reshape the landscape of California's biomes, renowned for their endemism and biodiversity. Wildfire and

hydroclimatic extremes have helped shape this landscape, particularly in mediterranean biome portion of the state, where biodiversity is promoted when low- to moderate-severity ground and surface fires occur (Keeley et al., 2012). Over the last two decades, however, wildfire has had increasingly long seasons in California, and forests throughout the U.S. Southwest and Cordilleran (Westerling, 2006). Recent widespread tree mortality in the alpine forests of the U.S. West have been documented, including California's coniferous forests (van Mantgem et al., 2009). The California Department of Forestry and Fire Protection spent nearly $550 million on fighting wildfires in 2015, marking its most expensive year since 1980 (Guerin, 2016). This is just one example of the potential economic drain that climate change will have upon the state.

These drier, warmer, and more flammable conditions may be unprecedented within ~150 years of scientific study and record-keeping, yet we know that ecosystems were present before under different precipitation and temperature regimes. This is where paleoclimate studies help extend our knowledge of climate and ecosystem composition and dynamics, and find past analogues to inform the modern management of national forests, wildlife, and water resources Southern California (Overpeck et al., 2013). Retrospective studies are also key to illustrate the potential range of variability for landscape response, and elucidate how a complex climate system operated and was teleconnected.

High-resolution Holocene studies have shown that prior arid events have occurred, with potential to be long-lasting. Termed "megadroughts" due to their decades-long duration, the Medieval Warm Period (1 – 0.7 ka[1]) in particular supported long periods of reduced precipitation (MacDonald et al., 2008; MacDonald and Case, 2005; Woodhouse et al., 2010). A recent review of Great Basin paleoclimate records from the last few millennia demonstrate that the Late

[1] Throughout the dissertation, "ka" denotes an approximate date in thousands of years before present, and "kyr" denotes "thousands of years"

Holocene Dry Period broadly impacted the region (Mensing et al., 2013). West of the Great Basin in the Sierra Nevada, Kirman Lake (Figure 1.1) showed a protracted arid period from ~8 – 3 ka (MacDonald et al., 2016). Records and studies that pre-date the Holocene are more rare, but similarly document long-lasting drought. At Lake Elsinore in Southern California (Figure 1.1), for example, a series of extended megadroughts were the norm just prior to the Last Glacial Maximum from 27.5 - 25.5 ka (Heusser et al., 2015).

Conversely, episodes of enhanced precipitation delivery to California are possible. The arrival of atmospheric rivers abruptly ended 33-40% of California droughts from 1950-2010 (Dettinger, 2013). Paleoclimatic records also show periods of anomalously high precipitation, particularly in Southern California. Physical and geochemical proxy data suggest pluvial episodes in a ~9,200 kyr record from Lower Bear Lake in Big Bear Valley of the San Bernardino Mountains (Figure 1.1) during the Early and Late Holocene (Kirby et al., 2012). In a recent review of records dating to the Last Glacial Maximum (LGM, c. 22 ka), Oster et al. (2015) found that Pacific-derived storms were steered toward Southern California at the LGM, creating unusually wet conditions. Lake highstands have been documented in the Lake Manix Basin (Figure 1.1) of San Bernardino County prior to the Last Glacial Maximum, with multiple episodes of basin overflow supporting times of sudden moisture influx to the region (Reheis et al., 2015).

Reconstructing these climate events, and their impact on terrestrial ecosystems, relies heavily upon lacustrine records. Lake records with continuous sedimentation can extend beyond the limits of dendrochronologic and before the Holocene. However, closed-basin lakes with continuous deposition prior to the Last Glacial Maximum are rare in Southern California and the U.S. Southwest, due to its natural aridity/semiaridity. Southern California, for example, only receives an annual total of ≤400 mm precipitation a year, compared with ≥1000 mm/yr in Northern

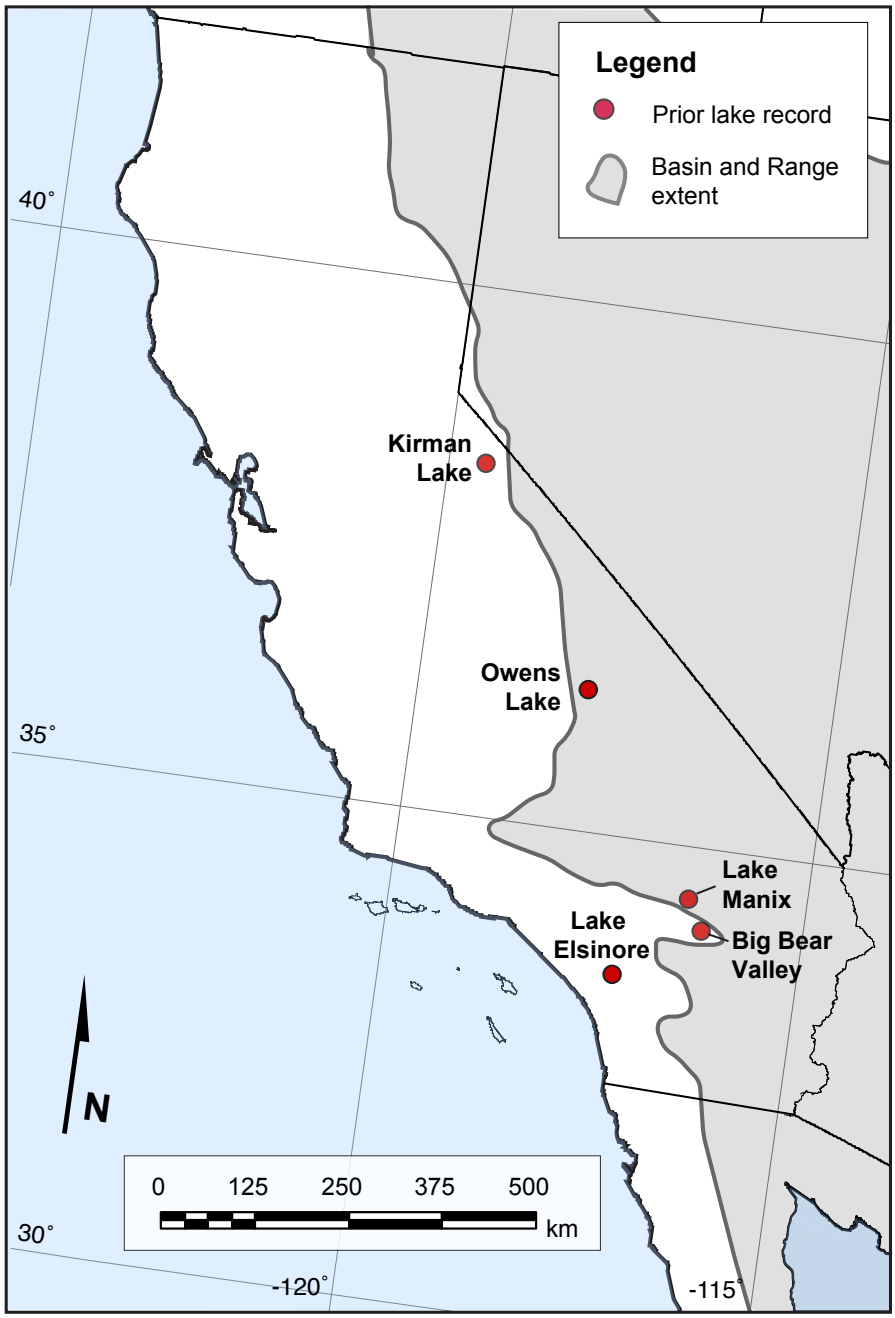

Figure 1.1 Location of paleoclimatic records mentioned in Ch 1 that exhibit paleohydrologic extremes (i.e. extended aridity, or moisture influx). The dissertation sites Baldwin Lake and Lower Bear Lake are located in Big Bear Valley, San Bernardino County.

California (Lyle et al., 2010). Drier-than-average events can therefore lead to desiccation of lake basins and disrupted sedimentation.

This dissertation focuses on a pair of lake records in Big Bear Valley (elevation 2060 m) of the San Bernardino Mountains, an alpine environment in Southern California. Situated at the transition between the Transverse Ranges and Mojave Desert (Figure 1.1), Big Bear Valley is sensitive to dynamic shifts in Pacific moisture delivery, vegetation and resulting sedimentation from the surrounding mountains. Over the past 125,000 years, it has possessed the rare set of circumstances that have allowed near-continuous deposition in Baldwin Lake before basin desiccation ~10 ka. The Big Bear Lake core began lacustrine deposition c. 10 ka (Kirby et al., 2012), which continued through most of the Holocene. Taken together, the records in Big Bear Valley's represent the longest high-resolution terrestrial record in Southern California that extends to Marine Isotope Stage 5e, the last interglacial. The primary two-part question guiding this research is:

Over the past 125,00 years in alpine Southern California:

1) how can temperature and available moisture changes at these lake sites inform our understanding of climate phenomena that affect California?

2) how has vegetation changed, and what role does wildfire play in past ecosystem dynamics?

In structuring this dissertation, I have parsed out different facets of the study, with more specific research questions, into four chapters. Chapter 2, **Palynology in California: Vegetation and Climate Change Patters over the past 130 kyr**, details the available pollen record throughout the state, and notes that forest contraction is a common signal linked to aridity. Chapter 3, **Insolation and North Atlantic Climate Forcing in alpine Southern California since 125 ka**, reports the age and lab results from the newly-recovered Baldwin Lake core

(BDL12), which suggest that local summer insolation and rapid warming events in the North Atlantic were long-term climatic drivers affecting Southern California. Chapter 4, **Terrestrial Organics, Vegetation, and Wildfire in alpine Southern California 120 - 10 ka**, include results of stable isotope, pollen, and charcoal analyses on BDL12, which further illuminate the hydroclimatic history of the site, changes in the forest canopy, and wildfire's active role in ecosystem dynamics for the majority of the last 125 kyr. Chapter 5, **Holocene Vegetation, Wildfire, and Hydroclimatic History from Lower Bear Lake, San Bernardino Mountains, Southern California**, applies similar methods to subsamples from the Lower Bear Lake core to show that proposed pluvial events in the San Bernardinos during the Holocene (Kirby et al., 2012) had a complex landscape response, in terms of forest composition and wildfire activity.

Throughout the dissertation, I contextualize the results from Big Bear Valley lake cores with other paleoclimatic and paleoecological sites from the Pacific margin, California, the Great Basin, and U.S. Southwest. I offer conclusions at the end regarding Southern California's responsiveness to climatic forcing, and most-important climatic drivers, including the role of local insolation and sea surface temperatures. This reconstruction of vegetation, wildfire, and precipitation in the SBM is timely, as it investigates the natural range of variability possible in this biome and these mountains prior to human occupation. This study can therefore inform 21st century expectations for ecosystem change in a Southern California future that is projected to be warmer and drier.

2. Palynology in California: Patterns, Challenges, and Future Research Potential from 130,000 years of vegetation data

2.1 Abstract

Pollen datasets from California were compiled, and examined for patterns in age, location, and ecological change during key climate events. These events included 1) the last interglacial Marine Isotope Stage 5e (MIS 5e, 130 - 120 ka, 11% of sites), 2) the Last Glacial Maximum c. 20 ka (LGM, 16% of sites), and the Holocene from 11 - 0 ka (73% of sites). Disturbance-loving *Alnus* typically indicated the onset of interglacial conditions at northern marine sites for both MIS 5e and the Holocene, followed by successive increases in *Sequoia sempervirens* and *Quercus*. Warming at terrestrial sites was best shown with a most-sensitive taxon, depending on the site's ecoregion. Aridity was widespread in Northern and Central California at the LGM with steppe expansion, while moist conditions prevailed in the south. The majority of pollen sites (73%) span only the Holocene, showing a pattern of complex change over the past 10 kyr. Aridity in the north was coeval with moisture in the south during the Early Holocene, then shifted to widespread drying in the south and Sierra Nevada during the Middle Holocene. The avariable Late Holocene was variably wet and dry, due to enhanced El Niño Southern Oscillation (ENSO). Almost universally, increases in herbaceous-shrub taxa, particularly *Artemisia*, signaled relatively arid conditions, while rises in coniferous taxa indicate enhanced forest cover and thus moisture. This review shows several gaps in the existing record, both in geography and usability. Prior work in southern California (i.e. below 35˚N) has primarily targeted available Holocene sites in coastal and marine areas, highlighting the need for work on long alpine records. Consistent data archival in the North American Paleoecological Database Neotoma is suggested as a best practice for future research endeavors to improve data accessibility and meta-analysis between sites, particularly for pre-Holocene work.

2.2 Introduction

Significant changes in ocean-atmospheric processes, moisture, and vegetation assemblages have occurred throughout the Late Quaternary. In this review, I discuss the available palynological record of California over the past 130,000 years, and how these data can inform 1) past change in vegetation cover, and 2) climatic conditions. I limit the geographic scope of this review to the political boundaries California, where the precipitation gradient from north-to-south is strongest (Lyle et al., 2010). The Pacific Northwest is dynamically different once it transitions to a marine ecoregion just north of the California-Oregon border (Figure 2.1, Bailey, 2009), with lower plant diversity and incidence of wildfire (Briles et al., 2011; DellaSala et al., 2011; Taylor and Douglas, 1995). As records are available, I include those dating to Marine Isotope Stage 5e (MIS 5e, 130 - 120 ka), the oldest limit of terrestrial sites discovered thus far in California. MIS 5e has generally been characterized as warm and climatically stable (Kukla et al., 2002; Maslin et al., 1998; Willis and MacDonald, 2011), and been examined as a possible analogue for Holocene climate and vegetation (Leduc et al., 2010; Maslin et al., 1998; Sánchez Goñi et al., 2000).

Currently, the terrestrial palynological record has been highly focused on mountain lakes, the northern part of the state, and the Holocene. Several of the longer records that capture MIS 5e came from marine cores. With the available record, the following can be asked to address the broader concern of how temperature and moisture change have driven past flora:

1) how does the terrestrial palynology record differ from marine studies?

2) are there identifiable ecological patterns to past climate change?

3) is MIS 5e a proper analogue for the Holocene?

Deciphering the record is a challenge for several reasons. Firstly, California's inherent landscape heterogeneity results in diverse vegetation cover, leading to the state's designation as the California Floristic Province (CFP), with unique and endemic floral species numbering over 3,500 (Mittermeier et al., 1999). Secondly, California experiences precipitation extremes on timescales that range from the seasonal (i.e. summer-dry conditions characteristic of mediterranean biomes) to multi-year, even decadal, mega-droughts (Heusser et al., 2015; Woodhouse et al., 2010). Dry conditions are not conducive to lake persistence and pollen preservation, which has left gaps in the microfossil record, particularly towards the south. Finally, data from several long sites and records are still not digitized, preventing broader meta-analysis that could include these sites.

2.3. Present-Day Pacific Dynamics and Terrestrial Vegetation

2.3.1 Ocean-Atmosphere Dynamics

Current oceanic and atmospheric dynamics of the Pacific include the persistent North Pacific High (NPH) in the eastern Pacific, and the North American Low (NAL) in the southwestern states (Figure 2.1). High moisture regions can be found along the coastline, particularly towards the north, and in high-altitude regions in California's many mountain ranges (Thompson et al., 2005). Both the seasonal migration and variations of the NPH and NAL influence several processes that impact West Coast climate, including directional changes in surface winds, the position of the jet stream and Westerlies wind belt, and storm tracks. The NPH migrates northward in the spring, resulting in three major changes: wind direction shifts towards the south, coastal upwelling is induced, and precipitation ceases for a summer season (Barron et al., 2003; Hendy et al., 2004; Sancetta et al., 1992). In summer, the NPH strengthens and migrates to a more central location that drives storms northward towards Canada. Both the

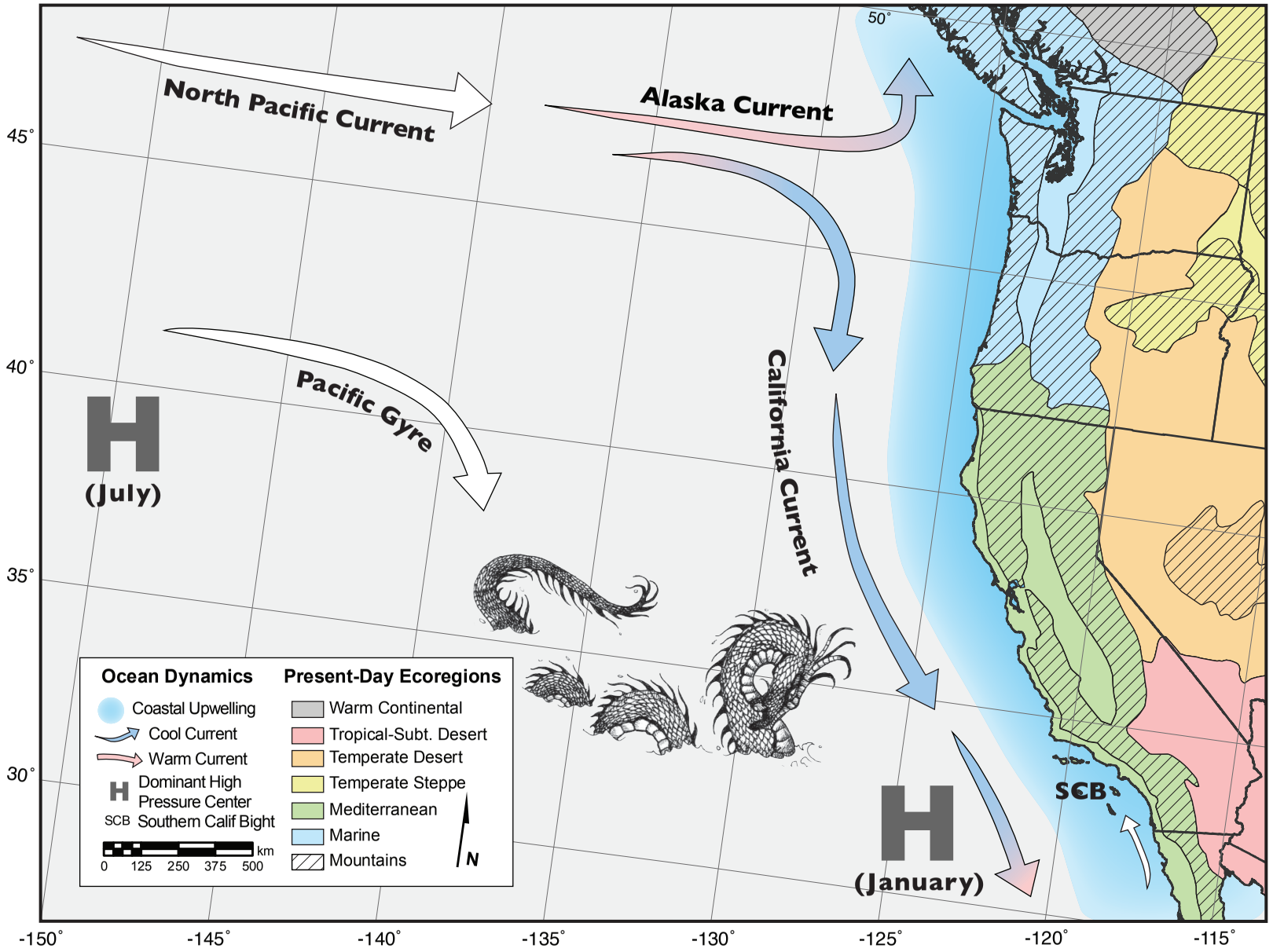

Figure 2.1. Present-day ecoregions of the North American West Coast, and ocean-atmosphere dynamics, inclduing currents.

NPL and NPH weaken during winter, with the NPH and the jet stream moving southward and changing the storm trajectory towards California (Barron et al., 2003; Lyle et al., 2010).

Major ocean currents include the North Pacific Drift, which flows eastward between 40 – 45˚N, partitioning at the coastal region just offshore of Washington and Oregon. The south-flowing portion becomes the California Current, and the northbound waters become the eastern section of the Alaskan Gyre (Figure 2.1; Pisias et al., 2001). Thus, maritime proximity and the prevailing westerly winds moderate West Coast climate, resulting in minimal temperature variation along the coast (Hendy et al., 2004; Heusser, 1992). Ekman transport supports strong upwelling along the coast to maintain cool, consistent sea surface temperatures (SSTs), a phenomenon that produces seasonal fog (Hendy et al., 2004) and influences primary productivity in the ocean surface (Poore et al., 2000).

Summer aridity is more pronounced towards in the Southwest, which experiences warm-weather, continental precipitation during the late summer and early fall. These processes include the North American Monsoon (NAM) and convective uplift in high-relief areas, and largely affect New Mexico, Arizona, and inland portions of southern California (Kirby et al., 2013; Sheppard et al., 2002). NAM moisture sources include tropically-sourced air surges that follow the Gulf of California northward, and from dissipating tropical storms of the eastern Pacific (Redmond, 2009; Vera et al., 2006). The Gulf of Mexico is a secondary source of moisture, with greater impact southeast of California (Adams and Comrie, 1997). In California, convective uplift can result in thunderstorms and late-summer precipitation. These variations in precipitation directly influence California's native vegetation.

2.3.2 Ecoregions and their dominant vegetation

In any geographic study, choosing appropriate boundaries to categorize change and

constrain discussion is a challenge, with several options available. I use the ecoregion boundaries of Bailey (2009), which capture elements of the physiography, temperature, and precipitation on the landscape that directly influence vegetation. Ecoregion boundaries have been actively adapted over the years, and now include the North American continent. Available at several scales, they are currently in use with the United States Forest Service, the managing entity for the San Bernardino National Forest and much of the SBM. While these ecoregion boundaries do over-generalize transition zones between vegetation groups and simplify the complexity of altitudinal zonation in mountains, this broad framework is appropriate for capturing floristic change that can be rapid over the physiographic boundaries on the West Coast (Thompson et al., 2005). Ecoregions also do not consider human-induced land use change, which, while significant and has influenced California's recognition as a biodiversity hotspot, has not impacted the landscape for the majority of the 130 kyr time span considered here. Finally, in this system, the distribution of dominant woody vegetation is used as a climate proxy to infer boundaries in many remote areas that lack empirical data from meteorological stations. Such an exercise bears some similarity to palynological work, where fossil pollen serves as a proxy for past vegetation assemblages and thus, paleoclimate (Bailey, 2009; Thompson et al., 2005). Figure 2.2 aggregates these ecoregions into three sectors based on overall climate, providing a simple framework in which to discuss paleoclimate sites located therein and the dominant vegetation.

California ecosystems are world-renowned for their high degree of diversity and endemism, with major plant structure of the different ecoregions described below. It is these woody taxa that tend to be the most telling indicators of past vegetation climate in palynology, as woodland expansion and contraction will occur with fundamental changes in moisture and temperature. Present-day distribution and diversity in the study region, with a focus on key

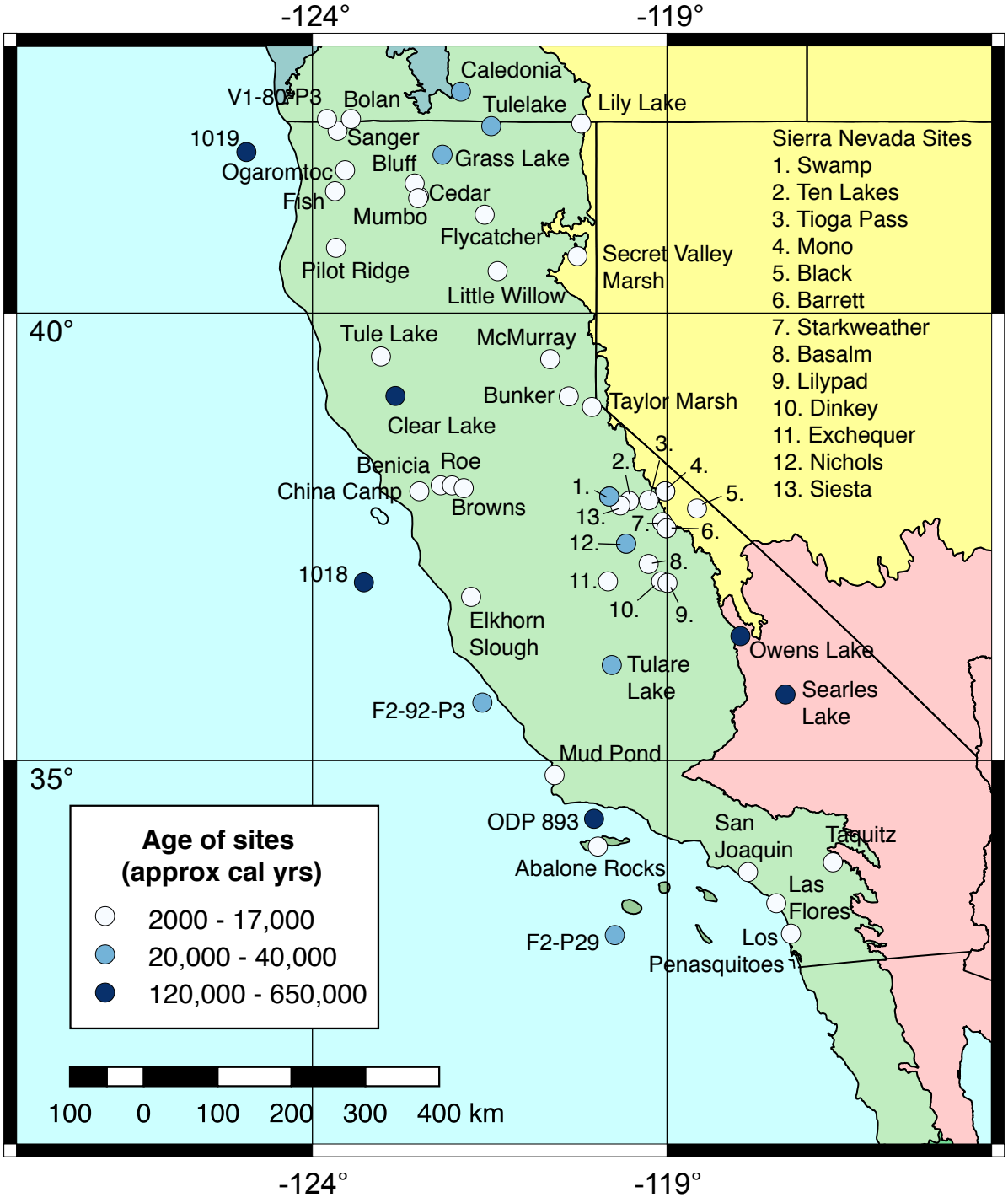

Figure 2.2. Map of marine, wetland, and lake sites with continuous palynological data that date to at least 2 ka. Sites detailed in Table 2.2.

arboreal taxa, are summarized in Table 2.1, alongside a summary of prevailing climate, ecosystem patterning, and present-day fire regime.

2.3.2.1 Mediterranean Ecoregion

The Mediterranean sector is located largely along coastal California (Figures 2.1, 2.2). Latitudinal annual temperature variation is low in California (in the range of 4-6 ˚C), but the precipitation gradient is much stronger, ranging from >1200 mm/year at the Oregon border, to <500 mm/year at the border with Mexico (Lyle et al., 2010). This strong moisture gradient drives diversity, in addition to genetic isolation during relatively recent mountain building (Calsbeek et al., 2003), high relief, and the frequent disturbance of wildfire. Mosaic habitats abound and lend to endemism, with significant taxa changes that often occur on a small scale with variations in hillside exposure, slope, soil composition, water table depth, and relief.

Vegetation undergoes a gradual change in forest structure from north to south. *Picea* (spruce) and *Tsuga heterophylla* (western hemlock) continue southward from the Pacific Northwest forests, with greater inclusion of endemic *Sequioa sempervirens* (redwood; Lyle et al., 2010; Poore et al., 2000). *S. sempervirens* requires persistent coastal fog and enhances moisture retention and drip within its forests, and is often associated with *Alnus* (alder) spp. (Lyle et al., 2010). Away from the foggy coast and in the rain shadow of the Coastal Ranges, the landscape inland and southward tends to be chaparral, scrubland, and oak woodland – by far the dominant land cover of this ecoregion at lower elevations, and a clear marker of decreased precipitation. Perennials flourish during wet months and die off during summer drought. Sclerophyllous shrubs and trees persist year-round on the landscape and are abundant in this sector, with hard leaves that are adapted to withstand several months of summer aridity, yet still maintain optimal surface area for solar intake (Bailey, 2009; Mooney and Dunn, 1970). Many shrub taxa naturally

Table 2.1. Summary of modern climate and vegetation characteristics of the three ecoregions (Figure 2.2) discussed in this review.

Sector	Climate	Ecosystem Patterning	Floral Diversity	Key Woody Taxa	Present-Day Fire Regime
Mediterranean	Temperature – some annual variability; monthly average never below freezing Moisture – precipitation during winter months originating from Pacific, 4-6 arid summer months, except at foggy coastline	Highly mosaic, due to variety of terrain, soil, and fire frequency	Very high, with high degree of endemism. Biodiversity hotspot (California floristic province), with thousands of plant species, roughly half endemic	*Quercus* (oak; interior woodlands), *Sequoia sempervirens* and *Alnus* towards northern coastline, *Pinus*, *T. heterophylla* at elevation, *Artemesia* (sagebrush) at southern coastline	Very important to regeneration; high frequency
Temperate	Temperature – high seasonality and degree of variation Moisture – generally semiarid; localized storm precipitation during summer months	Highly mosaic, high degree of altitudinal zonation due to complex terrain	Moderately high degree of endemism	*Artemesia* and xerix woody taxa at higher elevations, e.g. *Pinus*, *Tsuga menzeseii*, *Juniperus*, scant *Populus* (aspen) groves	Important to maintain open scrub and meadow, high frequency; recent suppression policy has had impact on encroachment
Tropical/ Subtropical Desert	Temperature – high diurnal variability; monthly average never below freezing Moisture – during winter months, summer monsoon from Gulf of California lasting few weeks	Highly mosaic, due to altitudinal variation, soil, and moisture; some small tracts inhospitable to most, if not all, vegetation	High diversity, esp. for vascular plants; endemism is moderately high, with highest concentration of endemics in Mojave Desert and mountains	*Larrea tridentata* (creosote), *Yucca*, pinyon-juniper, isolated stands of *Abies concolor,* Arecaceae (palm), *Salix* (willow), *Populus, Pinus longae*	Low frequency historically; recent proliferation due to invasive groundcover

produce flammable oils to promote burning, and wildfire is important to restore soil nutrients and facilitate plant regeneration. Sclerophyll scrub species grow densely together, creating highly impenetrable thickets that readily burn (Quinn, 2006). Chaparral is closely associated with oak and pine woodlands, and coastal sage scrub with deciduous, rather than evergreen, *Artemisia* (sagebrush; Quinn, 2006). In low-elevation woodlands, varieties of *Quercus* (oak) are the primary woody evergreen vegetation. *Pinus* (pine), *Abies* (fir), and *T. heterophylla* reappear at high elevations inland (Poore et al., 2000).

2.3.2.2 Temperate Desert Ecoregion

The Temperate Desert includes much of the Great Basin, the Modoc and Columbia Plateaus, and the western flank of the Rocky Mountains. In California, the eastern northeastern and east-central edge of the state lie in the rain shadow of the Sierra Nevada, and are designated as temperate desert. Much of the year's precipitation budget occurs as Pacific-derived winter snow. Evaporation is strong and can lead to salinization on dry lake beds (Anderson, 2003; Bailey, 2009). Due to changing relief, the temperate desert is highly mosaicked, with several subalpine, alpine, and riparian assemblages.

Plants are thus adapted to withstand this seasonal and interannual water stress (Redmond, 2009). Sagebrush scrub, comprised primarily of *Artemisia tridentata* (Big sagebrush), is common, often growing in association with *Sarcobatus vermiculus* (greasewood) and native bunchgrass in the nutrient-rich soils of low-lying regions (Baldwin, 2002; Booth et al., 2003; DeLucia et al., 1989; Naumburg et al., 2005). Other shrubs include: *Coleogyne ramosissima* (blackbush), *Ephedra nevadensis* (Mormon tea), *Grayia spinosa* (hop-sage), *Krascheninnikovia lanata* (winter fat; Baldwin, 2002). *Populus* spp. (cottonwood) occurs in riparian areas, and xeric pine species and pinyon-juniper assemblages create subalpine woodland. *Pinus* species include

monophylla, *jeffreyi,* and *ponderosa*, which are considered xeric, i.e., they are adapted to greater water stress and soil that is often nutrient-poor. Pygmy forests and some of the oldest trees in the world, *Pinus longaeva* (bristlecone pine), occur at higher elevations. Woodland gives way to alpine tundra at the highest altitudes of the region (Anderson, 2003; Baldwin, 2002; DeLucia et al., 1989).

2.3.2.3 Tropical-Subtropical Arid Southwest

The boundary between temperate and tropical-subtropical deserts is rather diffuse, with floristically similar plants, though they are increasingly adapted to aridity and warmer temperatures towards the south. Separated from the moisture source of the Pacific Ocean, the Mojave and Sonoran Deserts largely comprise the tropical-subtropical desert ecoregion. With a precipitation average of less than 200 mm a year, evaporation is strong and winter precipitation is episodic, occurring when the jet stream migrates southward to bring a supply of subtropical moisture to the region (Redmond, 2009). The North American Monsoon (NAM) delivers summer precipitation to the Southwestern states of Arizona and New Mexico, while the portion in California is at the farthest reaches of NAM extent (Metcalfe et al., 2015). A high degree of diurnal variability exists, but no monthly temperature average is below freezing (Bailey, 2009).

Vascular plants are highly adapted and diverse throughout southwestern deserts and varied terrain, and must survive extreme short-term temperature variability with long-term aridity. Endemic species are abundant due to geographic isolation and high relief (Baldwin, 2002). Surfaces that are inhospitable to all but the most specialized types of vegetation are common, including salt playas, shifting dunes, caliche, and desert pavement. *Sarcobatus* (greasewood), *Salicornia* (pickleweed), *Allenrolfea* (iodine bush), and *Distichlis* (salt grass) can grow on such surfaces (Collins, 1976). Mojave-type desert towards the north has greater

temperature extremes than Sonoran Desert, and *Larrea tridentata* (creosote bush) and *Ambrosia dumosa* (burro weed) are common (Redmond, 2009). The Sonoran Desert exhibits a warmer temperature gradient. Thriving taxa here include *Fouquieria splendens* (ocotillo), *Justicia California* (chuparosa), and *Olneya tesota* (ironwood; Baldwin, 2002). Perrennials appear after rainfall, and some plants are large enough to mimic an open woodland, such as the iconic *Yucca bevifolia* (Joshua Tree).

Arboreal vegetation is reserved for the higher altitude environments where lower temperatures control lower evaporation rates. As with the Great Basin, pinyon-juniper woodlands prevail in subalpine environments and along stream courses (Anderson, 2003; Bailey, 2009; Baldwin, 2002). Low-lying riparian habitats support cottonwood (*Populus*) and willow *(Salix*; Baldwin, 2002). Fire has historically been neither important nor frequent for deserts, where drought and high temperature remain the more significant ecosystem stressors. The fuel load is generally low, with a lack of dense ground cover and trees that do not readily burn (Brooks and Minnich, 2006). However, the spread of invasive grasses in low to mid-altitude regions in the desert southwest has allowed increased wildfire proliferation. This may be a fundamental ecosystem change, with the introduction of a new, more frequent fire regime (Brooks and Matchett, 2006).

2.4 The Nature of the Pollen Record

2.4.1. Pollen as a Proxy: Preservation Dynamics and Sources of Bias

Plants produce pollen grains that possess distinctive patterns on their exine (i.e. outer layer) that help differentiation at the family, and often, genera, level. Palynology uses fossil pollen, often from lake or marine deposits, to elucidate past vegetation assemblages. It is best-preserved in anaerobic depositional environments. Changes in the pollen assemblage over time

are a proxy for vegetation change on the terrestrial landscape, assuming that plant preferences and adaptations are unchanged (Bennett and Willis, 2001; Birks et al., 2010). The production, transport, deposition and preservation of fossil pollen is a suite of dynamic processes that can shift over time. Many of the processes involved can alter with changing climate, and further complicate the depositional history of a basin and its site interpretation.

Pollen deposition also varies widely between taxa, as plants have different pollen production, transport, and reproductive adaptations. For example, *Pinus* spp. tends to output pollen grains a few orders of magnitude greater than other conifers. Its overrepresentation is commonplace in pollen records from around the world, such as the Pacific Northwest (Heusser and Shackleton, 1979), the North Sea and northern Atlantic (Mudie and McCarthy, 2006), and in marine sediments globally (Tzedakis, 2004). Arboreal pollen usually disperses via wind and air currents, a process that allows mixing of taxa into a "pollen rain" (Bennett and Willis, 2001). The majority of airborne pollen is deposited close to its source area, but turbulent eddies can also keep grains aloft for long periods, often overcoming gravity and allowing transport over great distances for small-sized, robust grains with air bladders (Sofiev et al., 2013). *Pinus* is transported further afield than the similarly bisaccate, but larger, *Picea* (spruce; Heusser and Basalm, 1977). Analysis of *Picea* transport dynamics supports this, documenting long transport distances in fluvial systems and preferential sinking (Wu et al., 2013), and a high fall speed due to its size when transported in the atmosphere (Theuerkauf et al., 2012). Transport via runoff poses risk of destruction to grains, particularly those that are thin-walled; *Populus*, for example, is often damaged during sample processing, if it first survives original deposition. Insect-pollinated annuals, perennials, and members of the Poaceae family tend to be deposited locally, often never leaving the host basin (Heusser, 1972).

In lake systems, site size influences the pollen rain received. Small lakes provide insight to the specific locality, while larger lakes receive more of the "background" pollen rain and are therefore a better regional representation (Bennett and Willis, 2001; Sugita, 1994). In literature, the meaning of "large" varies somewhat, ranging from a minimum diameter of 1 km (Hicks and Hyvärinen, 1999) to 1.5 km (Sugita, 1994). By comparison, marine pollen deposition is subject to larger-scale processes that influence the quality and diversity of the record, including direction of prevailing winds, ocean currents, location of biomes with pollen-producing plants, runoff and stream intermittency, and anaerobic conditions. Deposition is also largely point-source driven, with greater abundance and diversity close to major stream outlets (Mudie and McCarthy, 2006), but this may not correlate with the position of the associated biome on-shore (Hooghiemstra et al., 2006). In the eastern Pacific, fluvial systems deposit much of the pollen off the coast of Chile where prevailing westerlies have little influence (Montade et al., 2011), and similar processes operate off the North American West Coast during interstadials (Heusser and Basalm, 1977). Marine and terrestrial records are by nature differentially suited for gleaning paleoclimatic information. As Ch 3 shows, the decadal- and centennial-scale arid phases can be "muted" in lakes, not readily apparent from multi-proxy analysis. Meanwhile, the signal of hydroclimatic shifts is challenging to detect in marine cores.

For the design of new investigations using fossil pollen, site selection must be informed by 1) an understanding of these biases, and how marine and terrestrial settings can be dynamically different, and 2) clear and focused research questions appropriate to the record likely to be recovered. The importance of site knowledge also cannot be understated, including present vegetation, glaciation history, hydrology, drainage, and local geology. These aspects of the site inform the vegetation reconstruction from the resulting pollen counts, and help selection

of other proxy analyses to aid the broader paleoecological and paleoclimatological interpretation (e.g. Dean, 2010).

2.4.2. Current Data Quality and Availability

Fossil pollen investigations have been conducted along the California coastline since the 1970s, with several sites dating to at least MIS 5e. Pacific-derived moisture and storms, orographic uplift, and fluvial deposition are dominant processes in this sector of the North American coastline (Montade et al., 2011), resulting in fluvially-dominated pollen transport (Mudie and McCarthy, 2006). Pollen grain abundance is highest (up to 10,000 grains/cm^3) in the outflow of large river systems, such as the San Joaquin-Sacramento Rivers (Heusser and Basalm, 1977). Arboreal taxa such as *P. menziesii*., *Abies*, *Tsuga*, *Pinus*, and *Picea* are common in the Pacific Northwest, and persist southward to the central coast of California, but with greater influence of *Sequoia sempervirens*, *Quercus* and *Alnus. S. sempervirens* disappears from the record south of the Southern California Bight, with the increased presence of herbaceous pollen in regions with coastal sage scrub (Heusser and Basalm, 1977; Lyle et al., 2010, 2012).

Well-preserved lacustrine records are more common with higher effective moisture, including towards the northern part of the state, and mountain ranges. Great Basin lakes in the Temperate Desert ecoregion are more prone to desiccation and the record may have hiatuses (e.g. Owens Lake, Searles Lake); further south into the Tropical-Subtropical Arid ecoregion from this site, continuous lake records are scarce. Palynology data have been recovered from packrat middens (e.g. Holmgren et al., 2010), which are omitted from this review. Compared to marine records, lake basins have rates of pollen deposition that can be orders of magnitude greater and range from 10,000 to 1,000,000 grains/cm^3 (Hooghiemstra et al., 2006). Lacustrine assemblages

are most dependent on the surrounding watershed, often with a key taxon or taxa (e.g. *Juniperus*, *Quercus, Artemisia*) that are most sensitive to climate change preserved at that locality.

Table 2.2 catalogues both marine and terrestrial pollen datasets from California (Figure 2.2). Most of those listed are archived at the North American Paleoecological Database (NeotomaDB.org; Grimm, 2008; Grimm et al., 2013); a current search within California's borders yields 78 results. For inclusion in Table 2.2 and Figure 2.2, selection criteria were 1) at least 10 horizons of continuous pollen counts during at least one of three climatic events listed below, 2) an age model, and 3) at least 2 kyr of data. Sites are grouped into three major climatic shifts most relevant to this dissertation: the Holocene, the Last Glacial Maximum, and MIS 5e (130 - 120 ka). This results in 37 sites from Neotoma, 66% of all listed in Table 2.2. Pollen datasets that include the last interglacial come from offshore coring, the Coast Ranges of Northern California, and the Mojave Desert. Of the datasets shown in Table 2.2 and Figure 2.2, 73% are from the Holocene, highlighting that younger sites are more prevalent, better preserved, and more often studied.

2.5. Patterns of Change

2.5.1 The Record from the Last Interglaical (MIS 5e, 130 - 120 ka)

In several global localities, the record of Marine Isotope Stage 5e (130 – 120 ka) provides evidence of the last sustained, warm interglacial. What climate and vegetation cover changes did this impose on California's landscape? Available site data are listed in Tables 2.2 and 2.3. A successional pattern is evident in Northern California marine sites, where disturbance-loving *Alnus* increased prior to, or at, the onset of the last interglacial c. 130 ka. This was followed by an increase of *Sequoia sempervirens* and *Quercus* (Figure 2.3a&b; Heusser, 2000; Lyle et al., 2010). Southward, *Quercus* peaked 125 ka in the Santa Barbara Basin at slightly higher

Table 2.2. California sites in California dating to at least 2 ka, organized by three major climate events: the last interglacial MIS 5e, the Last Glacial Maximum (c. 26 – 19 ka), and the Holocene. Color-coding matches the ecoregions described in text and shown in Fig 2.1.
*Dataset available on neotomaDB.org. Note that site elevation is not readily available from the database.
†Instances where original source reports ages only in radiocarbon years, and have been converted to calendar year estimates using www.calpal-online.de/index.html with a ±50 error.

Site Name	Lat	Long	Elev. (m)	Age (ka)	Reference(s)
Sites dating to MIS 5e					
ODP 1019	41.678	-124.933	-989	160 - 0	Heusser (2000)
ODP 1018	36.989	-123.276	-2477	613.6 – 2.7	Lyle et al. (2001), Lyle et al. (2010), Heusser, L. E. (2000), Poore et al. (2000)
Clear Lake	39.058	-122.831	404	130 – 0	Adam et al., (1981); Adam and Robinson, (1988); Adam and West (1983)
ODP-893	34.28	-120.03	-577		Heusser (1998, 2000)
Owens Lake	36.381	-117.966	1067	180 – 10.2	Benson et al. (1996); Litwin et al. (1997); Woolfenden (2003, 1996)
Searles Lake	35.716	-117.330	494	240 – 0	Litwin et al. (1999)
Sites dating to MIS 2					
Grass Lake*	42.662	-122.167	1537	35.5 – 0.5	Hakala and Adam (2004)
Tulare Lake†	36.029	-119.800	54	29.6 – 21.5, 11.6 – 0	Davis (1999a)
F2-92-P3	35.623	-121.605	-803	32 – 2	Heusser (1998)
F2-P29	32.915	-119.737	-1475	40 – 3	Heusser (1998)
Nichols Meadow*	37.424	-119.579		22.1 – 0	Koehler and Scott Anderson (1994)
Tulare Lake*	36.052	-119.78		29.6 – 0	Davis (1999)
Swamp Lake, YNP	37.128	-119.070	1554	20 – 0	Smith and Anderson (1992); Street et al. (2012)
Caledonia Marsh	42.311	-121.907	1263	38 – 0	Adam (1985); Colman et al. (2004); Hakala and Adam (2004)
Tulelake	41.95	-121.48	1231	27 – 0	Adam et al. (1989); Hakala and Adam (2004)
Holocene Sites					
Sanger Lake	41.902	-123.647	1550	14.5 – 0	Briles et al. (2008)
Benicia State Park*	38.073	-122.193	0	2.2 – 0	Malamud-Roam and Ingram (2004)
Roe Island*	38.072	-122.033	0	2.2 – 0	Malamud-Roam and Ingram (2004); May, (1999)
Taylor Marsh*	38.938	-120.060	1896	2.5 – 0	West, G. J. (unpubl)
Browns Island*	38.042	-121.868	0	2.6 – 0	Malamud-Roam and Ingram (2004); May, (1999)
Mud Pond*	34.788	-120.587	21	2.8 – 0	Anderson et al. (2015)
Fish Lake*	41.264	-123.683	541	2.9 – 0	Crawford et al. (2015)
Ten Lakes*†	37.9	-119.533	2743	3.6 – 0	Anderson (1987)
Ogaromtoc Lake*	41.486	-123.541	596	3.4 – 0	Crawford et al. (2015)
Los Penasquitos Lagoon*	32.931	-117.253	0	3.9 – 0	Cole and Wahl (2000)
Las Flores Arroyo*	33.291	-117.461	6	4.0 – 0	Anderson and Byrd (1988)
Dinkey Meadow*†	37.000	-119.083	1683	5.6 – 0	Davis and Moratto (1988)

Site Name	Lat	Long	Elev. (m)	Age (ka)	Reference(s)
CA-HUM-558 Pilot Ridge*	40.662	-123.670	1250	5.1 – 0	Hildebrandt and Hayes (1983)
Abalone Rocks Marsh*†	33.956	-119.977	0	6.0 – 0	Cole and Liu (1994)
Elkhorn Slough*	36.825	-121.764	0	6.5 – 0	Dietz et al. (1988)
San Joaquin Marsh*†	33.658	-117.858	2	7.7 – 0	Davis (1992)
Flycatcher* Basin	41.015	-121.573	924	8.1 – 0	Anderson et al. (2008)
Tule Lake*	39.490	-123.036	1340	8.9 – 0	West (1993)
Tahquitz Meadow*	33.772	-116.661	2399	9.2 – 0.4	Wahl (2002)
Balsam Meadow*†	37.196	-119.260	2015	11.2 – 0	Davis et al. (1985)
Tioga Pass Pond*†	37.908	-119.258	3018	11.6 – 0	Anderson (1990)
Secret Valley Marsh*	40.572	-120.265	1359	10.6 – 0	West and McGuire (2000)
Lily Lake*	41.977	-120.210	2047	10.8 – 0	Minckley et al. (2007)
McMurray Lake*†	39.460	-120.649	2438	13.8 – 0	Edlund (1996)
Cedar Lake*	41.207	-122.497	1737	12.3 – 0.1	West (1989)
Bunker Lake*	39.054	-120.386	1995	12.6 – 0	Edlund (1996)
Siesta Lake*	37.851	-119.660	2430	12.7 – 0	Brunelle and Anderson (2003)
Barrett Lake*†	37.560	-119.008	2816	15.9 – 0	Anderson (1990)
Exchequer Meadow*†	37.000	-119.833	2219	16.1 – 0	Davis and Moratto (1988)
Bluff Lake*	41.347	-122.560	1926	13.4 – 0.3	Mohr et al. (2000)
Mumbo Lake*	41.191	-122.511	1860	14.0 – 0	Daniels et al. (2005)
China Camp*†	38.008	-122.493	0	18.3 – 0	Malamud-Roam and Ingram (2004)
Lilypad Lake*	36.982	-118.994	1982	15.7 – 0	Edlund (1996)
Swamp Lake*†	37.95	-119.817	1554	19.0 – 0	Smith (1989)
Little Willow Lake*	40.412	-121.390	1829	16.2 – 0	West (2003)
Bolan Lake	42.025	-123.458	1638	17 – 0	Briles et al. (2005)
V1-80-P3	38.425	-123.796	-1600	16 – 1	Heusser (1998); Heusser and King (1988)
Starkweather Pond†	37.663	-119.068	2438	12.9 – 0	Anderson (1990)
Barrett Lake	37.596	-119.008	2816	13.8 – 0	Anderson (1990)
Black Lake	37.816	-118.578	1962	13.4 – 0	Batchelder (1970)
Mono Lake†	38.008	-119.026	1945	13.5 – 0	Davis (1999b)

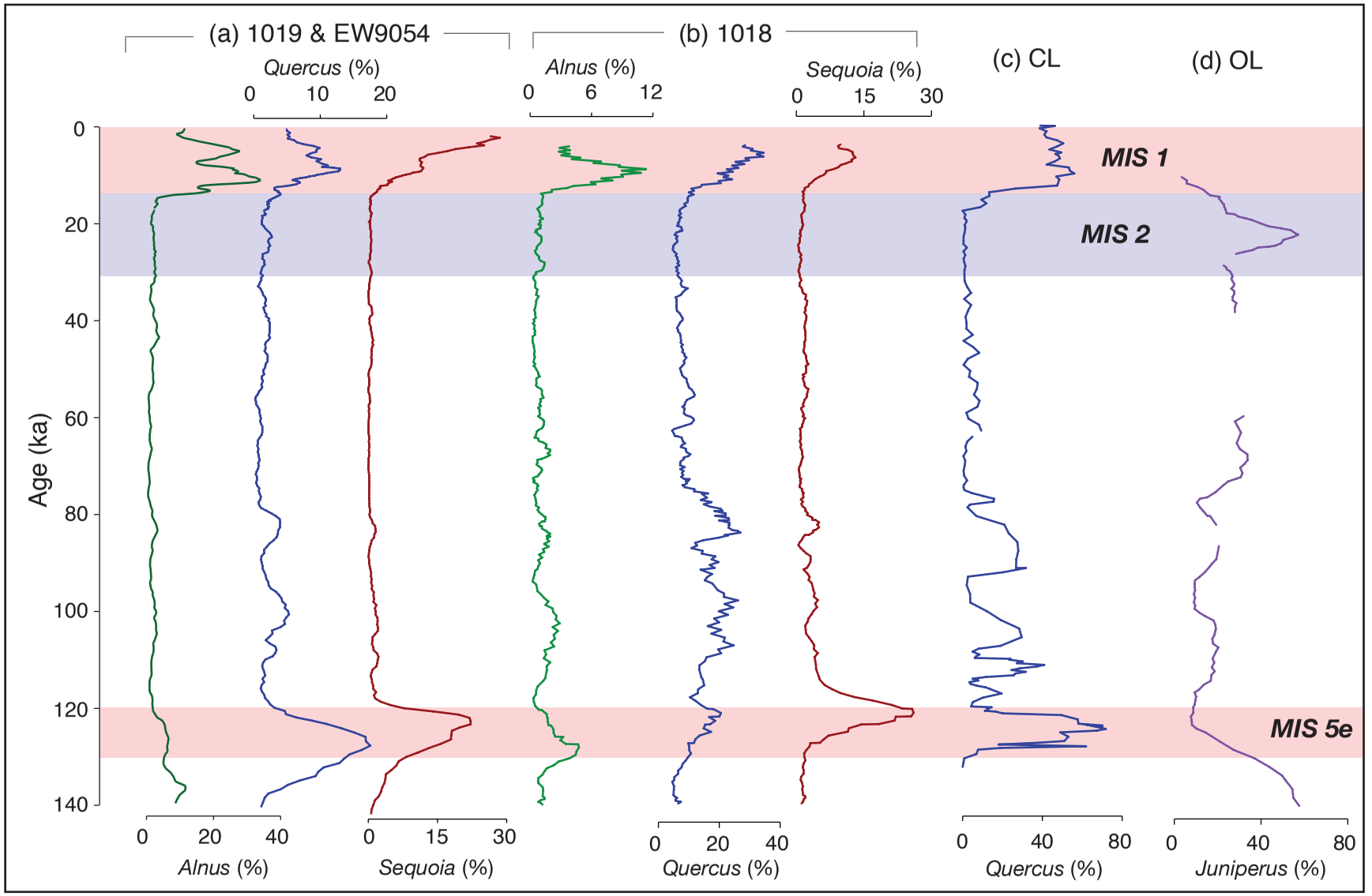

Figure 2.3. Pattern of ecosystem change to the last interglacial at two marine and two terrestrial sites in California. Key taxa from pollen data shown. 1019 & EW9054 data were combined in Heusser et al., 2000. Data arranged north-to-south from left; see Figure 2.2 for site locations. CL = Clear Lake and OL = Owens Lake.

Table 2.3. Summary of regional climate responses, derived from palynological records during the last interglacial (MIS 5e), and MIS 2. Ecoregion domains are subdivided into physiographic region, which notes sites key to regional interpretation, and 1. paleoclimatic conditions, and 2. important taxa upon which this interpretation is based.

	MIS 5e	LGM
Mediterranean Sites	**Marine NorCal (sites 1018, 1019)** 1. Wet and high amount of initial disturbance 2. sequence of *Alnus-Quercus-S. sempervirens* at 1018 and *Alnus-S. sempervirens-Quercus* at 1019	**Marine NorCal (sites 1018, 1019)** 1. relatively dry 2. herbs and shrubs expand
	Coast Ranges (Clear Lake) 1. warm and dry 2. *Quercus* more prevalent, and tied to marine $\delta^{18}O$ signal	**Coast Ranges (Tule Lake, Clear Lake)** 1. cool and wet at Clear Lake; dry and saline at Tule Lake 2. *Pinus*-dominated forest expansion at Clear Lake; *Sarcobatus*, herbs and shrubs abundant at Tule Lake
	western Transverse Ranges (ODP 893) 1. warm and dry 2. *Quercus* increased up to 30-35% of total pollen record	**Central Coast + western Transverse Ranges (893, F2-92-P3, F2-P29)** 1. moist and cool, with rainfall increase at LGM 2. assemblage of *Pinus*, Cupressaceae, Pinaceae,Taxodiaceae, Taxaceae and herbs; reduced *Quercus*; expanded range for *Homo sapiens cognatus*
		Sierra Nevada (Swamp Lake, Nichols Meadow) 1. cold and dry 2. *Quercus* declined and expansion of herbs and *Artemisia*-dominated steppe
		Central Valley (Tulare Lake) 1. cool and dry 2. xeric woodland assemblage at elevation (*Pinus-Quercus-Juniperus*); halophilic taxa local to basin (Cupressaceae, *Sarcobatus*, *Artemisia*)
Tropical-Subtropical Desert	**E. Sierra Nevada (Owens and Searles Lakes)** 1. rapid onset and drying 2. Arboreal taxa universally decreased, most strongly at Owens Lake: *Juniperus* contracted; lowlands had assemblage of *Ambrosia*, Chenopodiaceae, *Purshia* [bitterbrush], Asteraceae, *Ephedra*, and Fabaceae. At Searles Lake, TCT rapidly declined at onset while shrubs and herbs expanded.	**E. Sierra Nevada (Owens Lake)** 1. cold 2. *Artemisia* expansion, followed by *Juniperus*, with *Purshia*, *Artemisia*, *Atriplex*, and *Yucca brevifolia*. Decline of *Pinus.*
Temperate Great Basin		**Modoc Plateau (Tulelake, Caledonia Marsh, Grass Lake)** 1. dry and cold 2. widespread steppe, with reduced *Pinus* and expansion of Chenopodiaceae, *Ambrosia, Artemisia,* forbs

percentages, with no accompanying rise in *Alnus* nor *S. sempervirens*. This illustrates the north-south precipitation gradient in California, and the greater prevalence of a mosaic of oak woodland, chaparral, and sage scrub southward (Heusser, 1992).

The greatest *Quercus* increase to nearly 80% was documented at terrestrial site Clear Lake (Figures 2.2, 2.3c; Adam et al., 1981; Adam and Robinson, 1988). In both the Santa Barbara Basin and Clear Lake record, *Quercus* is invoked as a temperature proxy (Heusser, 1998), with its percent changes shown to be strongly correlative to the marine $\delta^{18}O$ record (Adam and West, 1983). The other two terrestrial pollen sites dating to the last interglacial are Mojave desert sites, where decreases in arboreal taxa occurred, most notably *Juniperus* at Owens Lake (Figure 2.3d; Litwin et al., 1999; Woolfenden, 2003).

2.5.2 The Record from the Last Glacial Maximum (26 - 19 ka)

MIS 2 is a global event that spans 29 – 14 ka (Lisiecki and Raymo, 2005), with the Last Glacial Maximum (LGM) is generally attributed to 26 - 19 ka (Clark et al., 2009). Sites dating to a minimum of 21 ka are considered here (Table 2.1). While cold conditions prevailed along the continental margin, precipitation conditions varied due to the high amount of topographic variability, and storm tracks that shifted along a north-south gradient. Mountain glaciation dominated the North American West Coast, and was often subject to regional climatic effects that caused the maximum extent of local glaciers to be asynchronous with continental ice sheet volume (Hughes et al., 2013; Thackray et al., 2008).

Herbaceous and shrubby areas expanded their range throughout Central and Northern California, largely replacing arboreal taxa. This paleoenvironment was prevalent at northern marine sites, the Modoc Plateau in northeastern California, the Sierra Nevada, and Central California (Table 2.3). Anomalously, Clear Lake is inset in this suite of paleoclimatic sites, and

showed *Pinus* expansions during the last glacial, with conditions interpreted to be cool (Adam et al., 1981). Southern California sites had a different response, with moist conditions during the LGM supporting forest expansion. Reduced *Quercus* indicates colder temperatures, while *Pinus*, Cupressaceae, Taxodiaceae, and Taxaceae increase in the Santa Barbara Basin (Heusser 1992). *Juniperus* expanded downslope in the Owens Valley (Figure 2.3d), though this taxon has been interpreted as a temperature indicator that expands during glacials (Koehler and Anderson, 1995; Woolfenden, 2003). During the LGM, *Juniperus* is associated with xeric taxa (e.g. *Yucca*, *Artemisia*), suggesting dry conditions overall.

2.5.3. The Holocene (10 – 0 ka)

Holocene pollen records are more abundant and often higher-resolution than well-preserved, continuous records dating to MIS 5e, and have thus illuminated finer-scale changes in temperature and moisture over the past 10 ka. Of 37 datasets extracted from Neotoma that satisfy the criterion of data spanning at least 2 ka, 92% are Holocene-age sites. As the Holocene sites represent, in aggregate, a greater number of sites often analyzed at higher resolution than older records, I have parsed the summary of their hydroclimatic history into Early (c. 10 - 7.5 ka), Middle (7.5 - 3 ka), and Late Holocene (3 - 0 ka; Table 2.4).

Although relatively warmer with more abundant forests statewide, prevailing moisture during the Early Holocene exhibited a dipole similar to the LGM. Drier conditions were present in the north, particularly in the Klamath Mountains, Sierra Nevada and Central Valley, while the Santa Barbara Basin and sites located southward favored moister-than-present conditions. Conditions during the Middle Holocene were relatively stable for several millennia. Aridity was widespread in the Sierra Nevada and southern California, while marine and northern sites underwent gradual change. For example, Klamath Mountain sites exhibited a slow transition

Table 2.4. Summary of regional climate responses, derived from palynological records during the Holocene. Ecoregion domains are subdivided into physiographic region, and three stages of the Holocene for terrestrial and high-resolution sites. The Early Holocene spans 10 – 7.5 ka, Middle Holocene 7.5 – 4 ka, and Late Holocene 3 – 0 ka. Text in cells notes sites key to regional interpretation, and 1. paleoclimatic conditions, and 2. important taxa upon which this interpretation is based. See Table 2.2 for references to specific papers reporting palynological data.

	Holocene		
Mediterranean Sites	**Marine NorCal (site 1018)** 1. EH moist; coastal fog present 2. *Alnus-Quercus-S. sempervirens* sequence occurred at onset; gradual decline of *Pinus*		
	Marine SoCal (ODP 893, F2-92-P3, V1-80-P3, F2-92-P29) 1. disturbance marking interglacial onset 2. *Alnus* increased at Early Holocene onset; *Pinus* and Cupressaceae declined while *Quercus* and herbs rose steadily throughout Holocene		
	Early Holocene	**Middle Holocene**	**Late Holocene**
	Central Valley (Tulare Lake) 1. warm and arid 2. xeric woodland assemblage at elevation (*Pinus-Quercus-Juniperus*); halophilic taxa local to basin (Cupressaceae, *Sarcobatus*, *Artemisia*)	**Central Valley (Tulare Lake)** 1. warm and arid 2. *Pinus* declined and *Typha, Sparganium,* and Cyperaceae encroached as shoreline receded	**Central Valley (Tulare Lake)** 1. cool and wet until 1 ka; aridity after 1 ka 2. *Pinus* and *Quercus* present until 1 ka; expansion of Chenopodieaceae-*Amaranthus*
	western Transverse Ranges (ODP 893) 1. EH cool and wet	**western Transverse Ranges (ODP 893, F2-92-P3, F2-P29)** 1. warm and arid	**NorCal (Benicia, Roe, Browns, China Camp)** 1. highly variable conditions
	Sierra Nevada (Swamp Lake and Tioga Pass Pond) 1. dry and warm 2. open montane chaparral with low *Abies* and *Tsuga*; expansion of *Artemisia, Sarcobatus,* Cyperaceae, Asteraceae, Poaceae	**Sierra Nevada (Swamp Lake, Balsam Meadow)** 1. MH moist and cool 2. *Abies* increase and *Quercus* upslope migration; Rosaceae decline	**Sierra Nevada (Balsam Meadow)** 1. generally moister than Mid-Holocene, punctuated by dry events 2. *Artemisia* steppe, expansion of *T. mertensiana*
	Klamath Mountains (Sanger, Bolan, Bluff, Cedar, Mumbo) 1. wet c. 10 ka, followed by EH drying 2. coniferous taxa (*Pinus, Abies*, *Tsuga*) decline in favor of *Quercus* expansion	**Klamath Mountains (Sanger, Bolan, Bluff, Cedar, Mumbo)** 1. relatively cool and moist 2. *Abies* expansion	**Klamath Mountains (Sanger, Bolan, Bluff, Cedar, Mumbo)** 1. Highly variable conditions throughout LH, and between sites
	SoCal (Tahquitz Meadow) 1. moist conditions 2. *Hypericum* prevalent	**SoCal (Tahquitz Meadow)** 1. relatively dry 2. *Hypericum* decline and *Populus* expansion	**SoCal (Tahquitz, San Joaquin, Abalone)** 1. terrestrial sites variable; maritime site moist

	Early Holocene	Middle Holocene	Late Holocene
Tropical-Subtropical Desert	**E. Sierra Nevada (Mono and Owens Lakes)** 1. lower effective moisture, warm 2. expansion of xeric taxa, e.g. Chenopodiaceae-*Amaranthus* and *Sarcobatus*	**E. Sierra Nevada (Mono Lake)** 1. moist	
Temperate Great Basin	**Modoc Plateau (Caledonia Marsh)** 1. wet and warm 2. *Pinus* and arboreal taxa flourished	**Modoc Plateau (Caledonia Marsh)** 1. aridity until 6 ka, subsequent return of moisture 2. *Juniperus* woodland with increased herbaceous taxa; coniferous forest expanded 6 ka	

towards wetter conditions from 8 - 3 ka (Briles et al., 2008) while ODP 1019 sea surface temperatures gradually decreased by 1˚C (Barron et al., 2003). A characteristic of the Late Holocene has been its widespread variation, often attributed to a higher degree of El Niño Southern Oscillation (ENSO) variability since 3 ka (Kirby et al., 2014; MacDonald et al., 2016). Sierra Nevada sites, for example, have been generally moist, punctuated by dry events lasting several decades or centuries. The Medieval Climate Anomaly (1 - 0.7 ka) and Little Ice Age (0.7 - 0.16 ka) have a documented hydroclimatic and sea surface temperature response statewide. These are centennial-scale events at a finer scale than the scope of this review, however, and are examined further in Ch 5 with the Lower Bear Lake record.

2.6 Summary

2.6.1 Review Questions

1) How does the terrestrial palynology record differ from marine studies?

Many of the records that date to the last interglacial MIS 5e were marine. California's north-south precipitation gradient, glaciation in the Sierra Nevada, and past megadroughts and arid states do not favor continuous lake deposition; long terrestrial sites are therefore rare. Marine patterns for interglacials (e.g. MIS 5e and the Holocene) towards the north tend to be successional, while documenting change at terrestrial sites across longer timescales has largely depended on an indicative temperature-proxy taxon (e.g. *Quercus*, *Juniperus*). Terrestrial sites have potential to be higher resolution, with more rapid sedimentation and pollen focusing in individual basins. This is particularly true for the Holocene, where detailed palynological studies have shown distinct centennial-scale climate events such as the Medieval Climate Anomaly and Little Ice Age, and decadal-scale phenomena such as ENSO.

2) Are there identifiable ecological patterns to past climate change?

In coastal Northern California, currently one of the wettest portions of the state, interglacial periods (MIS 5e and the Holocene) in marine records had the abovementioned distinctive signature with early and rapid *Alnus* colonization. Inland (e.g. Clear Lake) and southward (e.g. Santa Barbara Basin), *Alnus* and *S. sempervirens* were not present, and *Quercus* became more prevalent with enhanced aridity. Throughout the state and all climatic events examined, the expansion of herbs and shrubs — particularly *Artemisia* as an indicator of steppe — signaled long-term dry conditions. Conversely, the expansion of coniferous forest occurred under wet conditions. Higher moisture availability cannot be inferred from high arboreal or *Pinus* counts alone, examining the arboreal assemblage with *Pinus* is key. The combination of *Abies*, *Pinus*, Cupressaceae, Taxadiacaeae, Taxaceae and reduced *Quercus* has generally indicated enhanced moisture.

3) Is MIS 5e an analogue for the Holocene?

A direct comparison of MIS 5e and the Holocene conditions in California from available pollen data is problematic, largely due to varying resolution of studies between the two time periods, and age model uncertainties. While marine sites 1018 and 1019 followed similar successive "patterns" at interglacials, the most-sensitive taxa shown in Figure 2.3 for four sites often do not replicate the same abundance. Studies of non-pollen proxies have shown disparity between both interglacials: Holocene summer insolation was lower and declining than peak MIS 5e values (Laskar et al., 2004). The eastern Pacific has also shown a combination of high productivity and warm SSTs during the Holocene that were unique, and not replicates of MIS 5 conditions (Lyle et al., 2001).

2.6.2 Best Practices for Palynological Data

As data are increasingly generated and used to inform conservation and climate models, more sites will be available to examine these questions. Digital data availability is key to streamline this analysis, and to study the relationships between geographically disperse sites. I recommend Neotoma data archival as a best-practice for palynologists working on the West Coast, which is actively managed (Grimm et al., 2013), and increasingly integrated with mobile apps (e.g. Flyover Country; Myrbo, 2015) and R code packages to extract data (Goring et al., 2015).

3. Insolation and North Atlantic Climate Forcing in alpine Southern California since 125 ka

3.1 Abstract

Paleoclimatic records in the North American West have increasingly shown that solar radiation shifts and rapid change in the North Atlantic were important influences on past temperature and moisture regimes. However, their impact on terrestrial climate in Southern California over long timescales remains unclear. A new, multi-proxy record from Baldwin Lake in alpine Southern California spanning 125 – 20 ka shows that local summer insolation directly influenced lake temperature and productivity in MIS 5 (125 – 71 ka). From 60 – 57 ka, hydrological state changes and events occurred in California and the U.S. Southwest, though the pattern of response varied geographically. Intermediate, less variable levels of winter and summer insolation followed during MIS 4 – 3 (71 – 29 ka), which maintained moist conditions in Southern California that were interrupted with Dansgaard-Oeschger (D-O) events. Paleoclimate records in the region suggest that D-O events were times of enhanced sea surface temperatures (SSTs) and terrestrial aridity throughout the Southwest and Southern California, while Great Basin sites had a more varied response. Ice age conditions of low temperatures and reduced evaporation are widespread during MIS 2, though there is increasing evidence for moisture extremes 29 – 20 in Southern California. This record shows that prior to the last ice age, Southern California climate was impacted by 1) orbital-scale radiative forcing, and 2) rapid North Atlantic temperature perturbations.

3.2. Introduction

Throughout the U.S. Southwest and California, model projections for the 21st century suggest a response to increased radiative forcing that will manifest with enhanced temperatures, aridity, and climate variability (Overpeck et al., 2013). These projections prompt important questions about regional sensitivity to climatic change: what forcing mechanisms exert the most change? What teleconnections exist between regions? How do anticipated magnitudes of regional climate change compare to past variations? These questions are especially important in California, the adjacent Great Basin and Southwest, regions that are already water-stressed and increasingly populous (Georgescu et al., 2012).

Retrospective studies are crucial for deepening our understanding of large-scale climate dynamics and teleconenctions, and assessing the potential range of temperature and hydrological variability. Recent studies have documented long-lasting droughts in the West during the Late Quaternary (e.g. Brunelle and Anderson, 2003; Heusser et al., 2015; MacDonald and Case, 2005; Mensing et al., 2013), most of which were associated with warm intervals (Woodhouse et al., 2010). Conversely, extreme and long-lasting wet events were also a feature of West Coast climates (e.g. Bird and Kirby, 2006; Kirby et al., 2013, 2012). These prolonged hydroclimatic events have no analogue in the past 150 years of instrumental records.

A growing body of climatic records from the U.S. Southwest and Coastal Southwest suggests regional sensitivity to a variety of climate drivers that include an atmospheric-oceanic teleconnection with the North Atlantic (Asmerom et al., 2010; MacDonald et al., 2008; Oster et al., 2014; Reheis et al., 2015; Wagner et al., 2010), Pacific Ocean (Ingrid L. Hendy and Kennett, 2000; Heusser, 1998; Lund and Mix, 1998) boreal insolation (Lachniet et al., 2014), and migrating storm tracks (Garcia et al., 2014; Kirby et al., 2006; Owen et al., 2003). Offshore

marine cores have documented long histories through several Marine Isotope Stages (MISs), though the temporal resolution of records prior to MIS 2 is often low, and the response dynamically different from terrestrial sites (Heusser and Basalm, 1977; Hooghiemstra et al., 2006). The longer-term climate history of terrestrial Southern California throughout past glaciations and multiple MISs is lesser-known, compared to abundant studies on the Holocene and Last Glacial (MIS 2).

A newly-acquired core from Baldwin Lake, California in the San Bernardino Mountains (SBM) that dates to 125 – 10 ka provided insight to the long-term temperature and hydrology of Southern California, and associated climatic drivers. We use this material, in combination with other records from the Great Basin and Southwest, to address the following questions: What environmental changes occurred at the site over the past ~125 – 20 ka? How does the record of climatic variability at Baldwin Lake compare to other California, Great Basin and Southwestern sites? Finally, how did orbital-scale and millennial-scale climatic drivers influence the paleoenvironmental changes observed at the site, and throughout the broader region?

3.3. Setting

The SBM are part of the Transverse Ranges surrounding the Los Angeles Basin, with some of the highest elevation peaks in Southern California. They form a barrier between the interior Mojave Desert and U.S. Southwest, and the summer-dry, winter-wet Mediterranean conditions of the U.S. Coastal Southwest. The lateral strike-slip San Andreas and Mill Creek Faults bound either side of the range. Granitic rocks dating from the Triassic to Cretaceous dominate the range (Morton and Miller, 2006), with other allocthonous sedimentary terranes of Precambrian and Mesozoic age (Owen et al., 2003). High relief valleys and slopes are often covered with Quaternary deposits, including alluvium, talus, and fanglomerates.

Baldwin Lake (34.275˚N, 116.8˚W) lies at an elevation of 2040 m in the Big Bear Valley of the SBM, approximately 160 km east of the Pacific coastline (Figure 3.1). It is one of two major lake basins in the valley with a 79 km^2 watershed, and an intermittent lake (Big Bear Lake TMDL Task Force, 2012). To the west, the Big Bear Lake watershed is 96 km^2, and the basin supported a lake throughout the Holocene (Kirby et al., 2012; Paladino, 2008). Sugarloaf Mountain to the south (3033 m) is the source of most sedimentation into the Baldwin basin, with the 14 km^2 Sugarloaf fan (Flint and Martin, 2012; Leidy, 2006). Smaller-scale faults occur throughout Big Bear Valley, including a thrust fault <1 km east of Baldwin Lake on Nelson Ridge (Flint and Martin, 2012). During the last ice age (MIS 2), glaciation occurred at the highest elevations of the Transverse Ranges at Mount San Gorgonio (3,506 masl), with moraines still evident on the landscape (Owen et al., 2003) and in small, high-altitude lakes (e.g. Dry Lake; Bird and Kirby, 2006).

Mediterranean winter-wet and summer-dry conditions prevail throughout the SBM and Southern California, modulated by upwelling and currents on the North American Pacific margin. The configuration of the North Pacific High and North American Low, and westerly winds, drive this strong precipitation seasonality (Barron et al., 2003; Cayan and Peterson, 1989). Seasonal migration of the Polar Jet Stream (PJS) brings Pacific-derived moisture in the winter months, and Southern California's yearly precipitation averages 70-100 cm (Owen et al., 2003). Annual precipitation averages are comparatively higher in the mountains at ~220 cm/yr in Big Bear Valley (U.S. Climate Data, 2016), largely derived from North Pacific-derived winter storms (Owen et al., 2014; Wise, 2010). Other precipitation sources include orographic uplift, lateral snow drift (Minnich, 1984), and summer storms due to convection and the occasional dissipating

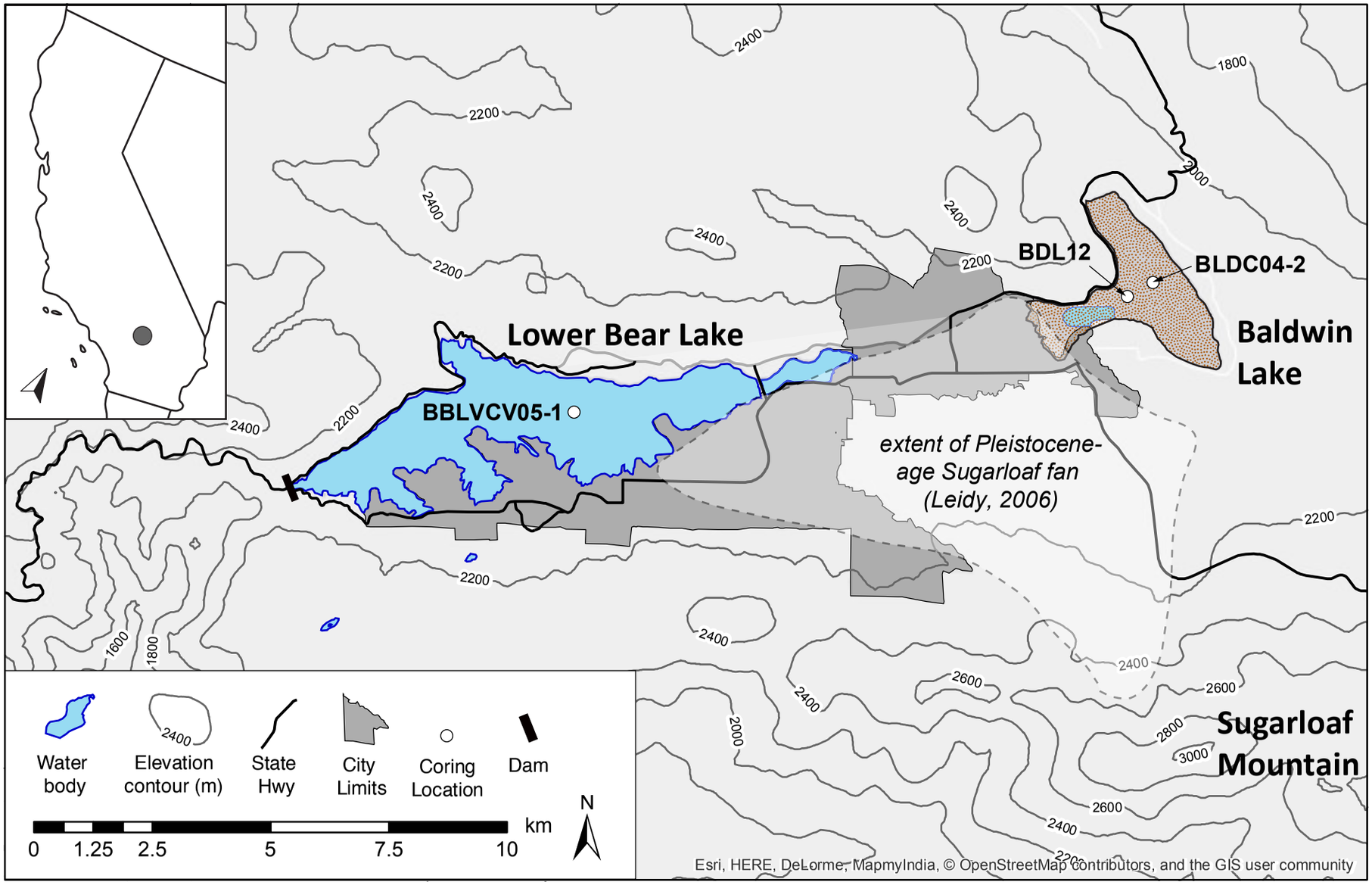

Figure 3-1. Map of Big Bear Valley, San Bernardino Mountains, California. Cores taken in the Valley include Lower Bear Lake (BBLVCV05-1; Kirby et al., 2012), Baldwin Lake (BDLC04-2; Kirby et al., 2006; Blazevic et al., 2009) and a second core from Baldwin Lake (BDL12; this study). Countour interval = 200 m.

late-summer tropical cyclones (Tubbs, 1972). Average July high temperature at Big Bear City is 27.2 ˚C, and January's average high is 8.3 ˚C (U.S. Climate Data, 2016).

3.4. Materials and Methods

3.4.1. Core recovery and Initial Core Description (ICD)

Baldwin Lake was re-cored August 2012 with a CME-95 truck-mounted hollow stem auger drill. We targeted the basin depocenter (34˚16.56633', -116˚48.61182'), located slightly west of the BLDC04-2 core site (Figure 3.1; Kirby et al., 2006). We refer to this sequence of cores as BDL12, which consisted of overlapping 2.5 foot sections from two separate holes. BDL12 is archived at UCLA. Cores were split at UCLA in 2013, then photographed and described at the Limnological Research Center (LRC) in 2014, following conventions for Initial Core Description (ICD; Schnurrenberger et al., 2003).

3.4.2. Chronologic control

Seven wood and charcoal samples from the upper 8 m of BDL12 (Table 3.1) were dated with accelerated mass spectrometry (AMS) radiocarbon methods. These macrofossils were preferable to the aquatic plant material, stems and bulk dates of the BLDC04 chronology (Kirby et al., 2006; Marty and Myrbo, 2014; Zimmerman and Myrbo, 2015). For the lower sections of core, Infrared Stimulated Luminescence (IRSL) single-grain analysis was conducted on two sections of the sequence with a high sand fraction (Buylaert et al., 2009; Rhodes, 2015). IRSL was applied to 150-175 μm K-feldspar grains, a technique increasingly used in Southern California, where quartz demonstrate low sensitivity in many locations (Garcia et al., 2014; Lawson et al., 2012). Four 20-cm sections of core were removed with a handsaw under luminescence laboratory lighting conditions, and a ~1.5 cm diameter cylinder of sediment extracted from the interior for IRSL dating. Once disturbed, these sections were not further

analyzed. Preparation procedures, measurement at UCLA, and analysis followed Rhodes (2015). Fading measurements were used to correct both the IRSL signal measured at 50˚C and the post-IR IRSL signal at 225˚C, which demonstrated mean g-values of 0.03 and 0.015 respectively. Dose rates were calculated using ICP-MS (for U, Th) and ICP-OES (for K) determinations at SGS, Vancouver, Canada.

We modeled age and depth with Bacon 2.2 (Blaauw and Christen, 2011) software, using default prior settings and the input of ^{14}C dates, luminescence dates, and five tie-points (Table 3.1, Figure 3.2a). Above the youngest radiocarbon date at 152 cm, the age and history of the modern lake surface is uncertain, and thus Bacon 2.2 extrapolated the model between 0 – 152 cm with no constraints. For the lower 8 – 27 m of core, we employ visual curve matching (Groot et al., 2014) between local summer insolation and BDL12's percent organic content proxy data. The two datasets shifted in tandem 40 to 20 ka in the already-dated section of BDl12. We believed that the correlation between primary productivity and organic content (described below) persisted throughout the sequence, illustrating the lake's rapid response to changes in local insolation. Record "tuning" with visual curve matching is often used in the absence of other chronologic data or techniques (e.g. Tzedakis et al., 2001), or to supplement existing dates (e.g. Cacho et al., 1999). Tie-points with a 2 kyr error (e.g. Mahan et al., 2014) were established between maxima and minima of summer insolation at 34˚N over the last 128 kyr (Laskar et al., 2004), and corresponding maxima/minima from a loess smooth of organic content (Figure 3.2b).

3.4.3. Sedimentary Analyses

Initial magnetic susceptibility data were collected at UCLA with a Bartington MS2e sensor, and replicated at LRC. Finer-resolution magnetics were recorded with a GeoTek Multi-Sensor Core Logger at LRC in 0.5-cm intervals. Loss-on-ignition (LOI) was conducted at 1-cm

Table 3.1. AMS radiocarbon dates, infrared-stimulated luminescence dates, and tie points used for BDL12's age model. Mean age from Bacon 2.2 (based upon IntCal13; Reimer et al., 2013) is used for the calendar-years age model; see text and Figure 3.2 for details.

Accelerated Mass Spectometry Radiocarbon Dates *W. M. Keck Carbon Cycle AMS Radiocarbon Lab, UC-Irvine*				
Sample No.	**Depth (cm)**	**Material**	**Raw ^{14}C Age**	**Approximate Calendar Age**
UCI-121791	152	charcoal	10,010 ± 320	~11,868
UCI-124533	262	charcoal	21,150 ± 810	~24,307
UCI-124534	389	charcoal	25,170 ± 280	~29,339
UCI-121792	440	pine cone piece	25,990 ± 140	~30,400
UCI-124535	529	charcoal	27,240 ± 180	~31,474
UCI-124536	745	charcoal	35,710 ± 790	~40,417
UCI-121793	815	twig	41,010 ± 700	~43,997
Post-IR Infrared Stimulated Luminescence dates *Earth and Planetary Sciences Dept., UCLA*				
Sample No.	**Depth (cm)**	**Material**	**50˚C IRSL Signal (cal yr BP)**	**225˚C IRSL Signal (cal yr BP)**
J0395	2075	massive silt	88,500 ± 6,200	87,800 ± 6,100
J0396	2173	clayey silt	55,800 ± 5,400	44,900 ± 3,900
J0397	2570	sand	117,000 ± 8,000	109,000 ± 8,000
J0398	2700	sand	136,000 ± 10,000	124,000 ± 8,000
Tie-Points for orbital tuning				
	Depth (cm)			**Age (cal yr BP)**
	1585			72,000 ± 2000
	1748			83,000 ± 2000
	2042			95,000 ± 2000
	2212			105,000 ± 2000
	2432			116,000 ± 2000

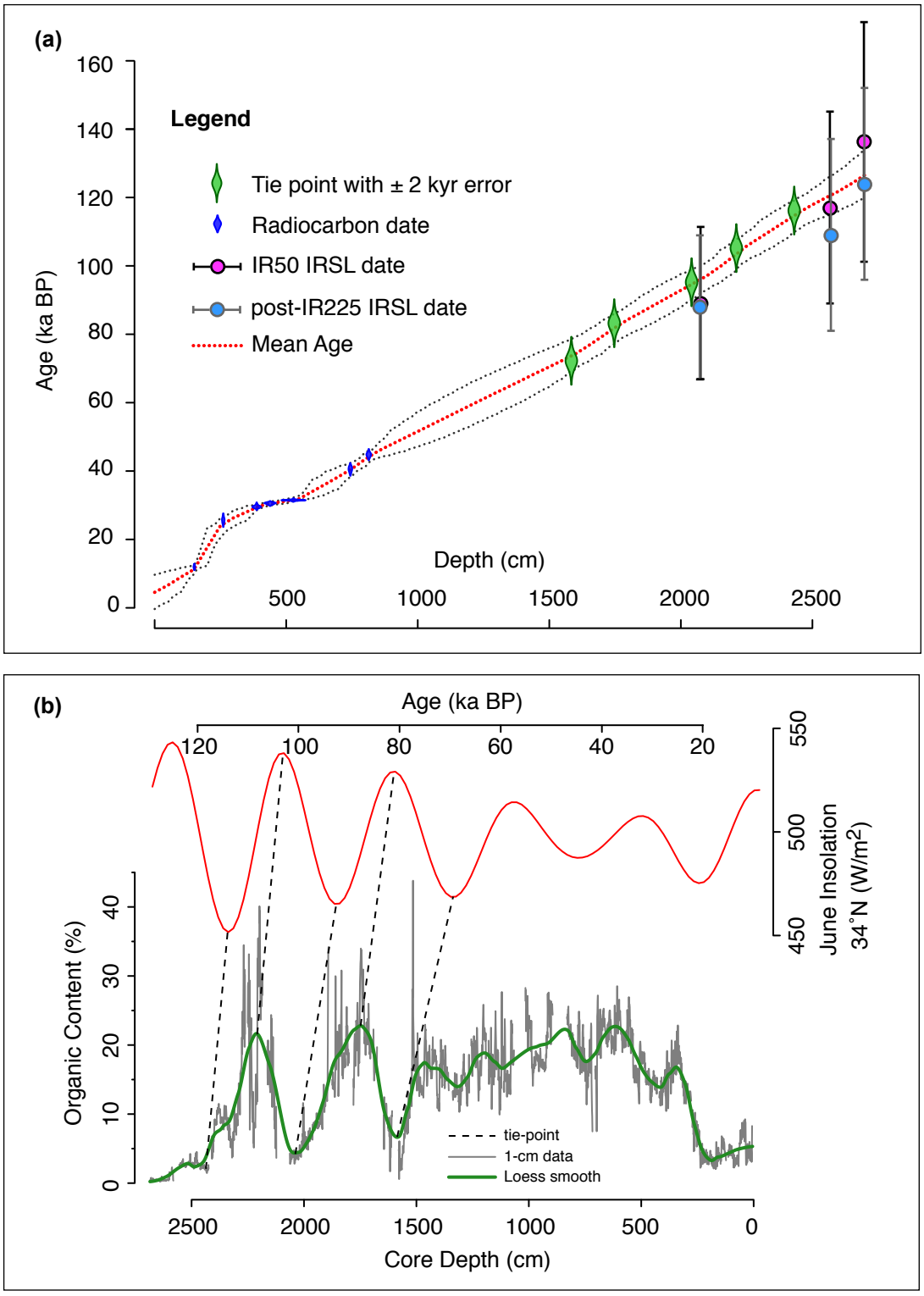

Figure 3.2. a) Bacon 2.2 age-depth model from radiocarbon and lumninescence dates, and tie-points (Table 1). b) Tie-points established between insolation peaks and troughs from summer insolation values at 34˚N (Laskar, 2004), and corresponding maxima amd minima from a loess smooth of high-resolution organic content data in BDL 12.

intervals throughout BDL12 to determine the organic and carbonate content of the sediment (Dean, 1974; Heiri et al., 2001). Organic content was determined from mass lost after 1-hour burns at 550˚C in a muffle furnace, and carbonate content was calculated after subsequent 1-hour burns at 950˚C. Core density was calculated from the dry weight values of the 1-cm^3 LOI samples. Bulk inorganic values are the remaining percent of core after percent organic content and carbonate content (both determined from the LOI analysis) were subtracted. The high-resolution LOI and MS data were used to determine the correlation between core sections. Mass accumulation rates (MARs) were calculated by multiplying a horizon's dry density by its sedimentation rate derived from the age model (Rack et al., 1995).

Grain size sampling was initially done at 50 cm intervals (Silveira, 2014), with later sampling that targeted the basal coarse-grained facies, and the slowly-deposited MIS 2 interval. Samples (n=93) were digested in 30-35% H_2O_2 to remove organics, 1N HCl to remove carbonates, and 1M NaOH to remove biogenic silicates, with intermittent centrifuging. Analyses were performed on a Malvern Mastersizer 2000 laser diffraction grain size analyzer. The results were combined with high-resolution grain-size data from core BLDC04 (Blazevic et al., 2009) after re-adjusting BLDC04's absolute depths (see Supplemental Data). We reported the grain size mode (μm) here, after averaging values at 25-cm intervals for the section above 15 m, and at 50-cm intervals for the section spanning 15 – 27 m. This was done to reduce noise and variable sampling resolutions throughout the ~27 m sequence. X-ray fluorescence (XRF) values were taken with a portable Innov-X Analyzer at 5 cm intervals along a split core surface that was lined with Ultralene film. Elements reported here include titanium (Ti), iron (Fe), calcium (Ca), potassium (K), and manganese (Mn).

3.4.4 Biogenic Silica (BSi)

We selectively analyzed biogenic silica (BSi) throughout the core in order to determine if organic content changes were driven by lake productivity, or terrestrial biomass. BSi wet-alkaline extraction followed the methods of Conley and Schelske (2002). Samples (n=32) from each of the Marine Isotope Stages were analyzed to characterize the relationship between organic content and BSi in the various core facies.

3.5. Results and Proxy Interpretation

3.5.1 Age Model

Age results from BDL12 range from 125 – 4.5 ka cal BP, with AMS ^{14}C dates converted to calendar years during Bacon 2.2 modeling (Table 3.1, Figure 3.2a). The 11.9 ka cal BP date at 152 cm was younger than expected from prior work (Kirby et al., 2006), and obtained from a 3-cm charcoal layer not captured in the BLDC04-2 core. Without any age constraints above 152 cm, Bacon 2.2 extrapolated to the core top, with dates that extend into the Middle Holocene. We had low confidence that this is the true age of the core top, and have excluded the desiccated upper 1 m of BDL12 from the ensuing figures and discussion. The fading-corrected IRSL ages measured at 50˚C and post-IR IRSL at 225˚C are in approximate agreement, and within range of the tie-points established (Table 3.1, Figure 3.2a-b). Sample J3096 was excluded from the age model, as it provided age estimates that were not in stratigraphic agreement with the other three samples (Table 3.1), had very low yield, and displayed non-standard TL during preheat measurements.

3.5.2 Sedimentology and Summary of Proxy Data

The BDL12 sequence was 91.9% complete, with some missing portions due to coring gaps and disturbances. Core stratigraphy and sedimentological data (dry density, inorganics,

MARs, and grain size) are shown by depth in Figure 3.3. Grain size mode results throughout the sequence were consistently in the range of silt (2-50 μm), except for the basal sand unit (mode >400 μm). We summarized important changes in Table 3.2, with modifiers "sandy," or "clayey" when these grain size fractions measured 20% or greater, and silt remained the dominant grain size (over 60%). Figure 3.4 shows proxy data by age and MIS, alongside shifting insolation for 34˚N. MIS 5 notations with numbers (e.g. MIS 5.1) represent times of peak conditions for its five substages, after the chronology of Lisiecki and Raymo (2005). Table 3.2 summarizes physical and geochemical results and important shifts in proxy measurements for each MIS. MIS 5 substages are referenced with letters here (e.g. MIS 5a), though Imbrie et al. (1984) note that the transition between these substages tended to vary geographically.

3.5.3 Relationships and Environmental Interpretation for Baldwin Lake Proxy Data

We assumed the following relationships between proxy data, environmental conditions, and local summer insolation in our interpretation of site history. We noted first a strong correlation between organic content and BSi throughout most of the sequence (Figures 3.4a-b; $r=0.8091$, $p<0.001$), suggesting that primary productivity was the most important contributor to organic variation (Colman et al., 1995; Conley and Schelske, 2002; Kaplan et al., 2002). Other sites at either high latitudes or altitudes have shown bulk organic and BSi correspondence to indicate lake water temperature (e.g. Blass et al., 2007; Hahn et al., 2013; McKay et al., 2008; Nussbaumer et al., 2011; Vogel et al., 2013), including a detailed study in the Sierra Nevada (Street et al., 2012). Light availability can be another control on length of the freshwater photosynthetic season (e.g. Colman et al., 1995; Hu et al., 2003) and seasonal ice cover of the lake surface (McKay et al., 2008; Melles et al., 2006; Prokopenko et al., 2006). We assumed that our LOI–BSi concentration recorded a similar connection to paleotemperature, and was largely

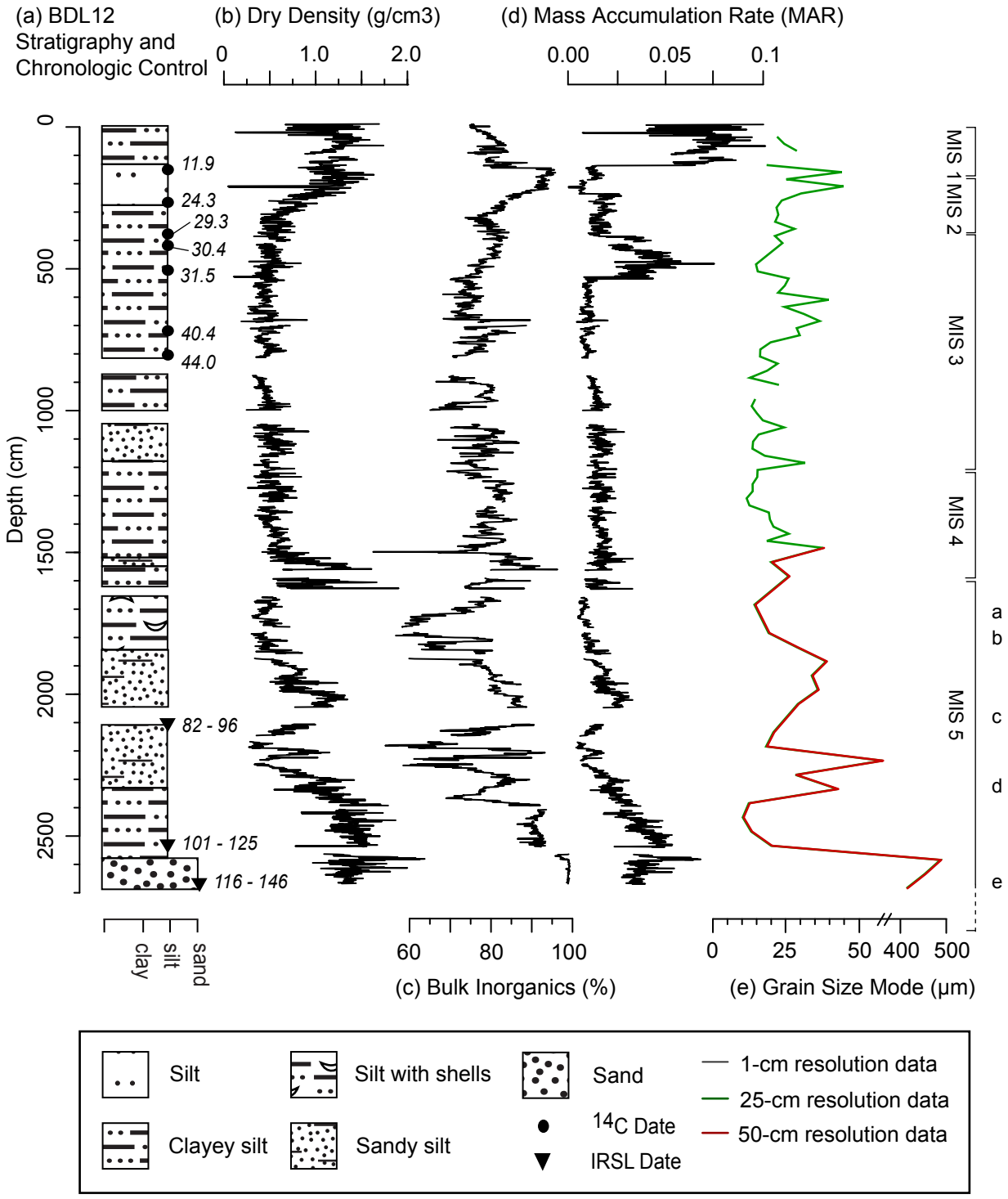

Figure 3.3. Stratigraphy, age horizons, and sedimentological data for BDL12, with approximate boundaries of Marine Isotope Stages after Lisiecki and Raymo (2005). The entire age range for three post-IR IRSL dates is shown. Substage lettering (MIS 5e-5a) is not bracketed at specific time points, due to this age uncertainty.

Table 3.2. Multi-proxy summary from Baldwin Lake core BDL12, by Marine Isotope Stage (MIS). MS = magnetic susceptibility, reported in SI units (10^5 of measured values). $CaCO_3$ = carbonate content from loss-on-ignition analysis. Trace element data (Ca, Fe, Ti, and Mn:Ti) reported as average for each MIS, unless otherwise noted. "Insolation" refers to summer insolation at 34˚N (Laskar, 2004), except for MIS 3, where both summer and winter are noted. For MIS 5, substages with letters (e.g. MIS 5b) refer to the span of the entire substage and its conditions, and are ordered alphabetically youngest-to-oldest. As boundaries between substages are not universally defined (Imbrie, 1984), MIS 5 notations with numbers refer to peak conditions of that substage (e.g. MIS 5.1 denotes peak conditions of MIS 5a, 83 ka), after Lisiecki and Raymo (2005).

Stage/Substages Cal Yr BP	**Key Changes in Insolation and Proxy Data**	**Key Paleoenvironmental Conditions/Events**
MIS 5e (127 to 120)	• short-term insolation shift from 543 W/m^2 at 127 ka, to 478 W/m^2 at 120 ka • sand facies throughout (grain size mode >400 μm); minimal clay (<1%) • high dry density (>1.2 g/cm^3), MS <7 SI throughout, with average value 3.2 SI • Ti (~2.4‰) and Fe (~8.5‰) remained low until rapid increase to 3.5‰ (Ti) and >20‰ (Fe) at 121 ka • low organic content (<1%), $CaCO_3$ (<3%) and Ca (~6.8‰) throughout; no BSi analysis	• High-energy fluvial setting
MIS 5d – 5c (120 to 95)	• insolation low 452 W/m^2 at 116 ka, rose to 538 W/m^2 by 105 ka, declined to 472 W/m^2 by 95 ka • fine-grained, inorganic clayey silt throughout, with fine sand (grain size mode = 58 μm) at 106 ka • MS rose from ~7 SI to ~16 SI from 121 - 118 ka, gradually declined to <5 SI by 112 ka, generally stayed generally below <6 SI until 95 ka, except for short excursion at 101 ka (51 SI) • high Ti and Fe (~3.5‰, 35‰) until 112 ka, lows of ~0.6‰ (Ti) and ~8‰ (Fe) at 107 ka and 102 ka, moderate-to-high levels of ~2.5‰ (Ti) and ~25‰ (Fe) began 98 ka • low-to-moderate Ca (~20‰) and $CaCO_3$ (5-10%) until peak at 112 ka (Ca ~109‰, $CaCO_3$ ~20%), declined to low-to-moderate values over next 8 kyr that persisted until 95 ka • low organics (<5%) until 113 ka, peaks ~33-39% at 106 ka and 103 ka, declined to <5% by 95 ka • BSi generally followed organics, with 1-3 mg/g background, peak of 11.3 mg/g at 103 ka	• Basin closure occurred near beginning of MIS 5d • Cool, deep, unproductive lake conditions during MIS 5d insolation minimum • High-erosion event 106 ka • Transition to more shallow, productive lake late MIS 5d, peak productivity during MIS 5c (103 ka)
MIS 5b – 5a (95 to 71)	• insolation rose from 472 W/m^2 at 95 ka to 529 W/m^2 at 83 ka, and declined to 468 W/m^2 by 71 ka • silt deposition throughout, with calcareous layers including mollusks that end abruptly 81 ka • MS low (<2 SI) between 86 – 76 ka; rose to 5 – 7 SI by end of MIS 5 • moderate Ti (~1.2‰) and Fe (17‰) at 95 ka, declined to <0.1‰ and ~6‰ by 83 ka, gradually increased to 1.7‰ and 18‰ by 71 ka. • moderate Ca (25 – 60‰) until 89 ka, then maxima 180‰ at 86 ka, and 160‰ at 83 ka. $CaCO_3$ ranged 5-15%, with peaks 22% at 86 ka, and 30% at 83 ka. Mn:Ti 0.84 at 83 ka and 0.74 c. 86 ka. • varied organic content: minima are <5% from 95 – 93 ka and 73 – 72.6 ka, maxima of ~33% at 88.2 ka and 81.6 ka. Maximum for BDL12 is 44% at the MIS 5a/MIS 4 transition (71 ka) • BSi varied with organics, with peak value 17.4 mg/g at 82.6 ka	• High-amplitude change in lake productivity that was paced with insolation and temperature. • Lowstand conditions evident for MIS 5.2 (87 ka) and MIS 5.1 (82 ka), with abrupt transition out of the latter, likely due to rapid shift in available moisture

MIS 4 (71 to 57)	• low insolation 468 W/m^2 at 71 ka increased to 518 W/m^2 by 57 ka • clayey silt (density ~0.70 g/cm^3) deposition that transitioned to organic silt (density <0.54 g/cm^3) • moderate-to-high organics (average = 16.5%); BSi at late MIS 4 (55-51 ka) was 9.8 – 11.5 mg/g • moderate-to-low MS, Ti and Fe throughout (MS ~5.0 SI, Ti ~1.5‰, Fe ~20‰) • shallow-water indicators were moderate at onset of MIS 4: Ca (22‰), $CaCO_3$ (<11%), but decline by 69 ka and remain low (Ca ~ 4.9‰, $CaCO_3$ <5%, Mn:Ti ~0.11),	• Basin shift occurred 69 ka towards deeper lake and sustained productivity that persisted after MIS 4
MIS 3 (57 to 29)	• summer insolation ranged between 487 – 508 W/m^2; winter insolation 186 – 200 W/m^2 and maintained 192 W/m^2 from 45 to 35 ka • fine-grained organic silt (mode 12 – 39 μm), dry density <1.00 g/cm^3 (average = 0.48 g/cm^3) • low MS (average = 3.9 SI); Ti decreased from ~1.7‰ to 0.9‰ by 37 ka, then increased to ~1.4‰ by 29 ka. Broad decrease and increase in Fe (ranged ~11-21‰) with rapid increases (~ 51‰) • suppressed Ca (~2.5‰) and $CaCO_3$ (<10%, average of ~4.3%) throughout MIS 3 • moderate organic content (average = 18.8%), with millennial-scale fluctuations ranging 10—28% • BSi relatively high throughout MIS 3, ranging 7.7 – 13.4 mg/g	• lowest-amplitude variation in both summer and winter insolation for nearly 30 kyr; reduced seasonality • Consistently productive lake that remained stratified and deep • Organic content does not shift in tandem with summer insolation, and millennial-scale fluctuations suggest a different, short-term climatic influence
MIS 2 (29 to 14)	• insolation low of 475 W/m^2 at 23 ka, reached 515 W/m^2 by 14 ka • predominantly silt deposition, with a coarser layer (28% sand) 28 ka; deposition rate declined by more than half (~0.05 cm/yr during MIS 3 to ~0.02 cm/yr for MIS 2m) • MS maximum at LGM start, with peak at 26 ka (~100 SI) above background values of 0 – 11 SI • high Ti (2.3-3.6‰) and Fe (average 26‰, with 56‰ peak) began 26.3 ka, maintained until MIS 1 • low Ca (6‰), $CaCO_3$ (generally <5%) and Mn:Ti (0.12) throughout • final organic content increase to 23% at 27.7 ka, then decline to <5% by 21 ka and thereafter • BSi decreased overall from 7.9 to 5.4 mg/g, though with peaks and lags separate from organics. *Pediastrum* are abundant 24 ka, and trace element phosphorus began increase 27 ka from ~7‰, reaching ~14 ‰ by 14.5 ka	• Low insolation, cold conditions, and deep water • last phase of moderate productivity at 27.7 ka not paced with insolation • BSi suggests moderate-to-low lake productivity during MIS 2, perhaps due to high K influx and abundant *Pediastrum* 24 ka
MIS 1 (<14)	• insolation continued its increase to 520 W/m^2 by 11 ka, declined to 493 W/m^2 by 5 ka • desiccated, inorganic clayey silt (mode grain size <29μm); dry density is high (0.67 – 1.74 g/cm^3) • erratic MS, varying between -2.6 - 8 SI; high Ca (~84‰), low Ti (~1.3‰), generally low Fe (18‰) with excursion ~73‰ at 11.8 ka, high Mn:Ti (0.58) • relatively high carbonate content; abrupt rise at 12.7 ka to ~15%; MIS 1 average 14.6% • low organic content (<10%, average 4.7%) and two moderate BSi horizons (4.5 – 7.8 mg/g)	• Transition to intermittent lake • Desiccation, low sedimentation, and uncertain age prevent study of environmental conditions after c. 12 ka

influenced by available light, variations in summer insolation at 34˚N, and the length of ice-free season. As BSi sampling resolution was low, we discuss the record in terms of relative temperature changes that affected the SBM.

Low values of magnetic susceptibility and dry density generally corroborated times of high biologic and autochthonous deposition (Table 3.2). Low MS values (<12 SI) throughout most of BDL12 (Figure 3.4, Table 3.2) suggest this proxy detected a largely diamagnetic fraction throughout basin history (Dearing, 1999). Magnetite-rich sediment was certainly produced from nearby granodioritic bedrock, yet the MS signal was dampened at times of episodic, high-energy clastic input. Likely magnetite-bearing sediment experienced oxidation at lake bottom, and magnetite was dissolved in whole or in part (Bird and Kirby, 2006; Dearing, 1999; Kirby et al., 2006; Nowaczyk et al., 2006).

Trace element data aided our interpretation of allochthonous deposition, lake level changes, and lake ventilation. Phases of increased detrital, non-biologic deposition produced relatively higher values of Ti and, in part, Fe (Kylander et al., 2011; Vogel et al., 2013). Warm water temperatures and lake regression can produce Ca saturation, and high values in the manganese to titanium ratio (Mn:Ti; Figure 3.4) have been interpreted as a proxy for a well-mixed lake with bottom ventilation (Kylander et al., 2011). Ca concentration generally changed in tandem with carbonate content ($CaCO_3$) as measured with LOI (Figure 3.4); taken together, we interpreted times of high Ca, $CaCO_3$ and Mn:Ti to reflect more shallow, ventilated, and warm lake conditions. At times when Ca, $CaCO_3$, Mn:Ti, and MS remained low, we interpreted the lake to be deeper, stratified, and anoxic at bottom.

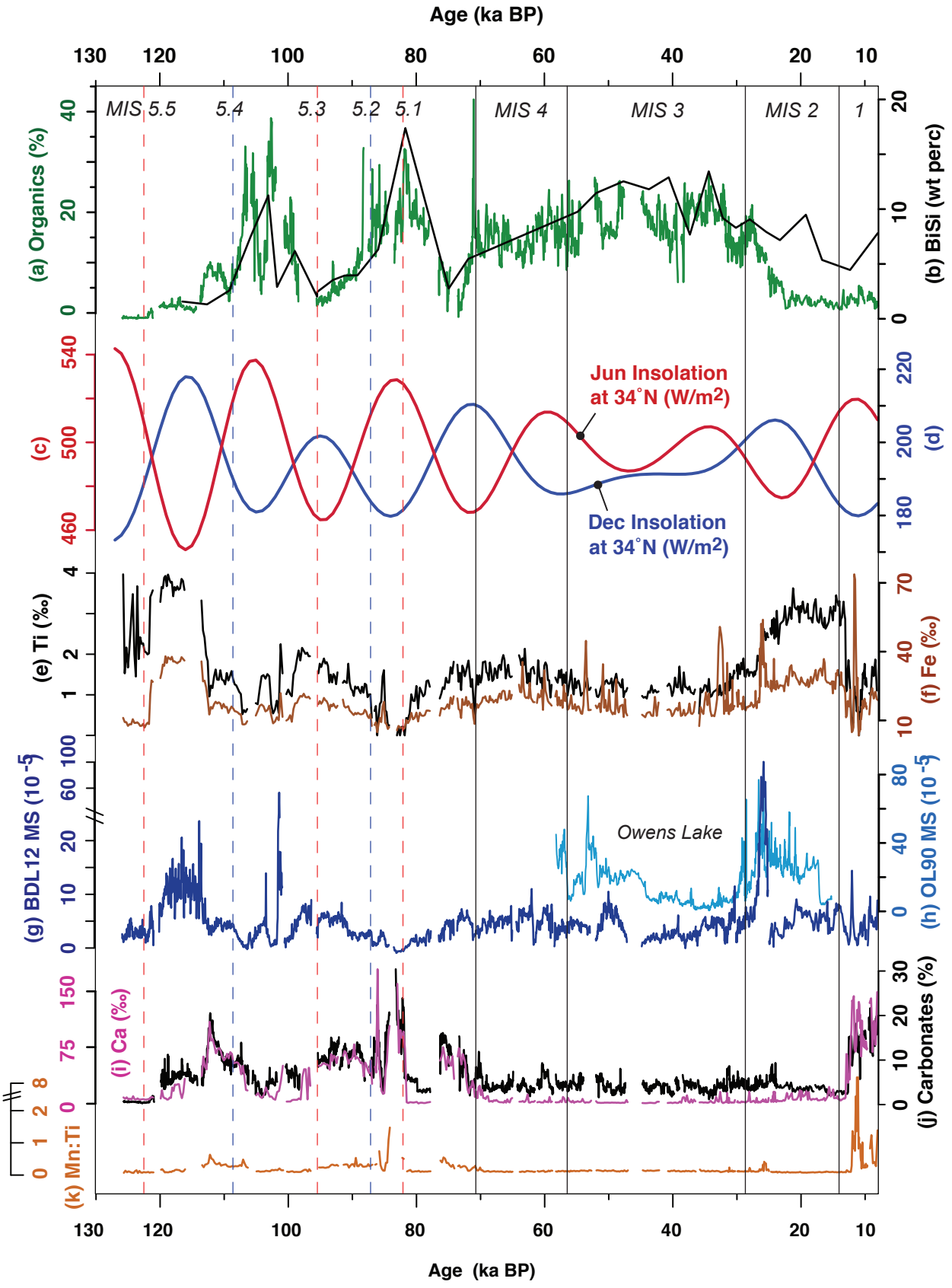
Age (ka BP)
130
120
100
80
60
40
20
10
MIS 5.5
5.4
5.3
5.2
5.1
MIS 4
MIS 3
MIS 2
1
(a) Organics (%)
0
20
40
(b) BiSi (wt perc)
0
10
20
(c)
460
500
540
Jun Insolation at 34˚N (W/m2)
Dec Insolation at 34˚N (W/m2)
(d)
180
200
220
(e) Ti (‰)
1
2
4
(f) Fe (‰)
10
40
70
(g) BDL12 MS (10-5)
0
10
20
60
100
Owens Lake
(h) OL90 MS (10-5)
0
40
80
(i) Ca (‰)
75
150
(j) Carbonates (%)
0
10
20
30
(k) Mn:Ti
0
1
2
8
Age (ka BP)

Figure 3.4. Physical and geochemical data, plotted by age and with Marine Isotope Stage boundaries noted. (a) Organic content, determined with loss-on-ignition. (b) Biogenic silica. (c) Summer and (d) winter insolation at 34˚N, the approximate latitude of the study site. (e) Trace element titanium (Ti). (f) Trace element iron (Fe). (g) BDL12 magnetic susceptibility (SI). (h) Magnetic susceptibility of Owens Lake core OL90 (Benson et al., 2002), adjusted to calendar years with a Bacon 2.2 age model based upon tie-points to NGRIP and radiocarbon dates of Benson et al. (2003). See Supplemental Data for details of OL90 age conversion. (i) Trace element calcium (Ca). (j) Bulk carbonate content ($CaCO_3$), determined with loss-on-ignition. (k) Manganese to titanium ratio (Mn:Ti).

3.6. Discussion

3.6.1. Baldwin Lake's Environmental Change from 125 – 10 ka

Luminescence dates support MIS 5e initiation of the BDL12 sequence, with high density, coarse grain size, and extremely low clay and organic content (both <1%). This sedimentology was likely produced in a high-energy environment, rather than closed-basin deposition. We hypothesize that fluvial and colluvial processes dominated erosion and transport in the alpine valley at this time. The transition to finer-grained clayey silt was abrupt and likely happened early MIS 5d. Rapid sedimentation from Sugarloaf Mountain, including possible landslide events, may have aided closure of the basin, and the separation of Baldwin and Big Bear Lake basins (Leidy, 2006; Stout, 1976). The ensuing deposition into Baldwin Lake was largely detrital, with high Ti and Fe and low organic content. It remained a deep, unproductive, cool lake for the first half of MIS 5d during an insolation minimum at 116 ka. Ca, $CaCO_3$, and organics later increased 112 ka while MS decreased, indicating the lake became warmer, shallower, and more productive.

The period between MIS 5.4 – 5.3 (109 – 96 ka, Figure 3.4) was the basin's first productivity oscillation apparently driven by summer insolation, with organic values reaching >30% twice from 106 – 103 ka, and BSi at 11.3 mg/g. Productivity reached minimal levels over the next 8 kyr to match the insolation low 95 ka. During MIS 5b – 5a (95 – 71 ka), productivity again increased and decreased, reaching >30% shortly after the insolation maximum 83 ka. Lowstand conditions accompanied this, with high Ca, $CaCO_3$, Mn:Ti. Abundant littoral mollusks *Lymnaea* and *Planorbella* spp. (Burch, 1982) indicates that the lake shoreline had reached the basin depocenter, where the core was taken. All Ca-based lowstand evidence quickly

disappeared at 82 ka, and organics surged to 33% by 81.6 ka in the deeper water, before declining alongside insolation to reach ~1% at 73 ka.

During MIS 4 and 3, these broad oscillations yield to a long-term state of moderate productivity, while seasonal insolation was less variable. Organics were already increasing from a low 73 ka, leading the insolation minimum at 71 ka by 2 kyr, and then maintained moderate values (average = 16.4%) Early MIS 4 had relatively high levels of Ca, $CaCO_3$, and Mn:Ti (Table 3.2, Figure 3.4) that tapered over the next ~5-6 kyr, while organic content rose, the lake deepened, and deposition became more rapid with the constant autochthonous biologic material. These conditions persisted into MIS 3, with continuous organic content (average = 18.8%) and that underwent millennial-scale fluctuations, a unique feature of this Stage.

Phases of subtle laminae occurred during the first half of MIS 3 (57 – 46 ka), and are described in greater detail for core BLDC04 (Kirby et al., 2006). While laminated and non-laminated sediment may indicate lake water level shifts (Retelle and Child, 1996), we do not find support for the alternating perennial-to-playa conditions during MIS 3 as proposed by Blazevic et al. (2009). The sediments and their chemistry are not consistent with playa conditions and the elemental "signature" of high Ca, $CaCO_3$, and Mn:Ti we found for Baldwin Lake's eventual desiccation in the Holocene (Figure 3.4). Instead, these elements are suppressed throughout MIS 3 along with low MS (Table 3.2, Figure 3.4), suggesting a lack of sustained bottom ventilation events in the lake. Low MS and well-preserved microfossils during MIS 3 also support persistent bottom anoxia. Baldwin Lake was thus a perennial, stratified lake for most of MIS 4 and the duration of MIS 3, a timespan of at least 35 kyr.

After a final millennial-scale fluctuation in organic content that peaked 27.7 ka, this proxy declined during the lower insolation and colder temperatures of MIS 2. Sedimentation

slowed significantly and was largely detrital, with Fe and Ti increasing into the Last Glacial Maximum (LGM, 26 – 19 ka). BSi declined to ~5 mg/g by the end of MIS 2, but its moderate values throughout MIS 2 (Table 3.2, Figure 3.4) suggest continued productivity during this cold time. Both an influx of potassium (K) to the basin (10-11‰, compared to prior averages of ~5‰), and high *Pediastrum* counts from preliminary pollen data, occurred during the LGM and indicate persistence of algae, despite lower light availability and temperatures. The highest MS excursion in the core occurred at 27 – 25.5 ka; aside from oxidation of the core since its collection, there are no other unique sedimentary structures, nor shifts in other proxy data, that correspond to this excursion. This likely represents a change in reducing conditions at lake bottom that anomalously preserved the magnetic signal (Dearing, 1999). Owens Lake, located ~250 km NNW of the SBM, underwent a similarly rapid, coeval magnetic susceptibility increase, before it shifted towards relatively higher magnetic values for MIS 2 (Figure 3.4h; Benson et al., 2002).

Organic silt deposition did not resume after MIS 2; instead, the lake transitioned to an intermittent, playa surface as summer insolation rose from 23 – 11 ka. Shallow-water indicators Ca, $CaCO_3$, and Mn:Ti increased suddenly 12 ka; afterwards, frequent dry episodes prevented further preservation of biologic material. While the Holocene is a notable omission in BDL12, studies on neighboring Big Bear Lake (Figure 3.1) have provided insight into Holocene climate of the SBM (Kirby et al., 2012; Paladino, 2008).

3.6.2 Important Climatic Drivers in California

3.6.2.1 Orbital-Scale Radiative Forcing

Summer insolation has been invoked as a key influence in long vegetation records. California pollen sites that date to MIS 5e have shown orbitally-induced landscape change, including the Santa Barbara Basin (ODP 893; Heusser, 1998), ODP 1018 (Lyle et al., 2010), and

Owens Lake (Woolfenden, 2003). ODP 1018 BSi and productivity also shifted with precessional cycles (Lyle et al., 2010). Total organic carbon (TOC) from an Owens Lake record was synchronous with summer insolation (Figure 3.5c, Benson et al., 2002). The influence of boreal summer insolation, largely credited with driving continental ice sheet mass, was a primary driver of change at interior Great Basin speleothem sites including the Leviathan, Pinnacle, and Lehman Caves (Lachniet et al., 2014), and Devil's Hole (Moseley et al., 2016). Baldwin Lake's history indicated that Southern California temperature and hydrology were sensitive to Milankovitch-scale orbital variations over the past 125 ka. Our new results confirm the first-order relationship between local insolation values and organic matter, first proposed by Kirby et al. (2006). The relationship between summer insolation and organic content is best evident during the high-amplitude changes in summer insolation during MIS 5 and its substages, a time encompassing 42% of the record.

Globally, MIS 4 conditions were milder than the preceding MIS 6 and subsequent MIS 2 stadials, including in the North American West and Sierra Nevada (Brook et al., 2006; Forester et al., 2005; Jiménez-Moreno et al., 2010; Phillips et al., 1996; Rood et al., 2011). In southern California, both summer and winter insolation likely drove short-lived cold conditions, and rapid recovery, compared to MIS 2. During intermediary MIS 3, both winter and summer insolation were less variable and local seasonality was reduced (Figure 3.4). Summer insolation only varied 487 – 511 W/m^2, while winter insolation was relatively static (Table 3.2). This allowed the lake surface to remain ice-free, and primary productivity to continue, for longer durations each year. During MIS 2, summer insolation declined to only 475 W/m^2 (23 ka) compared to 468 W/m^2 in MIS 4, but winter insolation was slightly lower (206 W/m^2 vs. 211 W/m^2). The rise of summer insolation to 520 W/m^2 at 11 ka was the first time in ~70 kyr it had reached such levels, and this

drove site desiccation at Baldwin Lake, as well as other sites in the semiarid ecoregions in California, including Owens Lake (Bacon et al., 2006) and /Death Valley (Li et al., 1996).

3.6.2.2 Millennial-Scale Forcing during MIS 3

Orbital variation is a slow cycle over several millennia, and while major productivity shifts in Baldwin Lake occurred at this pace, they are not without shorter-order minima and maxima, particularly during MIS 3. What rapid processes account for such change? Kirby et al. (2006) proposed these to be wet events corresponding to North Atlantic interstadials, or Dansgaard-Oeschger (D-O) events. D-O events were North Atlantic millennial-scale temperature oscillations that occur between 120 and 10 ka, first recognized in $\delta^{18}O$ data from the Greenland ice cores (Dansgaard et al., 1993). Interstadial-stadial couplets typically had a rapid onset, followed by gradual cooling (Grootes et al., 1993; Johnsen et al., 1992). The North Atlantic response included lower sea surface temperatures (SSTs), changes in freshwater flux to the North Atlantic, and often variations in Atlantic Meridional Overturning Circulation. Rapid transmission of a dynamic climate signal to the globe within decades was the net result (Elliot et al., 2002; Gottschalk et al., 2015), though regional response, duration and precise timing differed from the Greenland chronology.

Lund and Mix (1998) provided evidence that D-O events propagated to the North Pacific, and Hendy and Kennett (2000) have documented D-O events in the Santa Barbara Basin (SBB) with oxygen isotopes, and shifting benthic foraminifera assemblages. Right-coiling *N. pachyderma*, indicative of warmer SSTs that characterized the interstadial phase of these events, increased in parallel with the lighter-isotope events in Greenland (Figure 3.5a, 3.5b). Behl and Kennett (1996) noted laminations driven by anoxia during D-O events. Thus, the SBB response during MIS 3 interstadials was enhanced marine temperatures, driven by increased influx of

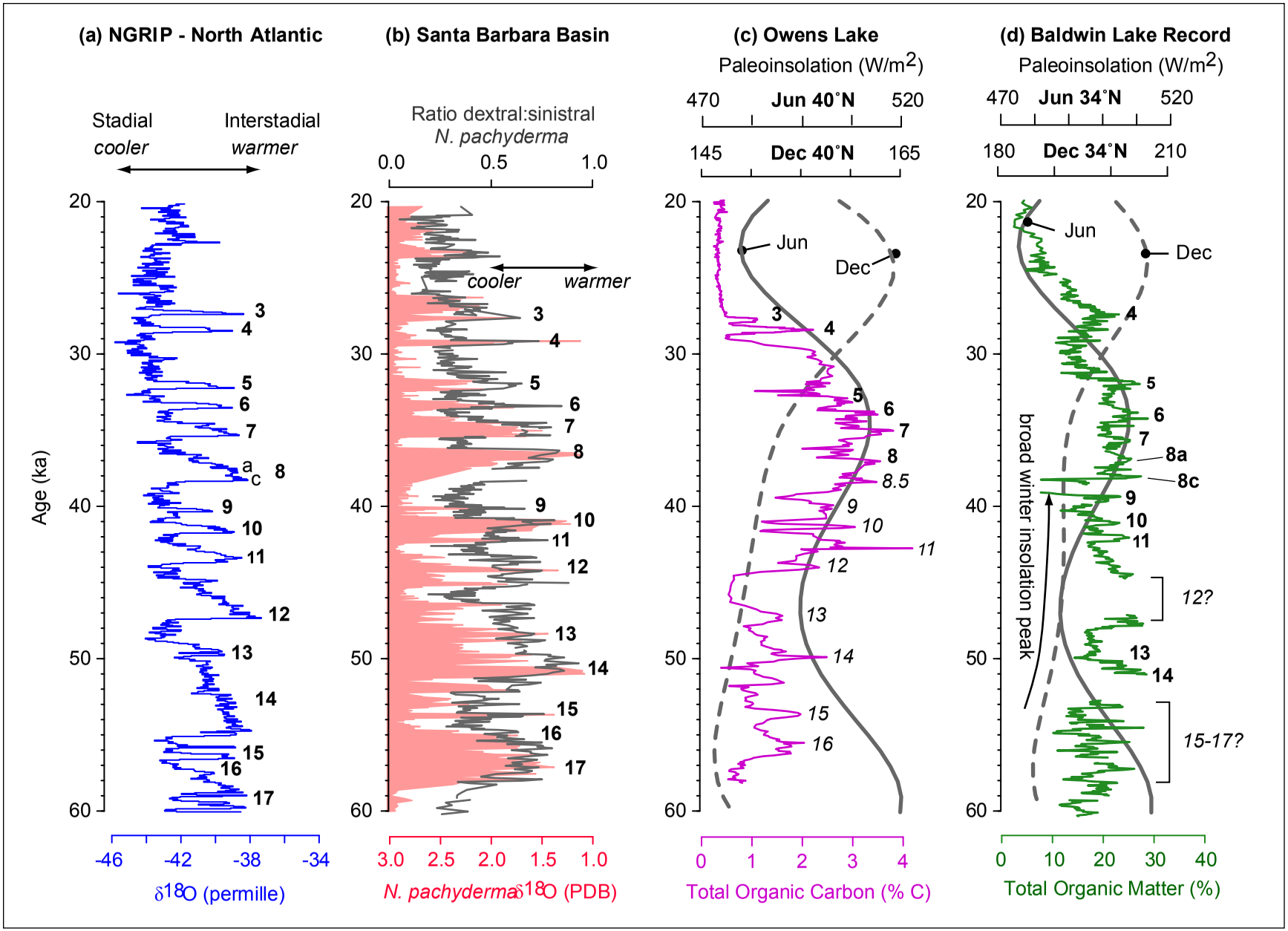
(a) NGRIP - North Atlantic
Stadial
cooler
Interstadial
warmer
Age (ka)
20
30
40
50
60
3
4
5
6
7
a
c
8
9
10
11
12
13
14
15
16
17
-46
-42
-38
-34
δ18O (permille)
(b) Santa Barbara Basin
Ratio dextral:sinistral
N. pachyderma
0.0
0.5
1.0
cooler
warmer
3.0
2.5
2.0
1.5
1.0
N. pachyderma δ18O (PDB)
(c) Owens Lake
Paleoinsolation (W/m2)
470
Jun 40°N
520
145
Dec 40°N
165
Jun
Dec
8.5
0
1
2
3
4
Total Organic Carbon (% C)
(d) Baldwin Lake Record
Paleoinsolation (W/m2)
470
Jun 34°N
520
180
Dec 34°N
210
broad winter insolation peak
8a
8c
12?
15-17?
0
10
20
30
40
Total Organic Matter (%)

Figure 3.5. (a) NGRIP $\delta^{18}O$ shifts from 60 – 20 ka, with Greenland Interstadial (GI) numbers (i.e. Dansgaard-Oschger events, Rasmussen et al., 2014). While many GIs have substages, only GI-8 has the substages shown for simplicity's sake. (b) Santa Barbara Basin core ODP-893, with interstadials labeled after Hendy and Kennett (2000) and latest age model (Hendy et al., 2007). (c) Owens Lake Total Organic Content (%) from OL90 (Benson et al., 2002), with summer insolation at 40˚N (Laskar, 2004). Bold D-O interstadial labels after Benson et al. (2003); later italic numbers our interpretation. See Supplemental Data for OL90 age conversion to calendar years. (d) Baldwin Lake core BDL12 bulk organic content from 60 – 20 ka, with summer and winter paleoinsolation trends (Laskar, 2004), and proposed D-O interstadial numbering.

subtropical waters and weaker California Current (Ingrid L. Hendy and Kennett, 2000). In Owens Lake, total organic carbon (%TOC, Figure 3.5c) fluctuated in millennial-scale events, with the longer-term influence of summer insolation at 40˚N apparent (Benson, 1999; Benson et al., 2003, 2002).

We found a similar response in Baldwin Lake's productivity and temperature. Within the limits of dating uncertainties, there was apparent synchronicity of these three California records with NGRIP $\delta^{18}O$ in timing, duration, and relative amplitude (Figure 3.5). We assign D-O event numbers for BDL12 (Figure 3.5d) and OL90 (Figure 3.5c) after the chronology and Greenland Interstadial (GI) numbering of Rasmussen et al. (2014). Core gaps and noisy data between 60 – 52 ka, however, complicated the BDL12 organic record, and winter insolation prior to 50 ka may have dampened the amplitude of potential D-O events (Figure 3.5b). Rasmussen et al. (2014) confirm that the North Atlantic response was complex at this time, with less defined D-O events prior to c. 48 ka. Higher-resolution Greenland ice core studies have detected additional events of similar amplitude since initial numbering. Thus, we do not assign GI 15 – 17 to a specific section of BDL12, and such events may have been muddled in Baldwin Lake and escaped detection. Despite these caveats, these records suggest that North Atlantic MIS 3 and MIS 2 perturbations were strong enough to act as a secondary climate driver to intermediate, less variable insolation in Southern California.

3.6.3 Pacific- and North Atlantic-induced events in California, the Great Basin, and Southwest

Insolation shifts explain first-order variation of Baldwin Lake's long-term, overall productivity over several millennia. However, changes still occurred that were more rapid than the slow cycle of orbital variation. We examined other paleoclimate sites in California, the Great Basin, and Southwest (Figure 3.6) for their response to rapid change, and asked 1) which events

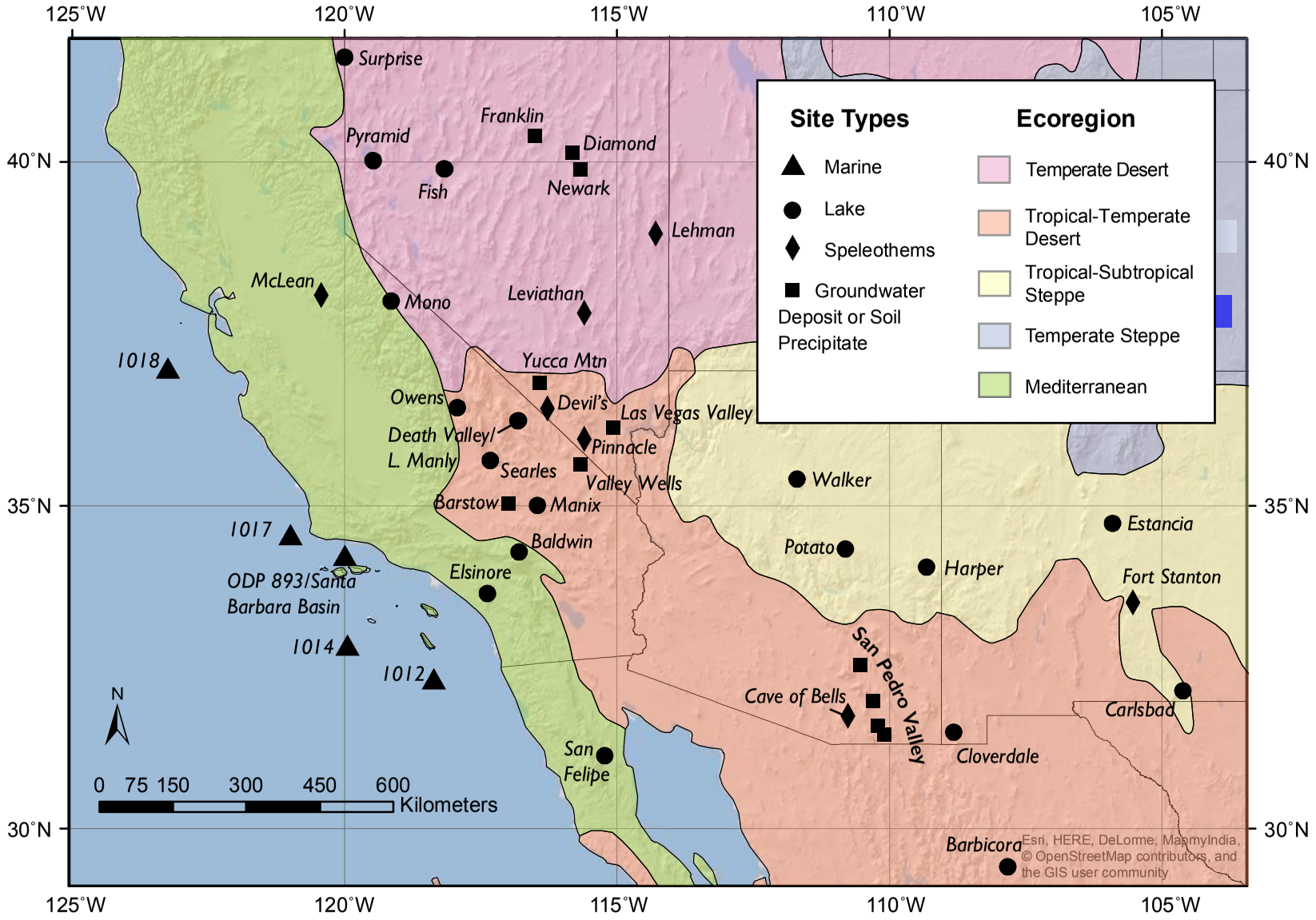

Figure 3.6. Paleoclimatic sites discussed in this review, with North American ecoregions shown (Bailey, 2009).

are coeval to environmental changes in the SBM, 2) was there a temperature and/or hydrological response at each site, and 3) is there a coherent geographic pattern of response? We focused largely on 85 – 20 ka, the period with the most comparative sites to Baldwin Lake, mapped in Figures 3.6-3.7 with the ecoregions of Bailey (2009).

MIS 5a events included lowstands at 87 and 82 ka, with the latter occurring during a marine highstand along the California and Southern Oregon coasts 84 – 76 ka (Muhs et al., 2012). Meanwhile, Devil's Hole reached maximum $\delta^{18}O$ values at 82.5 ±0.7 ka (Moseley et al., 2016). ODP 1017 SSTs increased at 82 ka, contemporaneous with Baldwin Lake's sudden transgression, and lasted until 58 ka (Seki et al., 2002). Elevated SSTs in late MIS 5a apparently coincided with greater effective moisture reaching the SBM and ending the lake lowstand.

The next time of widespread climatic change was the period 60 – 57 ka that included Heinrich Event 6 (H6; Hemming, 2004) and the MIS 4/3 transition at 57 ka. Several sites underwent state changes towards either warmer, or hydrologically different, conditions. This change generally persisted for several millennia and, in most cases, throughout MIS 3. Devil's Hole calcite growth ceased 60 ka, suggesting lower effective moisture in the northern Mojave Desert (Winograd et al., 2006). At the nearby Death Valley core, deposition changed to a more arid facies, shifting from mudflat to salt pan (Forester et al., 2005). Runoff to Lake Barbicora, located at the southernmost extent of the region shown (Figure 3.7), also reduced (Roy et al., 2013). In contrast, sites in Southern California became wet, including Baldwin Lake's deep phase throughout MIS 3, and the onset of groundwater flow in Valley Wells 60 ka (Figure 3.6; Pigati et al., 2011).

Offshore, SSTs increased, and a high-resolution BSi record at ODP 1018 provided insight to hydrological change. Enhanced marine productivity was linked to the suppressed upwelling,

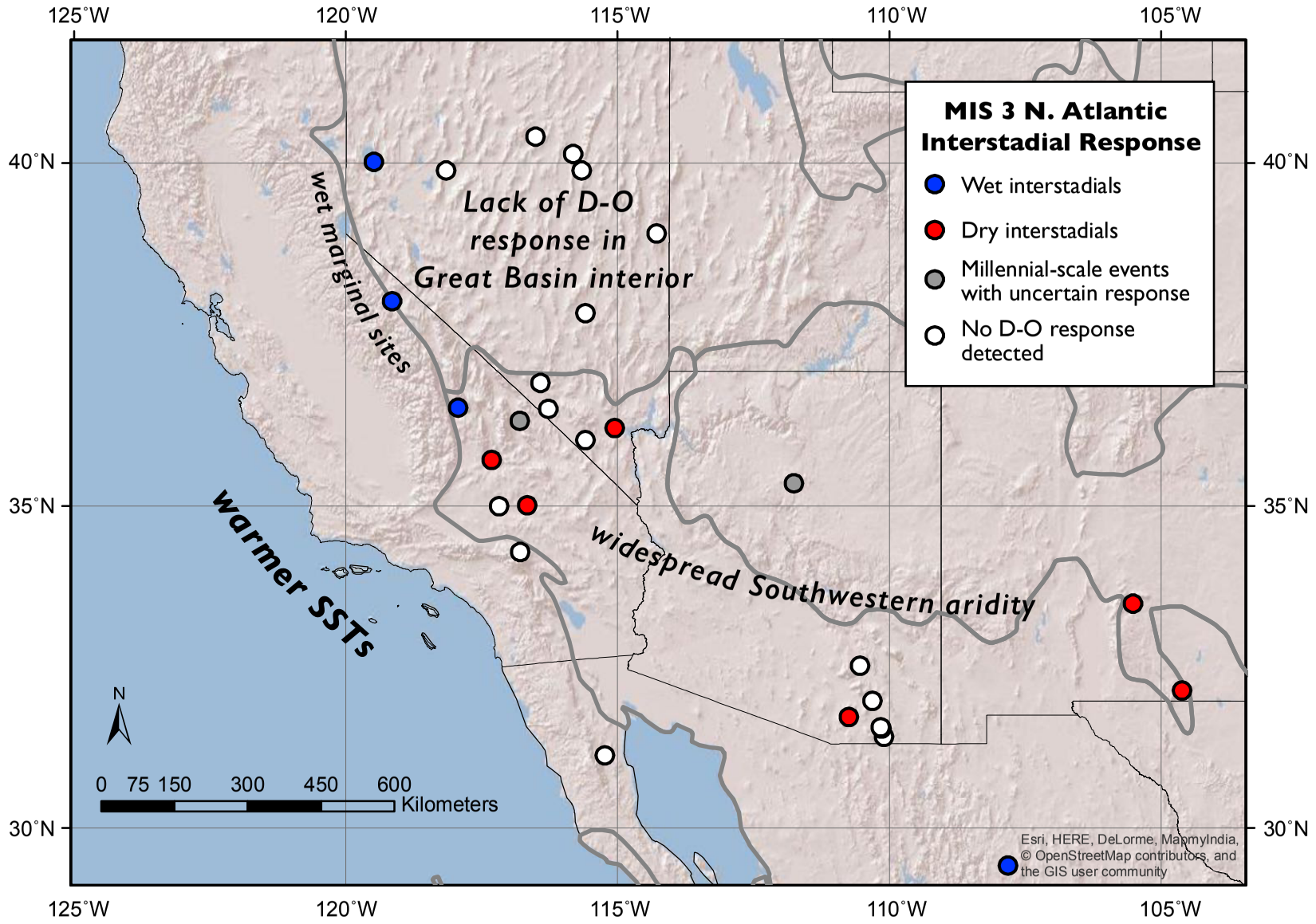

Figure 3.7. Response of regional sites to Dansgaard-Oeschger events during MIS 3 (c. 57 – 29 ka).

enhanced SSTs, and enhanced aridity. This combination of conditions began ~61 ka and lasted 8-10 kyr into MIS 3 (Lyle et al., 2010). Both 1014 and 1017 exhibited SST warming 59-58 ka (Hendy et al., 2004; Ingrid L Hendy and Kennett, 2000; Seki et al., 2002); SSTs at 1012 also gradually increased after the MIS 4/3 transition (Herbert, 2001). Finally, two sites towards the north on either side of the Sierra Nevada showed shorter-term change 60 – 57 ka. Peak moisture included a wetter phase from 61.7 ± 0.5 to 59.8 ± 0.6 ka at McLean's Cave, and then returned to relatively dry conditions (Oster et al., 2014). Meanwhile, ice-rafted debris from increased freshwater runoff reached a maximum 59 – 58 ka at Mono Lake (Zimmerman et al., 2011). Oster et al. (2014) ascribed changes at McLean's Cave to North Atlantic changes, with Heinrich 6 (60 ± 5 ka; Hemming, 2004) coinciding with wet conditions, and D-O events 15–18 coeval with aridity in the Sierra Nevada foothills. Ultimately climatic change is not uniform throughout California at the end of MIS 4, though wetter sites were largely grouped in the southern sector of the Mojave Desert and the SBM. The response of generally wetter conditions in Southern California to enhanced SSTs was similar to that observed at 82 ka in MIS 5a.

More studies have documented MIS 3, including a recent focus on sites that depend upon groundwater infiltration, including speleothem records, soil precipitates, and groundwater/desert wetland deposits. The trend of greater effective moisture in MIS 3 in the SBM has been observed in the Transverse Ranges of the Santa Barbara area (Heusser, 1998), Valley Wells in the Mojave (Pigati et al., 2011) and in the Great Basin (Maher et al., 2014). Millennial-scale fluctuations in temperature-driven lake productivity overprinted on "baseline" wet conditions at Baldwin Lake, episodes when SSTs further increased during D-O events (Figure 3.5). Terrestrial records in Figure 3.7 predominantly showed a hydroclimatic, rather than temperature, response.

High-resolution marine records ODP 1017 and 1014 responded to North Atlantic

warming D-O events with even warmer SSTs (Ingrid L. Hendy and Kennett, 2000; Hendy and Pedersen, 2005; Pak et al., 2012; Pospelova et al., 2015; Seki et al., 2002). Heusser (1998) detected millennial-scale increases in ODP 893 oak pollen, a dry-adapted taxa, that correspond to D-O interstadials. Enhanced aridity was the norm evident during D-O events at other terrestrial sites, including Southwestern speleothem records Fort Stanton, Carlsbad Cavern, and Cave of the Bells (Asmerom et al., 2010; Brook et al., 2006; Wagner et al., 2010). Not all sites in tropical-temperate desert south of the Great Basin recorded D-O interstadials; those that do initiated late at 35 ka, including Searles Lake (Lin et al., 1998), and Las Vegas Valley (Springer et al., 2015). Phases of enhanced aridity after 35 ka correspond with D-O events. Sites that experienced overall greater effective moisture throughout MIS 3, but did not exhibit consistent millennial-scale variability, include Valley Wells (Pigati et al., 2011), the San Pedro Valley (Pigati et al., 2009). Records in Mexico began to show a sensitivity to D-O events by mid-MIS 3 (42 – 40 ka), with warmer SSTs in the Gulf of California (Price et al., 2013) and enhanced moisture at Lake Barbicora (Roy et al., 2013).

Great Basin response to D-O events was the most complex, with enhanced moisture at its margins, and no apparent influence in the interior. Higher lake levels during interstadials occur at Mono, Pyramid, and Owens Lakes to the east of the Sierra Nevada (Benson et al., 2003). The northeastern Great Basin, proximal to the Laurentide Ice Sheet margin during MIS 2, underwent saline/hypersaline oscillations in the Great Salt Lake during MIS 3 (Balch et al., 2005), and Benson et al. (2011) interpreted higher lake levels and wet D-O interstadials for this sector of the Lake Bonneville Basin. Millennial-scale oscillations are absent from sites in the Great Basin interior (Figure 3.7), namely Lehman, Leviathan, and Pinnacle speleothem records (Lachniet et al., 2014), and groundwater precipitates (Franklin, Newark Valley, Diamond Valley, Barstow,

and Yucca Mountain, Figure 3.6-3.7; Maher et al., 2014). Marginal Great Basin sites may have been wet due to nearby glaciation.

In the SBM, Kirby et al. (2006) previously hypothesized that D-O events were wet episodes based on laminated deposits in deep water conditions, but the laminated horizons observed in BDL12 were not synchronous with the organic excursions we have identified as D-O events. Age chronology for both the BLDC04-2 and BDL12 cores is uncertain within the same range as these ~1.48 kyr events, a problem noted in other studies from the region (Benson et al., 2003; Denniston et al., 2007; Zimmerman et al., 2011). Recently-dated relict shorelines at paleolake Manix to the north, part of the Mojave River watershed with its headwaters in the SBM, showed that the stadials between D-O events were wet (Reheis et al., 2015). We revise our interpretation of SBM's hydrological response to D-O events, then, and propose that these interstadials were arid in the SBM, based in part on this new Manix lake level data. This interpretation also fits the emerging pattern throughout the Mojave Desert and Southwest (Figure 3.7), which was a response of enhanced aridity to D-O events.

Reduced insolation, reduced evaporation, and generally wet conditions prevailed through the MIS 3/2 transition and into the LGM. Groundwater infiltration in the Great Basin was active until 24 ka (Maher et al., 2014), while highstands persisted at Owens Lake (Bacon et al., 2006) and Lake Manly (Li et al., 1996). Cave of the Bells (Wagner et al., 2010) and the San Pedro Valley sites of Pigati et al. (2009) are wet from 25 – 20 ka. An arid episode just prior to the LGM was evident at several of these sites, best documented with a well-dated, highly-resolved pollen study at Lake Elsinore that showed a ~2 kyr drought from 27.5 – 25.5 ka (Heusser et al., 2015). Other brief lake regressions and/or arid phases, as determined with pollen, apparently interrupted conditions that were otherwise wet at several several sites, including Owens Lake at

25-24 ka (Bacon et al., 2006), Pyramid Lake at 29 ka (Benson et al., 2013), and a pair of lakes on the Colorado Plateau at 24.5 – 24 ka (Hay and Walker Lakes; Anderson et al., 2000). The high magnetic susceptibility excursion at Baldwin and Owens Lakes was contemporaneous with the Lake Elsinore drought, and could have been caused by rapid sediment burial or lake mixing (Dearing, 1999).

An influx of moisture, likely derived from the North Pacific, reached southern California by 22-21 ka (Oster et al., 2015). A highstand and possible valley spillover to the east are often mentioned as Big Bear Valley Ice Age events (Krantz, 1983; Leidy, 2006; Stout, 1976), but the evidence has not been previously dated. In the SBM, glaciation occurred on San Gorgonio, the highest-elevation peak of the range, reaching maximum extent 20 – 18 ka (Owen et al., 2003). Early MIS 2 drought, and subsequent moisture delivery, suggest that southern California had a complex and dynamic hydrologic history during the first half of MIS 2, with changes occurring on millennial, and perhaps submillenial, scales. Further study with tighter-resolution proxy analyses are necessary to better resolve these events in space and time.

3.7. Conclusions

New analysis from Baldwin Lake shows that southern California climate change was sensitive to orbitally-induced radiation over the past 125 ka. Variations in local summer insolation during MIS 5e-5a (125 – 71 ka) were large, ranging 452 – 543 W/m^2, and inciting an immediate response in lake productivity. Summer insolation exhibtied lower-amplitude change during MIS 4 – 3 (71 – 29 ka; 468 – 518 W/m^2), while winter insolation was relatively stable. During the combined effects of intermediate radiation and reduced seasonal variability, large portions of the West Coast were 1) broadly wet throughout MIS 3, and 2) highly sensitive to North Atlantic forcing, namely Dansgaard-Oeschger (D-O) events.

Response to D-O events throughout California, the Great Basin, and U.S. Southwest was geographically variable. In alpine Southern California, these manifested as short, rapid high-productivity, higher-temperature excursions in the Baldwin Lake core. While we have no direct measure of hydrologic change in BDL12 during these interstadials, we hypothesize that enhanced aridity was the likely response, as this was observed at several sites in the surrounding Mojave Desert and U.S. Southwest. Sites on the western and northeastern margins of the Great Basin were wet during D-O events, and no consistent millennial-scale events have been detected at Great Basin interior sites during MIS 3. MIS 2 brought depressed insolation and cold, glacial conditions with variable moisture. While summer insolation did not quite reach MIS 5 maxima (~530-540 W/m^2) at the MIS 2/1 transition, climate was warm and/or dry enough to cause site desiccation at Southern California lakes in semiarid ecoregions, including Baldwin Lake.

We show that the magnitude of past climate variation in the SBM and surrounding region was quite large, and highly sensitive to large-scale, distant climatic drivers, including long-term insolation shifts and North Atlantic SST depression. This highlights the need to better understand how the ocean-atmospheric system transmits change throughout the Northern Hemisphere, and its role in delivering precipitation extremes to the West Coast. This understanding is especially urgent at present, with a rapidly-melting Greenland Ice Sheet, and the potential for further water stress to Southern California and the Southwest. The region's sensitivity to global change, coupled with the radiative effect of enhanced greenhouse gases, support the findings of recent studies (e.g. Cayan et al., 2010; Diffenbaugh et al., 2015; Overpeck and Udall, 2010) that forecast an increasingly arid, high-temperature California.

4. Terrestrial Organics, Vegetation and Wildfire in alpine Southern California from 120 – 10 ka

4.1 Abstract

Macrocharcoal counts, fossil pollen counts, and coarse-resolution isotopic analysis were conducted on the Baldwin Lake core (BDL12), which lies at 2060 m at an ecotone between mediterranean alpine forest and desert in the San Bernardino Mountains of Southern California. Molar C:N values support that summer insolation was a key driver of organic production within the lake during the basin's history. Fossil pollen counts from 108 – 14 ka included significant shifts in coniferous taxa, and shrub and herb ground cover in the Asteraceae family. These changes revealed times of forest expansion and contraction. Shrubland largely replaced forests at 107.4 - 103.9, 88.8, and 69 - 68.2 ka, and 25.6 ka. Comparison with events in the Lake Elsinore pollen record suggested that in the BDL12 record, pollen data grouped by Asteraceae and coniferous taxa may serve as proxies for available moisture, with forests supported during wetter times, and dry conditions initiating landscape conversion to open shrubland (e.g. steppe). Forest expansion and contraction was well-paced with insolation shifts during Marine Isotope Stage 5 (MIS 5; 110 – 71 ka), with increased summer insolation brining drier conditions and vegetation, and summer minima allowing expansion of forests. Wildfire appeared to be most significant for a few kyr as summer insolation rose in the midst of forest-to-shrubland conversion, but was minimal during peak insolation. Vegetation cover, wildfire, and prevailing moisture shifted to be independend of summer insolation after MIS 5, with rapid collapse of the forest and increased wildfire at 71 ka. Forest recovered as a moist regime persisted in the SBM from 65 – 30 ka, bringing with it enhanced wildfire. A 2-kyr arid event before the Last Glacial Maximum (LGM) caused coniferous tree reduction and *Artemisia* expansion, but this recovered to reach a *Pinus*

maximum by the LGM at 22.5 ka. The anomalously warm onset of sea surface temperatures in Southern California during the last two glacials may explain the region's propensity for past extreme and rapidly-changing hydroclimates, as well as its divergence from a largely insolation-driven climate regime.

4.2 Introduction

Ch 3 described climate fluctuations over the past 125 - 12 ka that were detectable from physical and geochemical changes within Baldwin Lake sediment. Here, I aim to supplement this climatic history with additional proxies of stable isotopes, charcoal, and fossil pollen. These analyses provide insight into the paleoecological change in the San Bernardino Mountains (SBM) from 120 – 15 ka. Vegetation cover responds primarily to shifts in moisture availability in mediterranean biomes, and can influence the amount of runoff and erosion into lake basins. A paleoecological history that highlights landscape response helps construct a more complete picture of change already detected in the lake basin.

These analyses are guided by the following research questions on alpine Southern California's past ecosystems:

1) how has the vegetation shifted from 110 - 15 ka, and fire regime from 120 - 10 ka?

2) what prevailing climate conditions can be deduced from palynological data?

3) how do SBM paleoclimate conditions, and events, compare with regional studies?

The age and long-term anoxic conditions in Baldwin Lake have preserved fossil pollen well, creating an ideal candidate for palynological analysis. This history also shows the range of past variation in landscape cover, and may inform future expectations of vegetation change under increasingly warm conditions.

4.3 Background

4.3.1 Setting and Biogeographic Importance

Big Bear Valley (Figure 3.1) is a subalpine valley that lies in the northeast of the rugged San Bernardino Mountains (SBM). In this sector of the SBM, the diverse geology and extremes of climate influence the vegetation assemblage. The region receives some of Southern California's highest precipitation totals, due to the combination of east-traveling Pacific storms and rapid orographic uplift. The climate is mediterranean, with winter-wet and summer-dry conditions that support wildfire during the summer months, though summer thunderstorms also contribute to the annual precipitation total. The Valley itself has a dramatic precipitation gradient: as an example, 2010 precipitation data show a ~1300 mm/yr value at Big Bear Dam at the Valley's western end, while just 15 km away in the Baldwin Lake watershed, the total is ~850 mm/yr (Maurer, n.d.). Despite decreasing precipitation annual totals towards the eastern SBM, the proportion of moisture delivered during the summer months increases towards the east, largely derived from convection and orographic uplift (Anderson and Koehler, 2003).

This precipitation gradient is evident in the vegetation cover. Pine-dominated woodlands of *Pinus lambertiana, P. jeffreyi,* and *P. ponderosa* surround Big Bear Lake, with *Abies concolour, Calocedrus deecurrens* and *Quercus kelloggii* intermixed. Toward easterly Baldwin Lake (Figure 3.1), this assemblage transitions to pinyon-juniper woodland, with relatively xeric taxa (e.g. *Pinus monophylla*, *Juniperus occidentalis*, *Cercocarpus ledifolius*). This woodland co-occurs with Great Basin Sage Scrub (*Artemisia tridentata*) as ample ground cover, particularly in the higher elevations surrounding Baldwin Lake. The Basin surface itself and immediate terrain is categorized as Great Basin Sage Scrub (Minnich, 1976; Minnich et al., 1995). Within 1 km east of Baldwin Lake, desert taxa are admixed with the juniper-pinyon-sage woodland, including

Yucca brevefolia, Ephedra spp., and *Opuntia basilaris*. This is an ecotone between alpine mediterranean forest and subtropical-tropical desert; the Mojave Desert lies at the mountain range's eastern base, in its rain shadow.

In the Big Bear and the northerly Holcomb Valleys, there are clay and quartzite-rich "pebble plains" with markedly different soil and vegetation from the surrounding forests and woodlands. Absent of trees and shrubs, they are isolated much like biogeographic islands, with a few rare perennials adapted to grow in the hardpan soil (Ciano, 1984). A few of these perennials, including Caryophyllaceae *Arenaria ursina* (Big Bear Valley sandwort) *Eriogonum kennedyi* (southern mountain buckwheat), and *Linanthus killipii* (Baldwin Lake linanthus) are endemic to the San Bernardino Mountains, and listed as Forest Service Sensitive Species (Ciano, 1984; Stephenson and Calcarone, 1999).

Big Bear Valley is thus one of the most diverse locations for plant life in the already-diverse California Floristic Province, hosting at least 20 perennials that are endemic to the San Bernardino Mountains (Krantz, 1990). The rugged terrain promotes vegetation patchiness, due to microclimates, active wildfire, and diverse geology. Baldwin Lake is thus well-situated for the study of shifting climate, and plant ranges, over time.

4.3.2 Prior work

Prior analyses on Baldwin Lake cores have focused on the physical and geochemical changes of the sediment, and the long-term climatic drivers for these internal and within-watershed changes (Glover et al., submitted; Kirby et al., 2006). Pollen and charcoal analyses afford additional insight to landscape cover, its change, and moisture availability. Other lake studies from the SBM are confined to the Holocene and include the hydroclimate of Dry Lake (Bird et al., 2010) and Lower Bear Lake (Kirby et al., 2012). Pollen data from Lower Bear Lake

show abundant *Pinus* and fluctuations in wetland plants, though this record is low-resolution during the Late Holocene (Paladino, 2008).

Palynological work throughout Southern California generally derives from lower-elevation terrestrial sites, and marine and island records (Figure 2.1, Table 2.1). Lake Elsinore in Riverside County yielded a hydroclimatic record that spanned MIS 2 (Heusser et al., 2015). In a Diamond Valley deposit dating to mid-MIS 3 (c. 41 ka), Anderson et al. (2002) identified coniferous taxa that are typical of present-day montane environments at higher elevations of at least +900 m. The longest continuous pollen study in Southern California is the 160 ka Santa Barbara Basin (ODP 893) record, which showed depressed temperatures and wetter conditions during glacials. *Quercus* in particular tracked relative temperature change for the easterly Transverse Ranges (Heusser, 1998). Other pollen studies tended to target younger time periods, with a particular focus on paleoenvironmental change since the MIS 2/1 transition (c. 12 ka) and subsequent Holocene change.

Beyond Southern California, other California pollen records are similarly characterized by 1) post-MIS 2 studies that prevent direct chronological comparison to our record, or 2) discontinuity. Pollen studies from the Sierra Nevada (e.g. Anderson, 1990, 1987; Brunelle and Anderson, 2003) post-dated alpine deglaciation and the LGM. Mojave Desert paleoecology has been reconstructed with palynomorphs from pack rat middens that varied widely in time, though were largely from the Holocene (Holmgren et al., 2010).

Similarly, montane macrocharcoal studies in California are from postglacial lakes (e.g. Anderson, 1990; Brunelle and Anderson, 2003; Hallett and Anderson, 2010). Southern California charcoal largely come from the Channel Islands, and have shown increased biomass burning during the Bølling-Allerød (14.7 - 12.7 ka; Kennett et al., 2008) and the Middle

Holocene (Anderson et al., 2009). Microcharcoal counts were collected in the course of Lake Elsinore and Santa Barbara Basin pollen work, but are unpublished (Linda Heusser, pers. comm). This study thus represents the first continuous long record (c. 85 kyr, 110 - 15 ka) of changes in vegetation and fire regime from the Transverse Ranges that span multiple glacial phases.

4.4 Materials and Methods

4.4.1. Stable Isotope Analysis

Coarse sampling from various facies was conducted throughout BDL12, similar to BSi sampling. Horizons covering a wide range of organic matter values were targeted, and removed from the split core surface with a metal scoopula. Samples were then dried in an oven at 60˚C for 24 hours, disaggregated with a mortar and pestle, and weighed. The total $CaCO_3$ in each sample was estimated using bulk carbonate results from the 950˚C loss-on-ignition cook; a minimum of weight of 20 µg $CaCO_3$ was needed for analysis. Analysis was conducted at the University of Saskatchewan Isotope Laboratory for n=25 samples from 1.9 - 20.3 m depth in BDL12 (16.0 - 96.0 ka). Carbonate material was removed during acidification, then mounted in tin capsules for analysis. Both $\delta^{13}C$ and $\delta^{15}N$ were determined, converted to molar values, and reported here as the ratio of molar C:N.

4.4.2. Palynology

BDL12 was initially sampled at ~20 cm intervals from 0.8 - 24 m depth throughout the core; core gaps and later adjustment of absolute depths account for some discrepancy in the 20-cm spacing. Portions of MIS 2 (27.1 - 13.3 ka) were subsequently sampled at 10 cm intervals, due to the slow sedimentation rate during the last glacial. These 1 cm^3 samples underwent standard chemical digestion (e.g. Bennett and Willis, 2001; Faegri et al., 1989), with some

modifications. The initial processing utilized 10% HCl and then 10% KOH for acid and base treatment, with 1 *Lycopodium* tablet (Batch 1031, Lund University) added per sample during HCl digestion. Acetolysis was not performed after pilot sample batches, as grains were identifiable. Fine grains can obscure pollen grains and influence counting, but clay content was established as <20% throughout BDL12. Thus, sieving samples with a finer mesh (i.e. 7-15 μm) is a part of the standard processing that was skipped in this study.

Pollen identification and counting were conducted to a minimum of 300 terrestrial taxa for each sample (n=89 samples). Percents for each taxa were derived from dividing the number of a particular taxa counted over total terrestrial grains, computed automatically in Tilia 2.0.41 software. Pollen Accumulation Rate (PAR) was calculated for each sample with the following formula:

total # terrestrial taxa / (*Lycopodium counted* / 20,848) • sedimentation rate (cm per yr)

Sedimentation rates from Ch 3 were employed. The total percent of certain terrestrial vegetation taxa, e.g. trees and herbs+shrubs, were calculated in Tilia 2.0.41. Totals for 1) coniferous trees, and 2) all Asteraceae pollen, were subsequently calculated in Excel.

4.4.3 Charcoal

Wildfire exhibits a significant spatiotemporal variation, numerous ecosystem and climate interactions, and second-order effects within ecosystems (Pyne et al., 1996). Thus, characterizing this inherent dynamism remains a challenge, particularly in the heterogeneous landscape of mediterranean, alpine ecosystems in California (Parisien and Moritz, 2009; Whelan, 1995). Lake records offer the opportunity to examine wildfire fluctuations as a continuous time series from

accumulated charcoal fragments, which preserve well and withstand harsh chemical processing. Macrocharcoal fragments (>100 μm in diameter) are typically attributed to fires of local, within-watershed origin. Microcharcoal fragments (<100 μm in diameter) can travel over 100 meters, often via wind, and are considered the "background," or extralocal component (Figure 4.1a; MacDonald et al., 1991; Whitlock and Larsen, 2001).

Macrocharcoal core sampling for BDL12 followed Ballard (2009), with longer individual samples taken continuously through a core section (Figure 4.2b). While such analysis is often done in 1-cm intervals, this approach quartered the number of total samples needed and enabled analysis of the entire 27 cm core. Each slice was placed in an Erlenmeyer flask with 25 mL of 6% hydrogen peroxide (H_2O_2) for 72 hours at 50-60˚C to digest most organic matter. Samples were then sieved through a 125 μm mesh, and transferred to a petri dish. A few drops of 0.1% sodium hexametaphosphate were added as a deflocculant, then dehydrated at 50˚C (Myrbo et al., 2005). Some samples did not complete organic digestion after the first round of H_2O_2 processing; these were usually identified at the sieving stage, washed back into their flask, and left to dehydrate over the next 1-3 days. Another 25 mL of H_2O_2 was added, and the digestion and sieving repeated.

To count macrocharcoal, petri dishes were placed on a numbered grid and under a binocular microscope with 40-60x magnification, and counted. These were converted to Charcoal Accumulation Rate (CHAR) values, a measure of number of charcoal fragments deposited per cm per year. For each macrocharcoal sample counted, the number of counts was first divided by the number of centimeters sampled (typically 4), and then multiplied by the sedimentation rate of the mid-point depth of that sample.

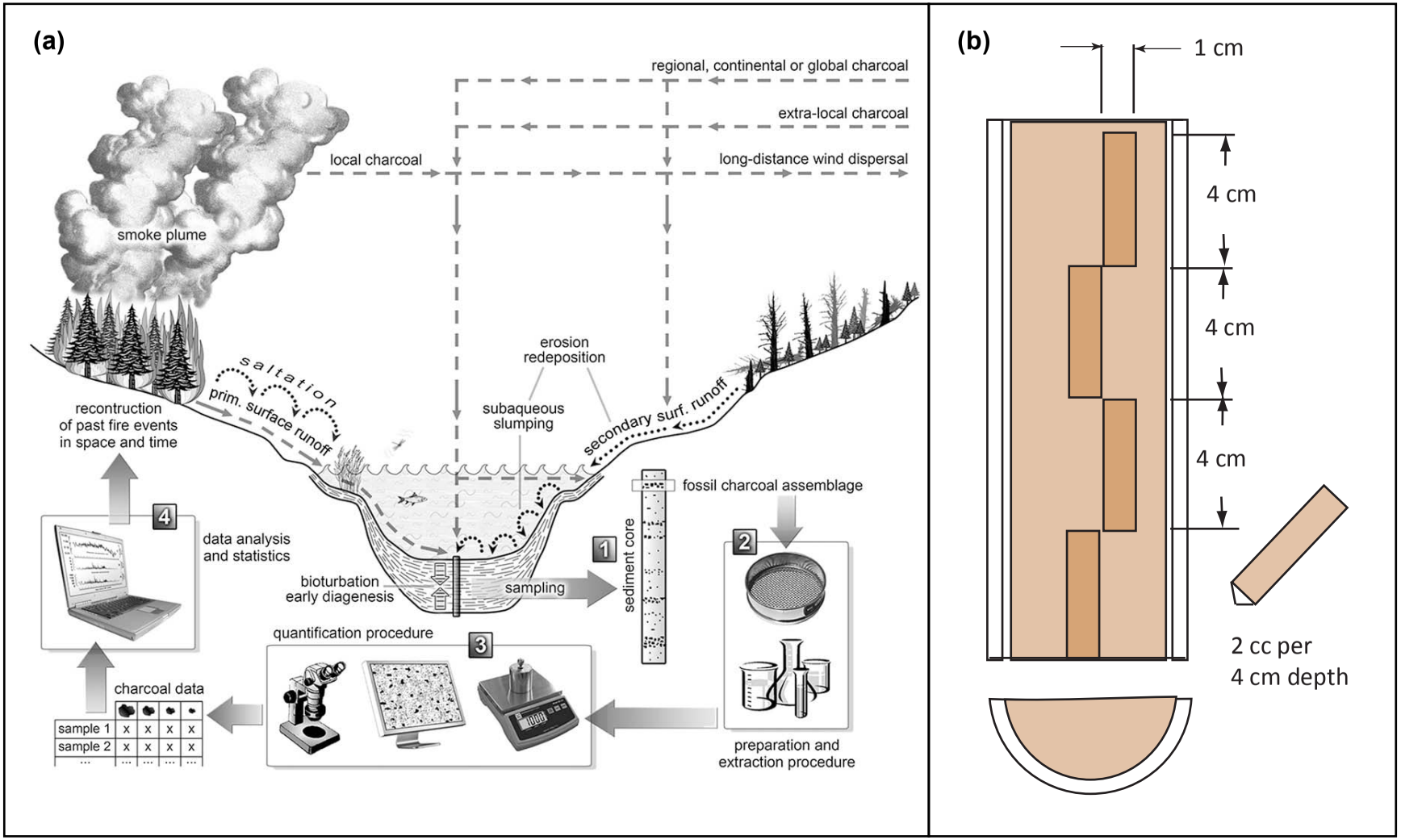

Figure 4.1. (a) Schematic of the stages of charcoal production from wildfire, its deposition into lakes, and analysis from sediment cores. Diagram from Conedera et al. (2009). (b) Coarse sampling strategy employed throughout Baldwin Lake core BDL12's charcoal analysis. Diagram from Ballard (2009).

4.5 Results

4.5.1 Stable Isotopes

Stable isotope data is shown in Figure 4.2(b), alongside relevant proxy data biogenic silica and organic matter from Ch 3. This coarse-resolution dataset generally tracked total organic matter in the lake, and summer insolation at 34˚N, over the period 96.0 - 16.0 ka. Molar C:N is low during MIS 5.3, at values <2. A section of higher-resolution sampling from 81.8 - 87.2 ka across MIS 5.1 and MIS 5.2 remained high, and highlighted the relationship to high summer insolation values (Figure 4.2b). Molar C:N values ranged 14.3 - 18.9 at this interval. Values then were relatively invariable for MIS 4-3 (75 - 29 ka), ranging between 6 - 9. By comparison, high-resolution molar C:N data from BLDC04-2, analyzed at the same lab, ranges from 11.6 - 19.1 during the interval 7.75 - 8.10 m (42.0 - 43.9 ka; Kirby, unpubl. data). During the last glacial, molar C:N declined in tandem with organic matter after the Last Glacial Maximum, and remained low (<2) until the last data point at c. 16 ka.

4.5.2 Fossil Pollen

Thirty-five different taxa groups were identified in the course of pollen identification and counting from samples that ranged c. 108 - 14 ka. A full list of identifiable taxa is shown in Appendix 4.1; some of these groups have very minimal presence in the dataset, and are not used in the ensuing figures and discussion. Those taxa that showed discernible change throughout the record were used for cluster analysis, and are shown in Figure 4.3, including tree and shrub taxa frequently found at other sites in California (e.g. *Pinus*, *Quercus*, *Artemisia*, Amaranthaceae). Notably, Poaceae, a common taxa in Sierra Nevada records, was largely absent in BDL12.

Cluster analysis revealed eight major zones throughout the record that largely correlate with shifts in *Pinus*, *Artemisia, Quercus,* Taxodiaceae-Cupressaceae-Taxaceae (TCT), and

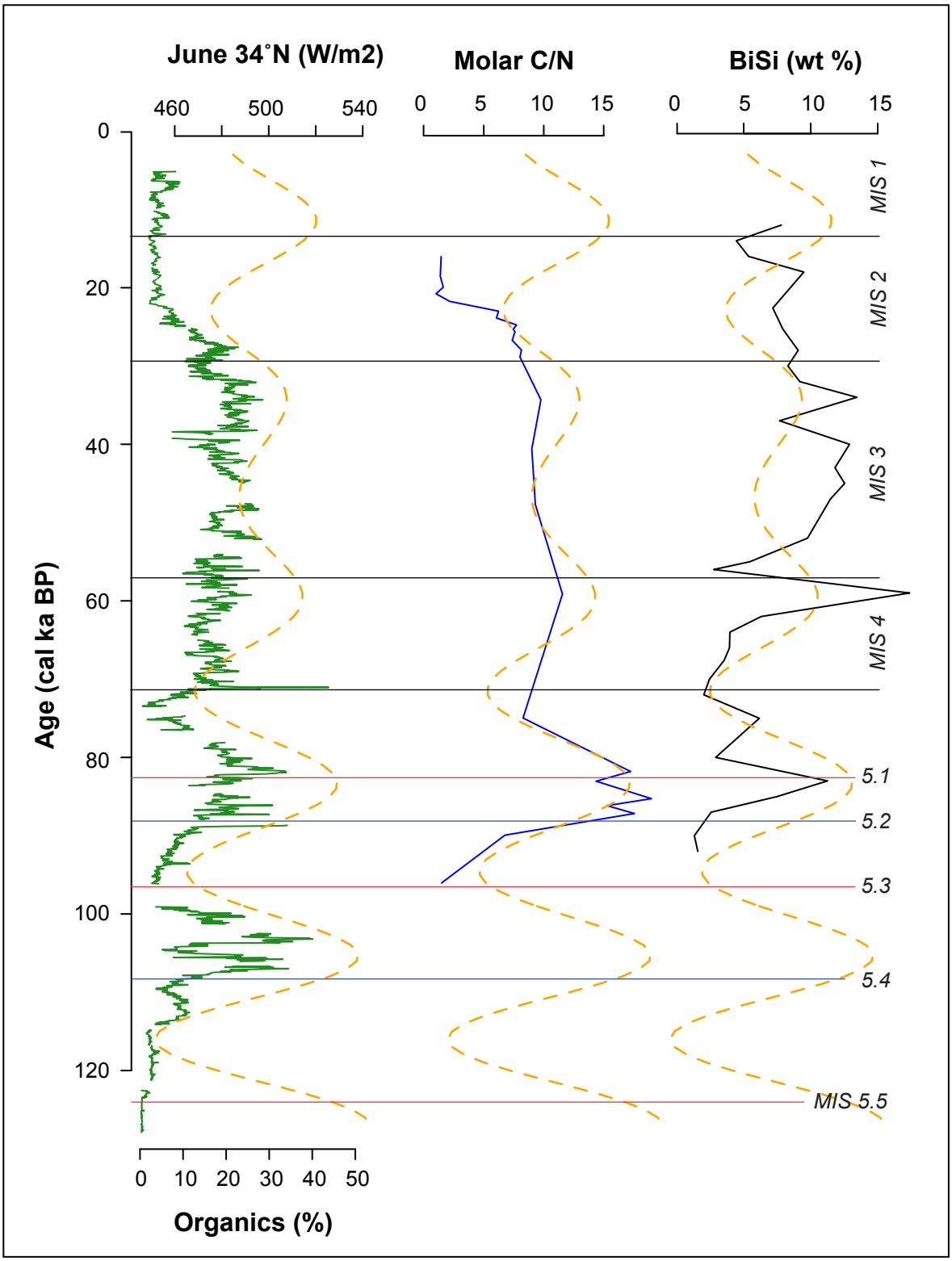

Figure 4.2. (a) Bulk organic matter (%) from loss-on-ignition and summer insolation at 34˚N, from Ch 3. (b) Molar C/N isotopic data with 34˚N summer insolation (same units and scale as [a]). (c) Biogenic silica (wt percent) and 34˚N summer insolation (same units and scale) from Ch 3.

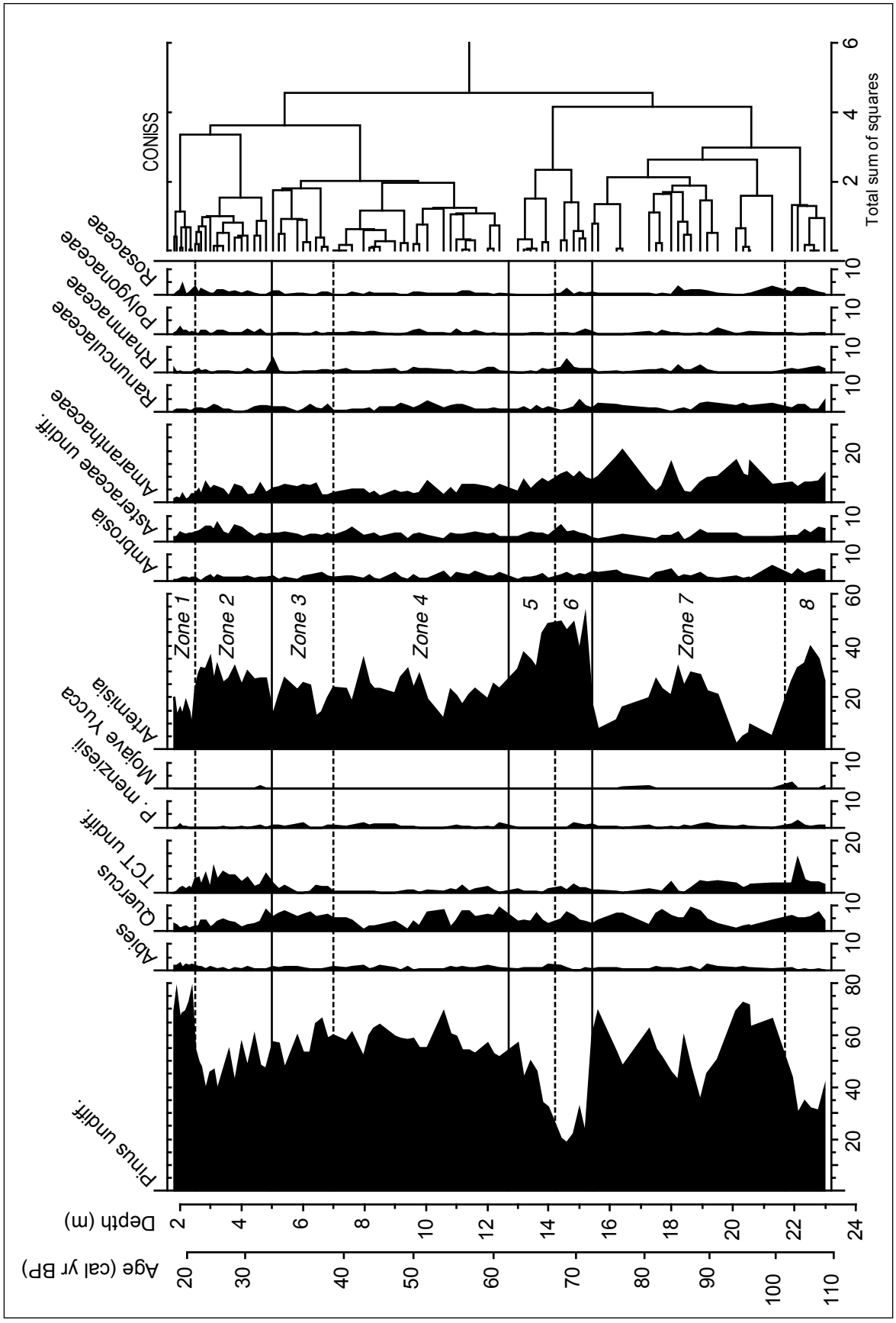

Figure 4.3. Selected pollen taxa (trees and herbs) used for cluster analysis in Tilia 2.0.41, and pollen zonation (solid and dashed lines).

Amaranthaceae. Shifts and percents of these groups that changed with each zone, and details on depth and age of each zone, are detailed in Table 4.1. About half of these zone boundaries occur at "breaks" in the cluster analysis that may be an artefact of sampling/core gaps of at least 2 kyr at these same horizons. Aquatic vascular plant taxa and algae underwent dramatic shifts throughout the record (Figure 4.4). *Pediastrum*, in particular, is over 80% of the total (terrestrial + aquatic plants) pollen at times. However, these aquatic taxa do not show an obvious synchronicity to other climate parameters known in the basin, or other proxy data.

The most striking shift in vegetation in Big Bear Valley since 108 ka was the ongoing fluctuation between *Pinus* and *Artemisia*, which remained anti-phased throughout the history of the basin. *Pinus* reached minima at 107.4 - 103.9 ka, 88.8 ka, 69 - 68.2 ka, and 25.6 ka. The plots for total coniferous trees and all Asteraceae (Figure 4.4) closely mimicked the shifts in *Pinus* and *Artemisia*, in timing and amplitude. The % *Pinus* was the largest contributor to the coniferous total, and % *Artemisia* the major component of total Asteraceae.

4.5.3 Charcoal

CHARs data (Figure 4.5) show that influx of charcoal to Baldwin Lake remained at low levels (<0.1 particles per cm^2/yr) until c. 70 ka. The highest relative influx during this phase of basin history was from 112.8 - 110.8 ka, and 91.1 - 84.6 ka. CHARs rose quickly at the onset of MIS 4 c. 70 ka and reached 0.1006 particles per cm^2/yr. MIS 3 was a time of charcoal production and deposition during the previous Stages. Peaks over 0.1 particles per cm^2/yr occurred during MIS 3 at 54.6, 54.4, 53.1, 50.4, 35.8, 31.7, and 31.3 ka. Of these, CHARs at 31.7 ka were highest for MIS 3, with 0.1859 particles per cm^2/yr. Charcoal counts declined steadily during the transition to MIS 2, with little-to-no charcoal production and deposition occurring. Values

Table 4.1. Key changes within pollen zones for BDL12.

Zone	Age and Depth	Key Pollen changes
1	14.7 – 23.8 ka 1.8 – 2.5 m	• *Pinus* 64-76%, peaked at 22.4 ka • *Artemisia* below 20% • slight rise in Polygonaceae to 2.5 % at 16.9 ka • *Abies* present throughout
2	23.8 – 31.0 ka 2.5 – 5.0 m	• *Artemisia* between 22 – 35% • *Pinus* gradually declined from 57% to 47% • TCT rises and sustains 6-7%
3	31.0 – 38.5 ka 5.0 – 7.0 m	• sustained *Quercus* (5-7%) and Amaranthaceae (5-7%) throughout; Amaranthaceae declined to 2.7% by 36.7 ka • variable *Pinus* (47-57%) and *Artemisia* (12-27%)
4	38.5 – 60.7 ka 7.0 – 12.4 m	• relatively stable *Pinus* with some variation (50-68%) • *Artemisia* fluctuates between 11-34%, variable *Quercus* (0.7 – 13%), low TCT (<1%) for most of zone
5	60.7 – 68.2 ka 13.0 – 14.0 m	• marked decline in *Pinus* (56% to 23%) • *Artemisia* rises (30 to 47%) and so does Amaranthaceae (7 to 10%)
6	68.2 – 72.0 ka 14.4 – 15.4 m	• lowest sustained *Pinus* (≤30%) in record • abundant *Artemisia* 36-50% • higher Amaranthaceae (9-12%), Ranunculaceae (up to 4%), Rhamnaceae (up to 5%)
7	72.0 – 99.3 ka 15.4 – 21.3 m	• change throughout, with high *Pinus* (68%) at onset and 93.9 ka, and minimum of 34% at 88.9 ka. • *Artemisia* had anti-phased change with *Pinus*, including lows 7.8% (72.8 ka) and 2% (93.9 ka). • Amaranthaceae fluctuated between 3.5-20% • *Quercus* variable (1.2 – 8%), very gradual rise of TCT throughout from <1% to ~4% at 88.8 – 91.2 ka.
8	102.9 - 108.4 ka 21.9 – 23.0 m	• variable TCT (3-12.8%), *Artemisia* rose and maintained levels at 26-38%. • high *Myriophyllum* (>20%) at 102.9 and 105 ka.

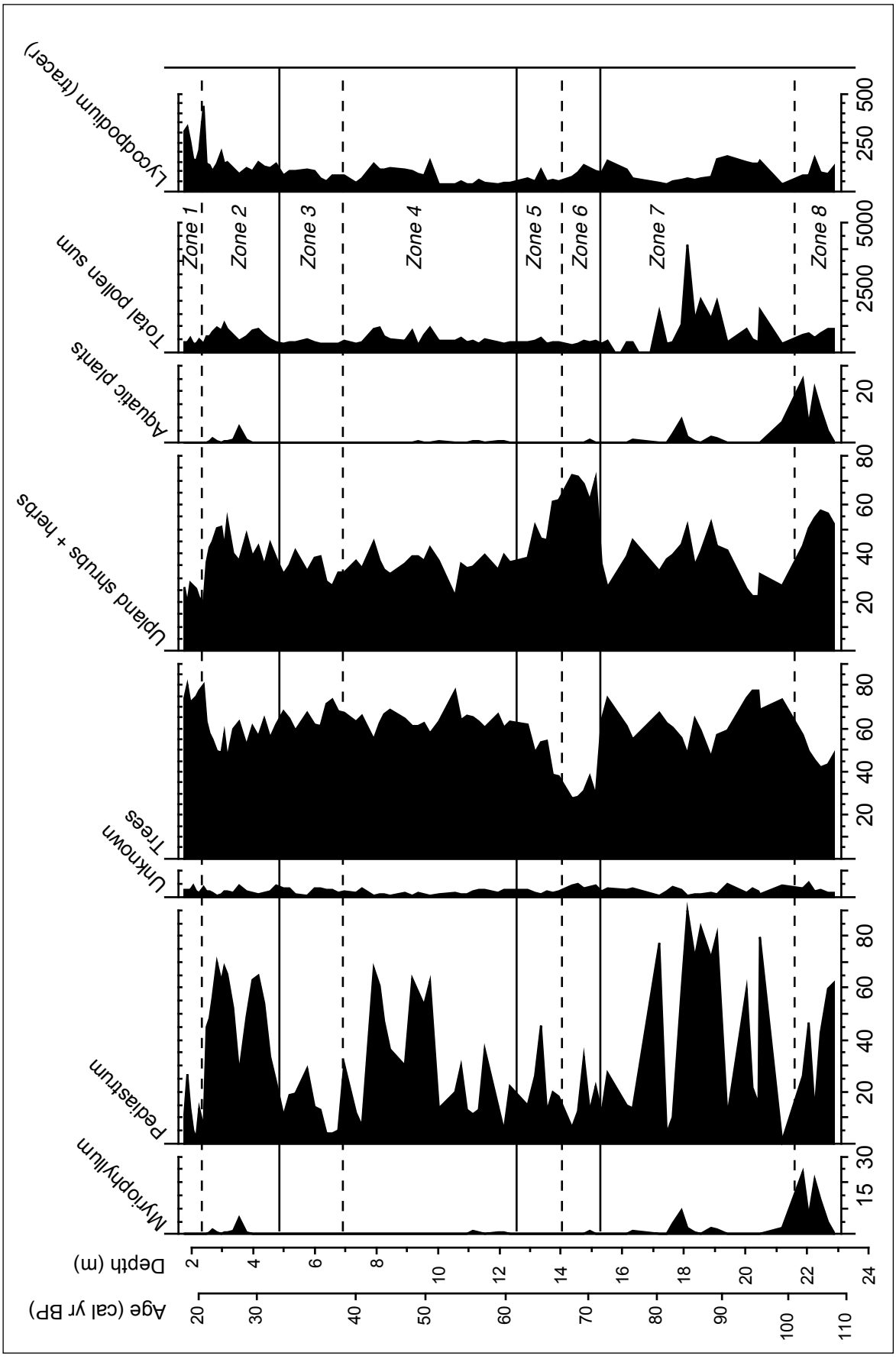

Figure 4.4. Aquatic, tracer, and pollen sum data from Baldwin Lake core BDL12.

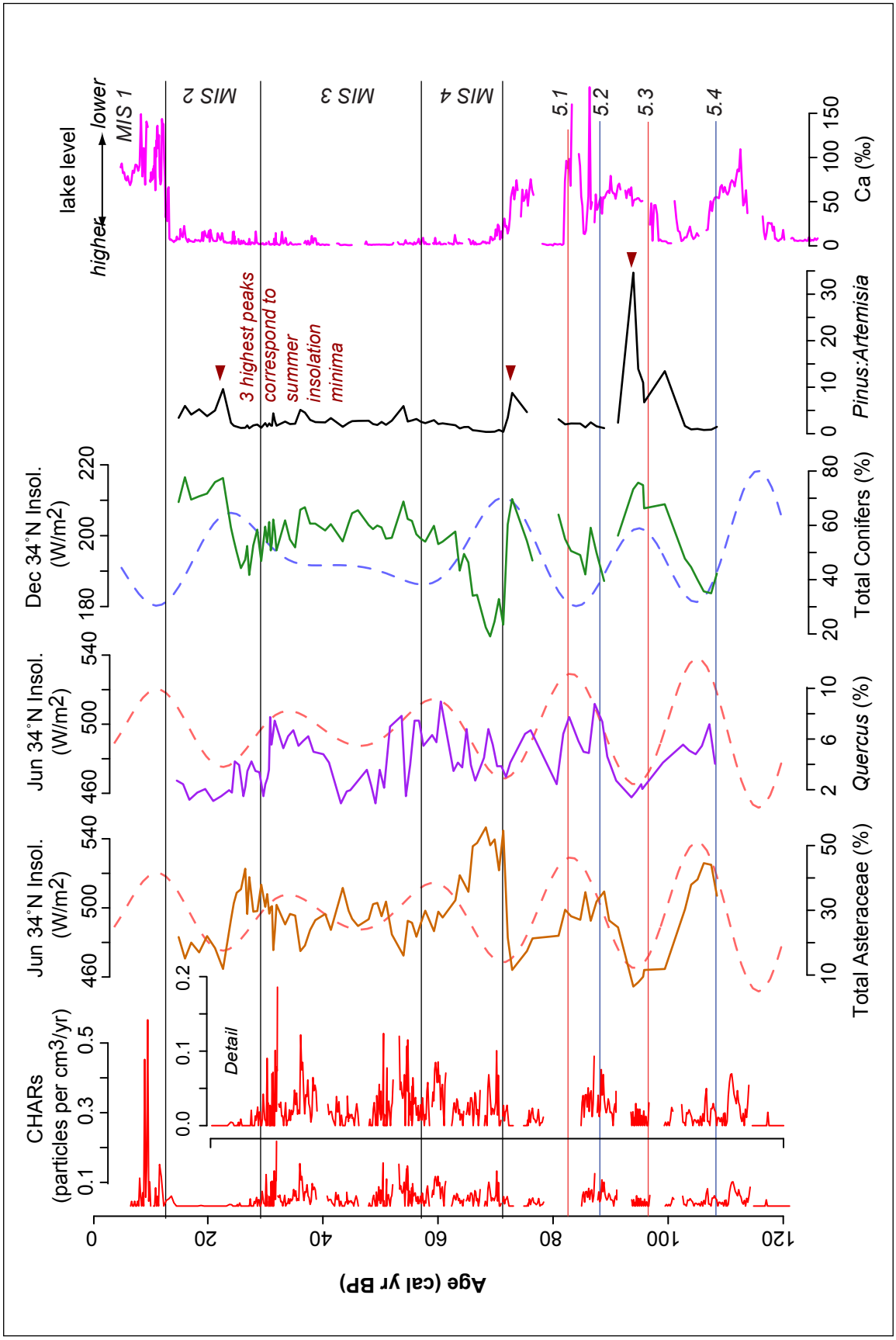

Figure 4.5. CHARs data, with selected pollen data, including aggregated coniferous taxa, all Asteraceae family counts, and ratio of *Pinus:Artemisia* counts. Calcium (Ca) pXRF data shown as proxy for lake level.

remain low from 29.0 - 11.3 ka, below 0.03 particles per cm^2/yr throughout, with mode = 0 particles per cm^2/yr.

The return to charcoal deposition at 11.3 ka was sudden, reaching its highest values in the record of 0.42 - 0.53 particles per cm^2/yr from 9.3 - 8.7 ka. This was one of the most chronologically uncertain sections of BDL12, however, with many previously-documented indicators of site desiccation by this time.

4.6 Discussion

4.6.1 Does isotopic data reveal organic matter source?

New isotopic data (Figure 4.2) generally showed that molar C:N, like BSi and total organic matter, changed in tandem with summer solar radiation values at 34˚N. This suggests that both terrestrial runoff, and primary productivity, were contributors to the total organic matter at long, orbitally-induced timescales based on summer solar radiation.

The interpretation that BSi tracks autocthounous production, while molar C:N shows allocthounous production, was not straightforward in this record. BSi in the Baldwin Lake core actually shows higher-amplitude change at the MIS 4/3 boundary and throughout MIS 3, compared to the relative staticity of molar C:N at values below 10. This suggests that the landscape was relatively stable, with a consistent runoff regime that persisted for ~40 kyr. The divergence and independent behavior of BSi and molar C:N data, with no clear link or antiphasing between the two as organic sources "switch," has been documented elsewhere (Brenner et al., 1999; Michelutti et al., 2005). Organic matter measured in lakes tends to be dominated by primary productivity (Dean and Gorham, 1998), and the $\delta^{13}C$ of organic matter can be affected by several processes that ultimately influence molar C:N values. These influences may include including macrophyte growth, atmospheric CO_2 exchange, and

photosynthesis rates within the lake (Brenner et al., 1999). Baldwin Lake may have been subject to some of these effects. Some evidence for that is the co-occurrence of *Myriophyllum* (water milfoil)'s secondary peak at c. 84 ka and the highest molar C:N detected in this analysis (~19).

Episodic change due to hydrologic extremes was not apparent in this isotopic dataset, likely due to the coarse sampling resolution. Finer sampling and analysis may reveal centennial- and decadal-scale changes, however, as the subset of MIS 3 data (Kirby, unpubl.) showed. In that dataset, a lighter sediment package with reduced organic matter reached molar C:N values over 12, values that have been linked to increased allocthonous organic input (Lami et al., 1994). Significant smaller-scale changes in basin erosion and runoff may have occurred during MIS 3.

4.6.2 Climate change from pollen data

In order to examine how Baldwin Lake's vegetation responded to known hydroclimatic events in the past, this dataset was compared to the high-resolution dataset at Lake Elsinore during the MIS 3/2 transition, and MIS 2 (Figure 4.6). Rapid increases in Asteraceae and *Juniperus* declines showed that arid conditions persisted from 27.5 - 25.5 ka, punctuated with brief reversals to wet events. Baldwin Lake total Asteraceae exhibited the same double-peak and reversal at this time, and a slow decline into the Last Glacial Maximum afterwards (Figure 4.6). Total coniferous taxa from Baldwin Lake changed in tandem with its lower-elevation *Juniperus* counterpart. Gradual decline started 32 ka, and reached minima during the arid phase; Heusser et al. (2015) noted that available moisture throughout Southern California began a slow decline 32 ka. At 25.5 ka, Lake Elsinore *Juniperus* recovered rapidly wihtin 2 kyr, while *Pinus* and other conifers at Baldwin Lake expanded over the course of 3 kyr to reach peak values at the LGM. Recent synthesis of West Coast paleoclimate sites noted widespread moisture at Southern

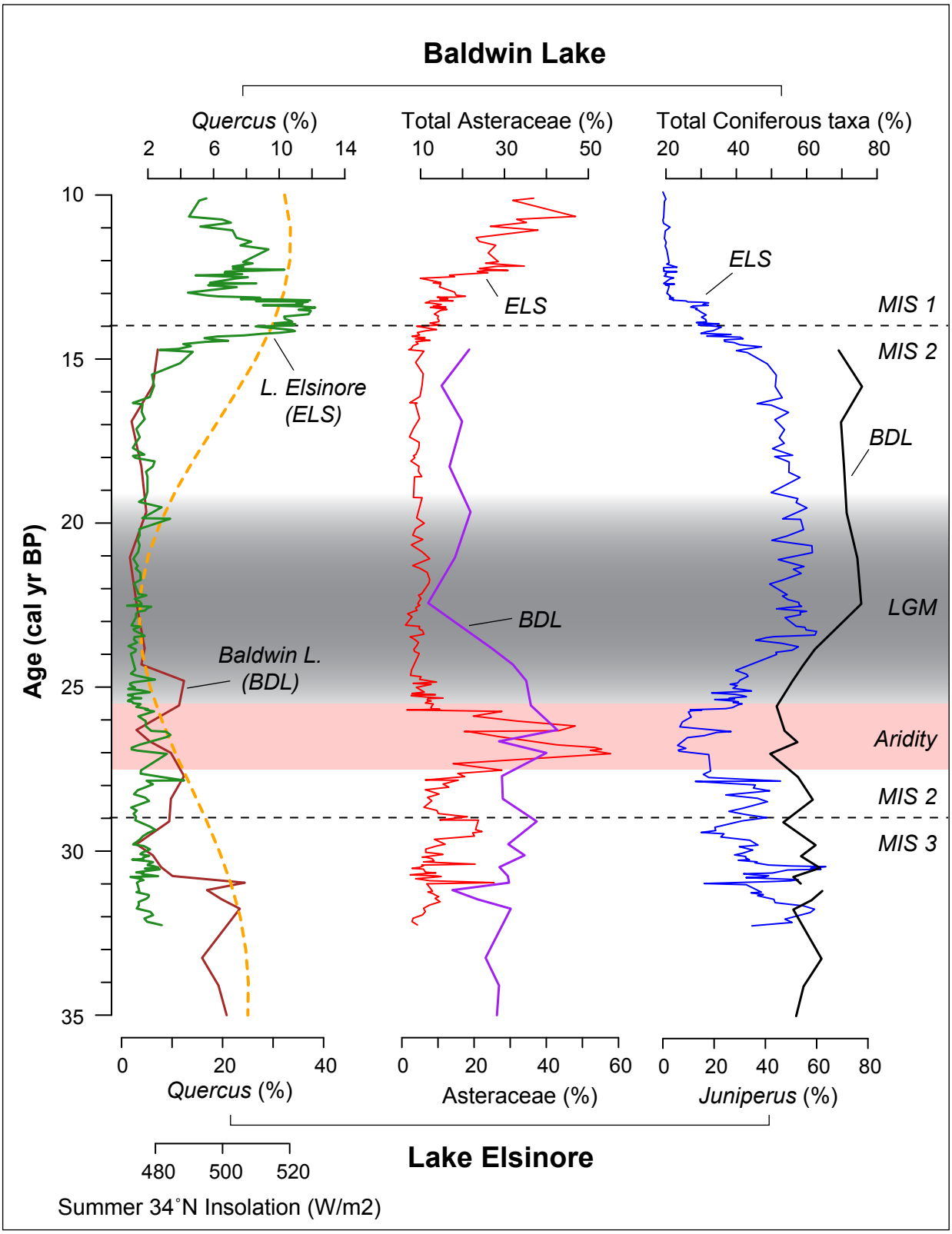

Figure 4.6. Comparison of selected pollen data from Lake Elsinore (ELS) and Baldwin Lake (BDL) during late MIS 3 and MIS 2, with LGM (26 - 19 ka; Clark et al., 2009), and southern California pre-LGM aridity (27.5 - 25.5 ka) identified in Heusser et al. (2015).

California sites during the LGM, and modeled that the most-likely cause of a moisture influx was a heightened pressure gradient that directed storms into the region (Oster et al., 2015).

The interpretation that abundant conifers signaled wet conditions, while Asteraceae signaled dry, was extended to the rest of the Baldwin Lake record. Several changes in forest cover were apparent, particularly during MIS 5, when coniferous expansion was correlated to increases in winter insolation. Summer insolation was coupled with the conversions to steppe-like shrub cover, including abundant *Artemisia.* This suggests that insolation and changes in available moisture from the Pacific were closely related from MIS 5d – 5a (110 – 71 ka).

This connection and tendency for slow, millennial-scale vegetation change was disrupted at the onset of the penultimate glacial at MIS 4. *Pinus* declined from 60% to 24% between 72.0 - 71.2 ka, a period <800 years when summer solar radiation was at a minimum. Conifers gradually recovered throughout MIS 4, paced with the increase in summer, instead of winter, radiation. Wet MIS 3 followed, including the longest sustained forest of the record. High abundance of coniferous taxa (>50%) continued for ~30 kyr until the above-mentioned arid, then moist, shifts during the last glacial from 27.5 – 22 ka. The increase in coniferous taxa to a maximum (77.4%) at 22.5 ka again does not follow its MIS 5 tendency to change with winter insolation, implying other forcing mechanisms.

These results suggest that two different climate regimes affected forests in the San Bernardino Mountains over the past 120 kyr: during MIS 5, high-amplitude shifts in insolation drive both locally-available radiation and moisture for vegetation. After 71 ka, hydroclimate and available moisture impacted the expansion and contraction of forests in alpine Southern California on more rapid scales, and by mechanisms other than solar radiation. Intriguingly, the past two glacials show different vegetation states: despite the decline of coniferous taxa from 29

– 24 ka, percents remained relatively higher and didn't exhibit the rapid contraction in under 1 kyr that marked the onset of MIS 4. Early MIS 4 was the sparsest forest in the record, with expansive dry, cold, steppe-like ground cover. Meanwhile, *Quercus* is the only taxa that exhibited shifts in its abundance that generally tracked summer insolation throughout the entire record, and across the MIS 5/4 boundary (Figure 4.5). *Quercus* has been invoked as a proxy for warmer temperatures in other California sites such as the Santa Barbara Basin (Heusser, 1998) and Clear Lake (Adam and Robinson, 1988), which may explain its response to available radiation, rather than moisture, over long timescales.

4.6.3 Linkages between wildfire, vegetation, and climate drivers

Despite the high-amplitude shifts of MIS 5 substages, charcoal deposition rates were modest prior to MIS 4. Available fuel from forests largely existed during cold, moist periods, climatic conditions that may have shortened the duration of California's typically dry summers, and suppressed evaporation. The highest charcoal deposition during in MIS 5 happened at the leading edge of summer insolation rises at 112.8 - 110.8 ka, and 91.1 - 84.6 ka. This suggests that a threshold in summer insolation (465 - 475 W/m^2) was needed to produce dry fuel.

Rapid increase in charcoal deposition occurred at 71 ka, concurrent with forest collapse. Wildfire gradually declined as shrubland persisted throughout MIS 4, and began increasing towards the MIS 4/3 boundary as forests expanded again. Wildfire exhibited its longest period of dynamic activity during MIS 3. With broad peaks in CHARs at 57 - 49 ka and 40 - 28 ka, and a decline in the middle spanning 47 - 40 ka, data of this proxy mimicked the low-amplitude cycle of summer insolation between 60 - 29 ka (Figure 4.5). The two summer insolation peaks reached over 500 W/m^2, times when abundant forest cover (and fuel) remained on the landscape.

The second-highest CHARs peak in the record occurred at 32 ka, coincident with the onset of drier conditions in Southern California (Heusser et al., 2015). Macrocharcoal deposition was suppressed throughout the last glacial in the Baldwin Lake basin for 18 kyr (28 - 14 ka), perhaps initiated with forest contraction during the arid phase from 27.5 – 25.5 ka. Declining summer insolation and lower evaporation rates in the mountains likely prevented the vegetation drying necessary for wildfire, though microcharcoal spikes occurred during the LGM at lower elevations (Pospelova et al., 2015; Heusser, unpubl. data). The highest CHARs peak in BDL12 coincided with the large charcoal pieces recovered from a trash layer and radiocarbon-dated to ~11.8 ka. Comparable fossil pollen data was not well-preserved after 14.6 ka, however.

4.6.4 The Role of the Pacific

Herbert et al. (2001), in a review of alkenone-derived sea surface temperatures (SSTs) along the California Coast, noted that Southern California SSTs were tightly coupled in timing, pace and duration with global benthic oxygen records during MIS 5 and MIS 4. Comparison of the LR04 stack (Lisiecki and Raymo, 2005) with Southern California sites ODP 1012 and ODP 1014 show this similar pacing during MIS 5 and 4 (Figure 4.7). After MIS 4, SST warming along the California coast was 5-10 kyr premature to terrestrial deglaciation, with the largest anomaly in Southern California. Herbert et al. (2001) attribute this to a weaker California Current, which would have lessened cooler water brought to Southern California, and allowed greater propagation of subtropical waters northward. In the Western Pacific, SSTs off the coast of Japan are anomalously colder as southern California SSTs warm prematurely during the last glacial at 24 ka. A weaker North Pacific High (NPH) would have produced these temperature differences at opposite ends of the Pacific (Yamamoto et al., 2007).

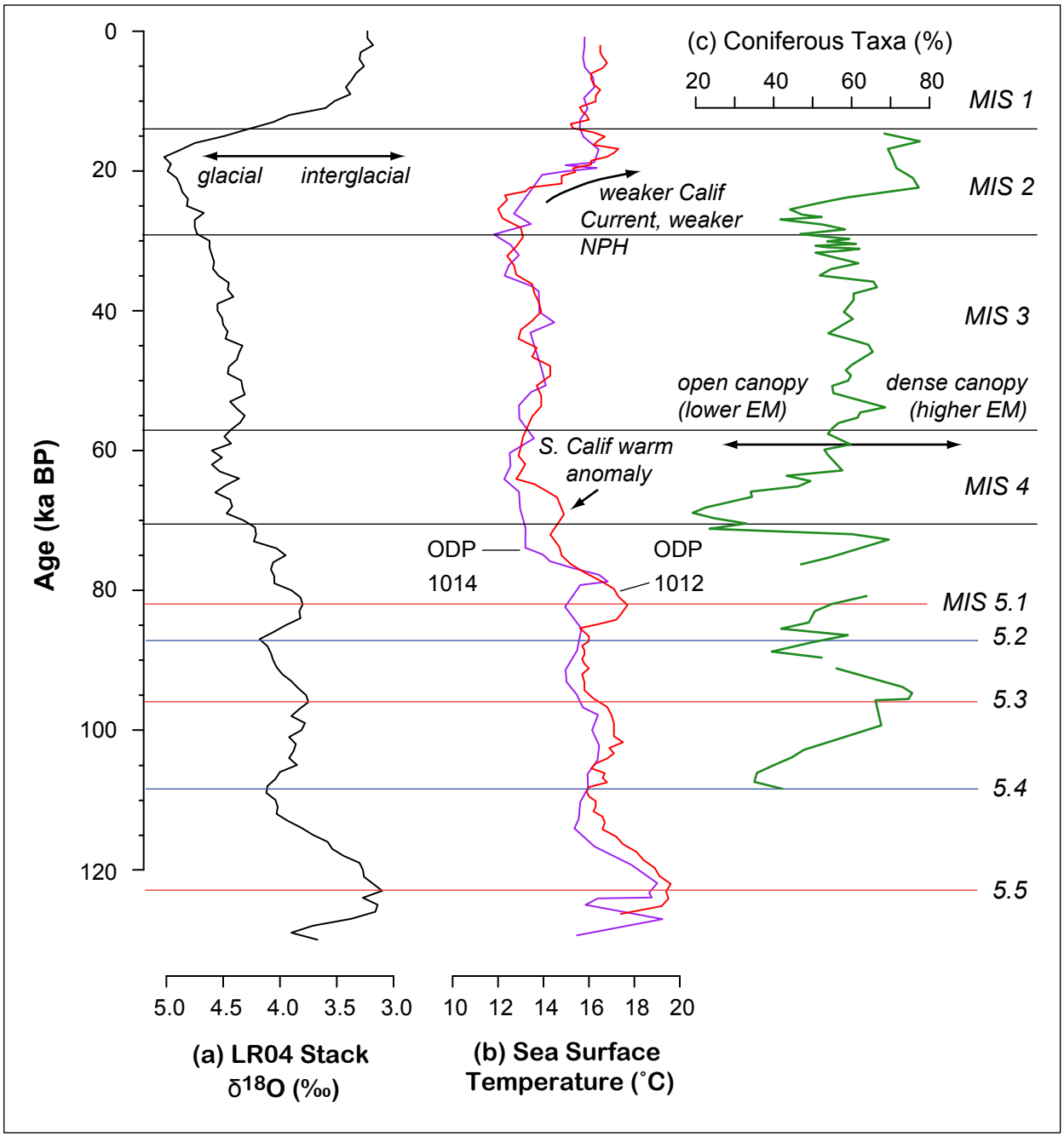

Figure 4.7. Comparison to oceanic change, including (a) benthic $\delta^{18}O$ stacked data (Liseicki and Raymo, 2005). (b) Sea surface temperature data from Southern California margin sites ODP 1012 (Herbert et al., 2001) and 1014 (Yamamoto et al., 2007). (c) Total coniferous pollen counted in Baldwin Lake. NPH = North Pacific High, EM = effective moisture.

SST data from ODP 1012, the closest to the Los Angeles Basin, show that Southern California's divergence from global benthic isotopes may have started during MIS 4. SSTs increased in the first half of MIS 4, a perturbation not observed at ODP 1014, nor at other northerly offshore sites (Herbert et al., 2001). This was coeval with the widespread aridity and contraction of forests observed in the SBM during early MIS 4.

Both ODP 1012 and 1014 showed the "early onset" of warm SSTs during MIS 2, with a slow rise that began 25 ka, and led the increase of the global benthic record by 4-5 kyr (Figure 4.7). Notably, ODP 1012 increased over 2˚C from 23.5 - 21.8 ka, during summer insolation minima, the midst of the LGM, and enhanced moisture delivery to southern California (Oster et al., 2015). This enhanced moisture supported the forest expansion that began c. 25 ka in the San Bernardino Mountains, and warmer SSTs may indicate that offshore southern California was a potential source. A weaker NPH and California Current has been invoked as causes for these warmer SSTs (Yamamoto et al., 2007), though this does not agree with a stronger NPH, the suggested cause for moisture influx to southern California during the LGM (Oster et al., 2015).

4.7 Conclusions

New coarse-resolution stable isotope data from BDL12 showed coupling between molar C:N values, summer insolation, and total organic matter from 100 – 16 ka. Finer-resolution analysis would be necessary to examine times when terrestrial runoff contributes more or less to this organic matter than biogenic silica, another coarse-resolution dataset that serves as a proxy for lake primary productivity.

Pollen data largely revealed the influence of available insolation and moisture on the vegetation in alpine Southern California. *Quercus* abundance was closely tied to changes in local summer solar radiation throughout the record. Pollen in the Asteraceae family and aggregated

coniferous tree taxa were also influenced primarily by solar radiation during MIS 5 (108 – 71 ka). Conifers expanded with winter radiation increases, while herb and shrub cover expanded with summer radiation. This suggests that moisture availability shifted over long and gradual timescales, with winter insolation increases as the primary driver that promoted moisture delivery to southern California. CHARs remained below 0.1 particles per cm^2/yr, implying that wildfire was not a major agent of landscape change compared to modern fire regimes. Fire largely appeared at the leading edge of summer insolation rises just prior to MIS 5.4 and MIS 5.2, as vegetation shifted from forest cover to more open shrubland. Offshore SSTs were predictably paced with global isotopic shifts during MIS 5.

Rapid decline of coniferous pollen occurred at 71 ka, with a large increase in charcoal production. Coniferous forests ultimately recovered by 65 ka and persisted for ~30 kyr throughout wet MIS 3. Available fuel and some fluctuations in summer insolation produced a more dynamic fire regime. Pollen data from Lake Elsinore and BDL12 show that the onset of the last glacial (MIS 2) was hydrologically dynamic, with heightened aridity 27.5 – 25.5 ka, and regrowth of dense coniferous forest by the LGM (22.5 ka).

Overall, southern California paleoclimate and vegetation since the penultimate glacial (c. 71 ka) shows the influence of local insolation shifts, but this was not the primary driver for hydroclimate and vegetation. Rapid (2-3 kyr) vegetation response at terrestrial southern California sites, including Baldwin Lake, suggests that rapid changes in moisture delivery to the region occurred. Anomalously warm SSTs developed 4-5 kyr early offshore of southern California during glacial periods MIS 4 and 2; this may have in turn influenced anomalous local aridity, though the mechanisms of this potential feedback are not fully understood. A weaker

California Current would have allowed these warm pools to develop locally, though the state of the North Pacific High during the LGM remains uncertain.

Appendix 4.1 Pollen taxa identified in BDL12. *=those taxa used in cluster analysis, and shown in Figure 4.3.

Trees
Pinus undiff.*
*Abies**
*Quercus**
Fagaceae undiff.
Betula
Caryophyllaceae
TCT undiff.*
Pseudotsuga menziesii
Alnus
Julgans
Yucca spp.*
Celasteraceae
Polemenaceae
Sequoia sempervirens
Papavaraceae
Grossulariaceae
Tsuga
Upland Herbs and Shrubs
*Artemisia**
*Ambrosia**
Asteraceae undiff.*
Amaranthaceae*
Ranunculaceae*
Rhamnaceae*
Polygonaceae*
Convolvulaceae
Poaceae
Rosaceae*
Umbelliferaceae
Ephedra
Onagraceae
Aquatic Vascular Plants
Myriophyllum
Typha spp.
Potamogeton spp.
Nymphaceae *Nuphar*
Algae
Pediastrum
Unidentified pollen and spores
Unknown

5. Holocene Vegetation, Wildfire, and Hydroclimatic History from Lower Bear Lake, San Bernardino Mountains, Southern California

5.1 Abstract

Prior sedimentological and geochemical work on a 4.5 m sequence from Lower Bear Lake showed that enhanced Pacific moisture delivery reached the San Bernardino Mountains throughout the Holocene as a series of centennial-scale pluvial events. Here I present a new age model, stable isotope analysis $\delta^{18}O$ of *Valvata* mollusk shells, charcoal counts, and pollen counts to examine landscape response to Lower Bear Lake's hydroclimatic history. Tree taxa, especially conifers, showed the highest degree of change during pluvial episodes. Amaranthaceae increased throughout the Middle Holocene, suggesting underlying aridity that has been documented northward in the Owens Lake Valley and Seirra Nevada. Charcoal deposition, and by extension wildfire, is most active in the Early Holocene, and second half of the Late Holocene. Supported in part with $\delta^{18}O$ data, Lower Bear Lake's hydroclimate reflects paleoclimate conditions that extended throughout California, the Great Basin, and U.S. Southwest. These widespread events include Early Holocene wet conditions 9.2 – 8.6 ka, the onset of aridity at 8 ka, a generally dry Middle Holocene, wet conditions from 3.3 – 3.0 and 1.5 – 0.9 ka, and dry conditions 3.0 – 2.1 ka that are coeval with the Late Holocene Dry Period. Overprinted on these events are centennial-scale wet episodes, detected with highly-resolved physical and geochemical analyses, that demonstrate the complex, variable nature of Southern California's Holocene hydroclimate.

5.2 Introduction

Holocene (10 – 0 ka) records are abundant and the subject of high-resolution study in California (Figure 2.2), particularly in alpine regions. Such work has improved our understanding of climatic shifts, terrestrial response, and how climate change manifests in the Pacific Ocean and can impact moisture availability in a state subject to water stress. Several megadroughts have been documented during the Holocene in California, at decadal-to-centennial timescales much longer than the current drought (MacDonald and Case, 2005; Mensing et al., 2013, 2004; Stine, 1994). Wet events are extreme and long-lasting in their own right, as evidenced in coastal areas such as the storm events documented at Lake Elsinore (Figure 3.6, Kirby et al., 2013) and the Santa Barbara Basin (Hendy et al., 2012). These events have no analogue in the past 150 years of instrumental records in the Western U.S.

Stratigraphy and analyses from Ch 3 show that Baldwin Lake did not have the continuous sedimentation, nor preservation, for a reliable Holocene history to test the veracity of hydroclimatic events in the San Bernardino Mountains (SBM) that have been documented elsewhere. Here, I supplement the Baldwin Lake record with new analyses of the lake core from the neighboring basin, Big Bear Lake (Figure 3.1). The Big Bear Lake core, referred to as Lower Bear Lake in scientific literature, has been well-dated and the subject of prior sedimentological and geochemical study (Kirby et al., 2012). New trace element, charcoal, and stable isotope datasets and are presented, and past datasets re-examined for insight into moisture delivery and landscape change in the Big Bear Valley during the Holocene. The motivating research questions are:

1) What was Holocene vegetation and wildfire response at a semi-arid montane site during the Holocene?

2) Do new data support the current hydroclimatic interpretation for the SBM, which is a series of Holocene pluvial events?

3) Is the Lower Bear Lake record sensitive to wet and arid episodes documented throughout southern California, the U.S. Southwest, and Great Basin?

5.3 Background

Our current understanding of Holocene climate change in California is one of highly variable hydroclimatic states, with wet and dry extremes that varied in time, or by region. Summer insolation values were highest during the Early Holocene (10 - 7.5 ka), supporting a wet southern California (Heusser, 1998; Holmgren et al., 2010) and aridity in the northern sector of the state and Pacific Northwest (Briles et al., 2008; Hakala and Adam, 2004). The Middle Holocene (7.5 - 3 ka) was a time of widespread warmth and aridity at marine sites (Heusser, 1998), and low-lying terrestrial sites throughout the state (Davis, 1999a; Wahl, 2002). Higher-elevation sites in the Klamath Mountains and the western Sierra Nevada exhibited moist conditions (Briles et al., 2008; Davis et al., 1985; Street et al., 2012), yet Kirman Lake on the eastern flank of the Sierra Nevada entered its driest state (MacDonald et al., 2016). During the Late Holocene (4.0 ka - present), hydroclimatic variability was more widespread as the Pacific Decadal Oscillation strengthened and the influence of El Niño Southern Oscillation (ENSO) expanded northward into California (Barron and Anderson, 2011).

In the SBM, sedimentological analysis of Dry Lake (2760 m) during the Early Holocene supports enhanced storminess and moisture delivery from 9 - 7.5 ka (Bird and Kirby, 2006). A lake lowstand occurred 5.5 ka during an arid Middle Holocene, though sedimentation rates began to increase 4.5 - 4 ka as the Late Holocene approached, coeval with Lake Mojave highstands (Bird et al., 2010).

The Big Bear Basin, a watershed area of 96 km^2, lies north of Dry Lake and the Sugarloaf Mountain ridge in the Big Bear Valley (Figure 2.1). Lower/Big Bear Lake is in the western sector of the valley, and presently a reservoir. Prior to damming in the 19th century, this basin had up to 3000 acres of wetland meadow habitat (Krantz, 1990). As described in Ch 4, this section of the valley is wetter and more diverse in its mesic vegetation than the Baldwin Lake Basin. Prior work on the Lower Bear Lake core showed five horizons of markedly higher total organic matter and molar C:N throughout the ~9 kyr record, interpreted as times of increased terrestrial biomass delivery into the lake, transported via enhanced runoff. These proposed pluvial episodes suggest more episodic, rapid delivery of moisture to southern California and the SBM than the general hydroclimatic history in the region (e.g. a wet Early Holocene, dry Middle Holocene, variable Late Holocene). Enhanced atmospheric rivers to Southern California, due to insolation shifts, variable Pacific atmospheric conditions, and sea surface temperatures, may have produced these wet episodes (Table 5.1; Kirby et al., 2015, 2012). The pollen data reported in Paladino (2008) support the more general Holocene moisture trends for Southern California, rather than punctuated pluvial episodes, though this may be due to differences in analytic resolution between the two studies.

5.4 Materials and Methods

5.4.1 Bayesian Age Modeling

Core BBLVC05-1 was dated with accelerated mass spectrometry (AMS) radiocarbon dating on 33 samples, including 31 discrete materials (e.g., seeds, wood, charcoal) and two on bulk organic matter (Kirby et al., 2012). The Lower Bear Lake chronology has been updated here, in order to utilize the most recent radiocarbon calibration curve (IntCal13; Reimer, 2013), Bayesian age modeling software Bacon 2.2 (Blaauw and Christen, 2011), and improved

Table 5.1. Lower Bear Lake pluvial episodes (Kirby et al., 2012), adjusted for new age Bacon 2.2 age model.

Pluvial Episode	Initial timespan (yrs BP) and duration	Adjusted timespan (BP) and duration
PE-V	9170-8250; 920 yrs	9241 – 8586; 655 yrs
PE-IV	7000-6400; 600 yrs	6913 – 6428; 485 yrs
PE-III	3550-3000; 550 yrs	3317 – 2962; 355 yrs
PE-II	850-700; 150 yrs	834 – 745; 89 yrs
PE-I	500-476; 24 yrs	239 – 164; 75 yrs

understanding of suitable lacustrine macrofossil material that yields optimal radiocarbon dates (Marty and Myrbo, 2014; Zimmerman and Myrbo, 2015). The initial age model interpolated between 23 dates after 10 were rejected for various reasons (Kirby et al., 2012). Re-examination of the initial dataset of 33 included the original set of 23 in the new age model, and an additional date from wood (sample #32; Kirby et al., 2012). Nine dates were still excluded, on the basis of either being 1) bulk material, 2) generated from lower quality material (e.g. roots, stems or leaves), or 3) duplicates from woody material that exhibited an offset from another date at the same horizon on preferable material (e.g. seeds). Bacon 2.2 was run at 5-cm intervals with default priors for the 0 – 450 cm sequence, and extrapolated to the core top and bottom. Since the lake has been highly modified during the last ~150 years (e.g. dredging, impoundment), the exact age of the sediment-water interface is unknown.

5.4.2 Charcoal Analysis

Preparation for charcoal counts was conducted at 1-cm resolution for 0 - 400 cm of core BBLVCV05. Subsampling was done at CSU-Fullerton, with 2 cm^3 sample volume taken from 1-cm intervals. Half of each of these subsamples (1 cm^3 volume) were dissolved for charcoal counting, following the methodology of the Limnological Research Center (2005). Samples were digested in individual Erlenmeyer flasks with 25 mL of 6% H_2O_2 for 48 hours at 50-60˚C. Samples were then rinsed upon a 125 μm mesh sieve, and the remaining fraction washed onto its own petri dish. A few drops of 0.1% sodium hexametaphosphate were added as a deflocculant, then dehydrated at 50˚C. Some samples did not complete organic digestion after the first round of H_2O_2 processing; these were usually identified at the sieving stage, washed back into their flask, and left to dehydrate over the next 1-3 days. Another 25 mL of H_2O_2 was added, and the digestion and sieving repeated.

To count macrocharcoal, petri dishes were placed on a numbered grid and under a binocular microscope with 40-60x magnification, and counted. These were converted to Charcoal Accumulation Rate (CHARs) values, a measure of number of charcoal fragments deposited per cm^2 per year.

5.4.3. Mollusk identification, and geochemical analyses

Mollusks and ostracods had been separated and counted in 10-cm intervals; mollusk-rich horizons of BBLVCV05 include 20 cm, 140 - 160, 180 - 280, and 290 - 320 cm (Kirby et al., 2012). Carbonate-rich samples from the charcoal petri dishes were inspected for shell and precipiate material, and ostracods, mollusks, and $CaCO_3$ precipitates (e.g. *Chara* stems and calcified seeds) were removed and separated. We identified mollusks to family and (when possible) genus level with the aid of Burch (1982). *Valvata* spp. shells, the most-abundant obligate aquatic organisms in the sample collection, were sent for stable isotope analysis at the UCSB Marine Science Institute. For their preparation, samples were weighed, sonicated in distilled water, dehydrated, and disaggregated with a mortar and pestle. At UCSB, 200 μg of sample were analyzed with a Finnigan Gas Bench and Delta XP Isotope Ratio Mass Spectrometer for $\delta^{13}C$ and $\delta^{18}O$.

X-ray fluorescence (XRF) values of the BBLVCV05 subsamples were taken with a portable Innov-X Analyzer at 5 cm intervals. Remaining subsamples of ~1 cm^3 volume were removed from Whirlpaks into individual weighing trays, and covered with a 4 x 4 cm square of Ultralene film. The pXRF device was then pressed into the covered sample to take a 2-minute close reading. Detectable elements include potassium (K), calcium (Ca), titanium (Ti), manganese (Mn), iron (Fe), zinc (Zn), strontium (Sr), and zircon (Zr).

5.4.4 Fossil Pollen Data

Chemical processing methods for pollen data are reported in Paladino (2008), with pollen counts typically achieving at least 200 total terrestrial grains. Pollen counting was conducted at 5-10 cm intervals for the lower 1.5 m of the record, which spanned 9.2 - 4.5 ka. Sample spacing ranged 20-30 cm afterwards, with the exception of the uppermost 10 cm of the core, where I added counts from samples at 5 cm and 10 cm. Data of Paladino (2008), the original sample vials, slides, and counting notes were reviewed. Most grains initially reported as "unknown" in Paladino (2008) had been carefully sketched; I moved these counts into identifiable groups. For the most part, these unknowns resemble Ranunculaceae, Rosaceae, or *Quercus.* Terrestrial pollen totals represent all trees, upland herbs, and shrubs, while the total pollen sum includes these plus aquatic plants and unknown spores, pollen, and palynomorphs. These were used to calculate percentages in Tilia 2.0.44 software, and the adjusted dataset was replotted with the new age model, and resultant cluster analysis.

5.5 Results

5.5.1 Bayesian Age Modeling

The new age model (Figure 5.1) shows a 300-400 year deviation for boundaries of the Early Holocene, compared to the one presented in Kirby et al. (2012). Although the boundaries of the Early, Middle, and Late Holocene are not substantially changed, the timing of PE-V, the earliest and longest lasting of the pluvial events, starts about 300 years earlier. The extrapolation to the bottom of the core (450 cm) shows a large degree of uncertainty, but this extends beyond the relevant paleocological data reported here, which are limited to the finer-grained sediments of the upper 4 m of core. The age of the top 25 cm of core is younger than the model of Kirby et

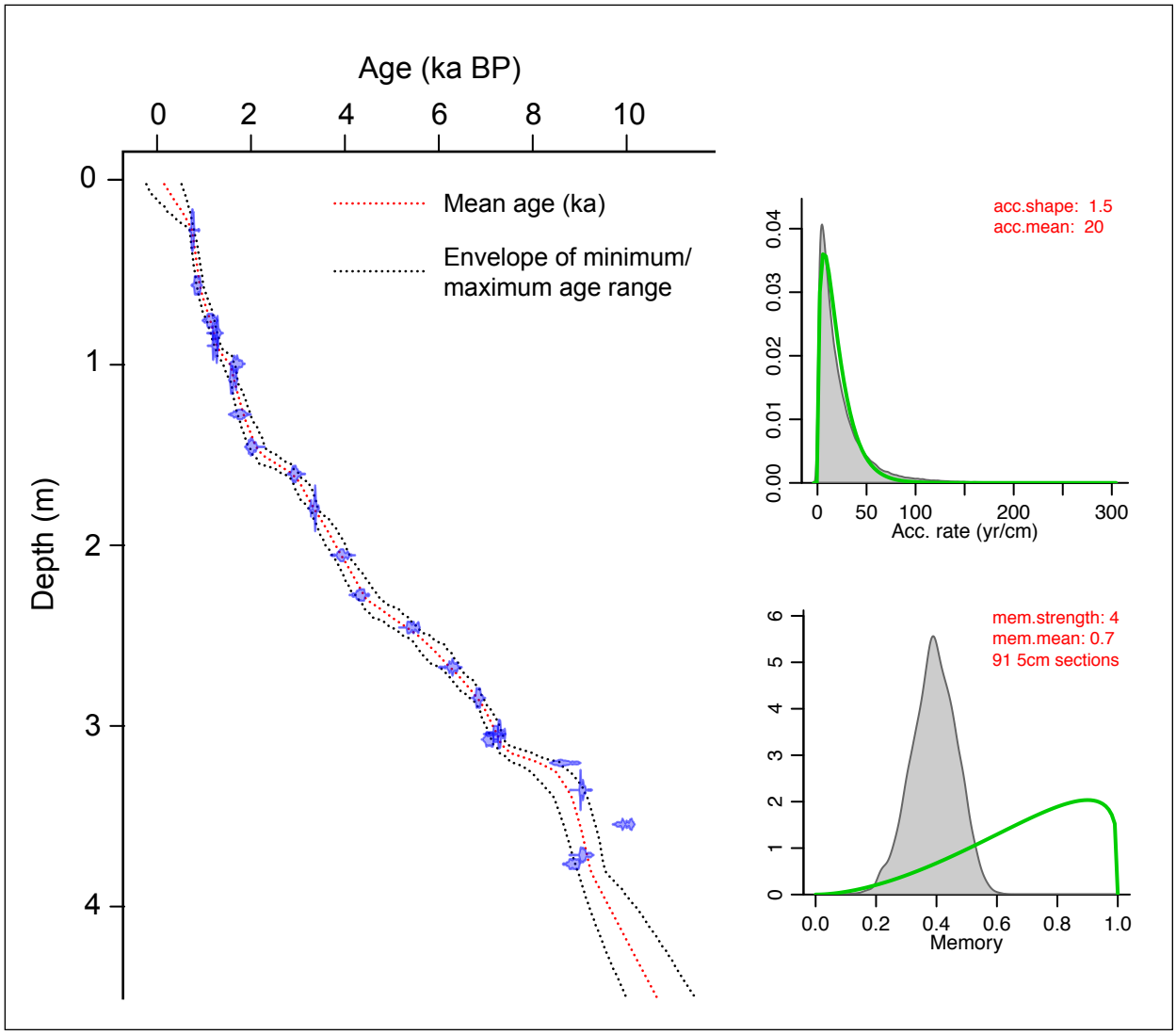

Figure 5.1 Bacon 2.0 age model for Lower Bear Lake, based upon 24 ^{14}C dates from Kirby et al. (2012).

al. (2012) by ~300 years, and the ages of the pluvial events have shifted to those shown in Table 5.1. Notably, the first pluvial (PE-V) is shorter by 265 years with this new chronology.

5.5.2 Charcoal

Charcoal Accumulation Rate (CHARs) ranged from 0 to 28.12 particles per cm^2/yr, values higher than Baldwin Lake results by up to two orders of magnitude. The longest sustained maximum in CHARs occurred during the Early Holocene from 9.1 - 8.9 ka, during the first half of pluvial PE-V and corresponding to an increase in trace element Ca and molar C:N (Figure 5.2g). Charcoal deposition was quiescent during the rest of the Early Holocene. During the Middle Holocene, values were generally low (≤4) but noisy, with moderate excursions of up to 8.5-9.29 particles per cm^2/yr that were centered around 7.3 and 4.4 ka. In the Late Holocene, the longest span of lowest CHARs transpired after pluvial PE-III, lasting 2.9 - 2.0 ka. CHARs maxima of the Late Holocene did not occur until after 2 ka; excursions above 10 particles per cm^2/yr are shorter-lived (<50 years duration) than their counterparts in the Early Holocene, the last time charcoal deposition approached such values. These Late Holocene increases in charcoal deposition occurred 1.68, 1.25, 1.01 - 1.00, .92 - .88, .74-.71, and .29 ka (Figure 5.2g).

5.5.3 Mollusk Identification, Stable Isotope, and Trace Element Geochemical Data

Mollusks identified in the Lower Bear Lake sediments include members of the families Planorbidae and Lymnaeidae, including organisms that largely tend to occupy the littoral (shoreline) area of freshwater systems. Of the extracted mollusks, *Valvata* spp. is the most reliably obligate aquatic (Saxon Sharpe and Peter Hovingh, pers. communication). *Valvata* spp. are valve snails adapted to a specific lake environment: alkaline water, with a tolerance for total dissolved solids up to ~6000 mg/L (Sharpe and Forester, 2008). Mollusk shells were present to ~380 cm in BBLVCV05, but not substantial enough for isotopic analysis below 310 cm (c. 7.3 ka).

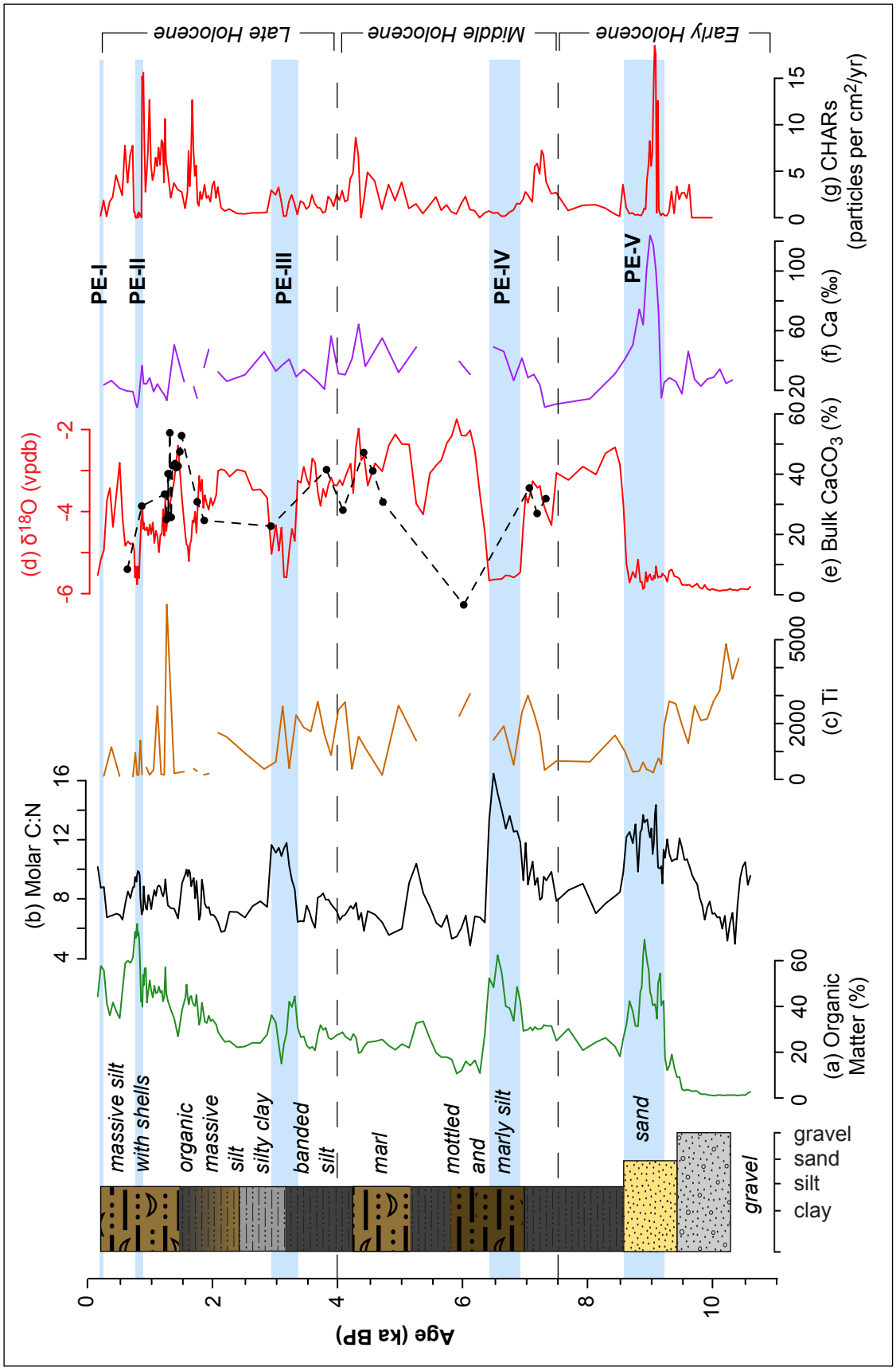

Figure 5.2 Stratigraphy of Big Bear Lake core CCLVC05-1 plotted against new age model, with physical, geochemical, and charcoal data. Organic matter (a), molar C:N (b), and bulk carbonate (e) data are from Kirby et al. (2012). Light blue shading and labels PE-*x* show pluvial episodes of Kirby et al., (2012), adjusted for new age model.

Values for $\delta^{18}O$ are reported as Vienna Pee Dee Belemite (vpdb), and range between shells that are most-enriched in ^{18}O at 1.3 ka ($\delta^{18}O$ = -2.081 vpdb), and the least-enriched ^{18}O shells at c. 6.0 ka ($\delta^{18}O$ = -6.274 vpdb; Figure 5.2d). They generally shifted in tandem with bulk carbonate in the record (Figure 5.2e), with a few exceptions. The paucity of samples below 310 cm (c. 7.3 ka) yielded only one sample during the Early Holocene, with $\delta^{18}O$ = -3.686 vpdb at 7.3 ka. Seven samples of largely moderate ^{18}O enrichment ($\delta^{18}O$ = -4.046 to -2.561 vpdb) span the Middle Holocene from 7.2 - 4.1 ka, and include the least-enriched sample ($\delta^{18}O$ = -6.274 vpdb) at 6.0 ka. This anomalously low observation is the only one available from the period 7.1 - 4.7 ka, the core part of the Middle Holocene. Mollusk shells were especially abundant during the Late Holocene; 18 of the 26 samples analyzed are younger than 4.0 ka, and nearly half (n=12) of the total samples analyzed span the period from c. 1.5 - 1.2 ka. This higher-resolution section shows that *Valvata* $\delta^{18}O$ was relatively stable and highly enriched from 1.51 - 1.32 ka; $\delta^{18}O$ values range between -2.927 to -2.081 vpdb, with one outlier of -4.139 vpdb at 1.34 ka. *Valvata* $\delta^{18}O$ enrichment then decreases to -4.192 to -3.078 vpdb for the next 0.6 kyr (1.24 - 1.30 ka).

Of the trace element x-ray fluorescence data, Ca and Ti are reported here (Figure 5.2c and 5.2f). The Ti record initiated at relatively high values (4000-5000 ppm) alongside coarse-grained deposition until 9.5 ka, then remained <3000 ppm for most of the record, with the exception of a short excursion above 6000 ppm at c. 1.27 ka. Ca was highest during the Early Holocene, peaking at ~124‰ c. 9.0 ka in the midst of the first proposed pluvial PE-V (Figure 5.2; Kirby et al., 2012). Values for Ca remained relatively stable and below 60‰ after this excursion. Unlike the Baldwin Lake record, Ca from trace element analysis and Ca deposited to the basin as bulk carbonate ($CaCO_3$) do not correspond throughout its history (Figure 5.2d and 5.2f).

5.5.4 Fossil Pollen

Coniferous taxa observed and counted included undifferentiated *Pinus, Abies, Pseduotsuga mertenzii*, *Tsuga,* Taxaceae, Cupressaceae, and *Juniperus.* Of these, *Pinus* was the most abundant, ranging 41.1 - 86.1% throughout the record (Figure 5.3); *Abies* ranged 0 - 3.7%, and TCT (combined Taxaceae, Taxodiaceae and Cupressaceae) up to 14.2%. Remaining coniferous taxa are not shown in Figure 5.3, as they were 0% for the majority of samples counted. Most abundant of the hardwood trees was *Quercus*, ranging 1 - 8.2% throughout the record. Ranunculaceae, Rosaceae, undifferentiated Asteraceae, *Ambrosia*, *Artemisia*, Malvaceae and Amaranthaceae were perennial and shrub pollen that were present throughout the record, typically in amounts that varied between 0 - 20%. Rhamnaceae did increase to 33.2% at c. 7.2 ka, and fluctuations for individual taxa are discussed in more detail in the following section, along with environmental interpretations.

Aquatic taxa identified throughout the core included Cyperaceae, *Typha latifolia*, *Myriophyllum*, Nymphaceae, and *Potamogeton.* Cyperaceae varied throughout the sequence, with values up to 16.2%. *Typha latifolia* is most abundant from 9.1 - 4.4 ka, and *Myriophyllum* from 7.3 - 6.7 ka, and 2.3 - 0.3 ka. Cluster analysis to the second order demarcated four zones, 9.1 – 7.1, 7.1 – 6.5, 6.5 – 4.1, and 4.1 – 0.3 ka (Figure 5.3). Vegetation data are generally limited for the Late Holocene, comprising only eleven samples with up to 400-500 years between horizons sampled.

5.6 Discussion

Paleoenvironmental and paleoecological change within the Lower Bear Basin during the Holocene is discussed below by the Early, Middle, and Late stages of the Holocene. Overall, the Bayesian age model has refined the BBLVCV05 sequence, but boundaries between the Early, Middle, and Late Holocene are not markedly different from prior work (Kirby et al., 2012).

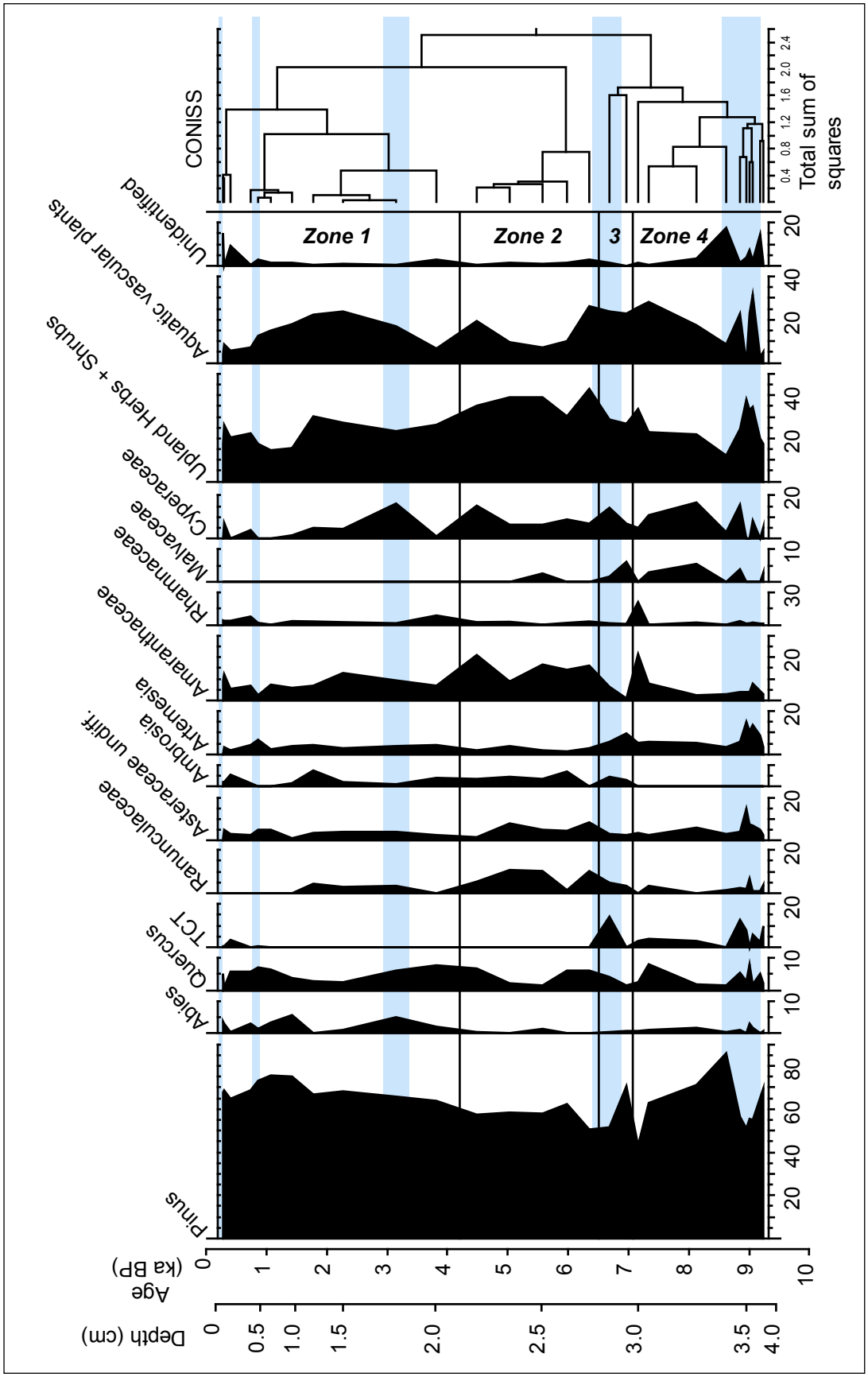

Figure 5.3 Lower Bear Lake pollen, most data from Paladino (2008). Replotted with new grouping, age model and cluster analysis. Zonation done to second-order cluster analysis.

Evidence that led to interpretations of paleoclimatological events described below is detailed in Table 5.2, along with briefly-summarized events from other regional sites.

Coarse-grained deposition marked the onset of the Early Holocene in the Lower Bear basin, with lake sediments and anoxic preservation of fossil pollen beginning 9.5 - 9.2 ka. Sand was still being deposited during PE-V (9.2 - 8.6 ka), and the highest Ca values of the record at this time, along with high CHARs, support high-energy deposition. *Pinus* reduced during PE-V while *Artemisia* expanded towards this end of the valley, suggesting a more xeric vegetation assemblage, though other conifers appear at this time (e.g. TCT). During 9 ka, summer solar radiation averaged 515 W/m^2 at 34˚N, compared to today's 481 W/m^2 (Laskar et al., 2004). The enhanced radiation may have driven shrub expansion, while still the supporting wetter-than-modern conditions that have been documented in the Mojave Desert (Holmgren et al., 2010; Kirby et al., 2015) and at Lake Elsinore (Kirby et al., 2007) during the Early Holocene. Such wet conditions may have supported the *Pinus* re-expansion by the end of PE-V at 8.6 ka. Evidence for a more arid landscape in the Lower Bear basin began 8.1 ka, with lower-energy sedimentation, high $CaCO_3$ values in lake deposits, and gradual expansion of herbs and shrubs. Onset of similar dry conditions occurred in the Sierra Nevada (MacDonald et al., 2016; Street et al., 2012) at 8–7.5 ka. This dry regime lasts until c. 6.9 ka at Lower Bear Lake.

Centered around 7.2 - 6.9 ka at the beginning of the Middle Holocene, episodic sedimentation occurred including charcoal deposition, and Rhamnaceae reaches unprecedented levels of 33% of pollen counts. Intriguingly, zonation independently identified a distinct pollen zone that is near-parallel with PE-IV, spanning 7.1 - 6.5 ka. TCT reappeared for the duration of PE-IV, but other aspects of the vegetation response are ambiguous on moisture conditions: shrubs and herbs continued to expand throughout, and wildfire was quiescent. If PE-IV was

Table 5.2 Summary of Lower Bear Lake basin events during the Holocene, supporting evidence, and comparison to regional records.

Sedimentological, Geochemical, and Paleoecological Evidence	Paleoenvironmental Interpretation	Regional Records
Late Holocene (4 – 0 ka)		
0.83 – 0.75 ka: CHARs are <1 particles per cm^2/yr **1.4 – 0.9 ka**: high *Pinus* (75-75.5%) and *Abies* (5.6% at **1.4 ka**); three CHARs excursions ≥10 particles per cm^2/yr **1.5 – 1.3 ka**: ^{18}O-enriched shells (average: -2.085 vpdb) **3.1 – 2.1 ka**: Aquatic plants expand; *Typha latifolia* declined permanently while *Myriophyllum* expanded. Low organics, CHARs <1 particles per cm^2/yr **2.8 – 2.2 ka**. **3.3 – 3.0 ka**: increased molar C:N and organics; increases in *Abies* and Cyperaceae at **3.1 ka** **4 – 3.5 ka**: static vegetation similar to Middle Holocene values; *Quercus* rose while aquatic taxa declines	**0.83 – 0.75 ka**: PE-II suppressed wildfire **1.5 – 0.9 ka**: $\delta^{18}O$ suggests decreasing evaporation with time **3.0 – 2.1 ka**: low energy deposition and limited wildfire, aquatic plants expand in quiet waters **3.3 – 3.0 ka**: PE-III moisture supported *Abies* expansion **4.0 – 3.5 ka**: relatively warm, dry and stable conditions of Middle Holocene continued	**0.4 ka:** Silver Lake wet **0.8 ka:** Silver Lake wet **1.0 – 0.7 ka**: Medieval Warm Period in Sierra Nevada **1.5 – 1.4 ka**: enhanced sedimentation at Dry Lake **2.7 – 2.0 ka**: prolonged aridity in California Central Coast (Zaca Lake, Dingemans et al., 2014) **2.8 – 1.85 ka**: Late Holocene Dry Period throughout Great Basin (Mensing et al., 2013) **3.2 – 1.8 ka**: Lake Elsinore dry (Kirby et al., 2010) **4.0 – 3.0 ka**: Sierra Nevada cool and wet (Street et al., 2012)
Middle Holocene (7.5 – 4 ka)		
4.4 ka: increased charcoal deposition **6.4 – 4 ka**: low organics, high carbonates, *Pinus* in the range 50-62%, shrub+herb totals range 27-43%, Amaranthaceae particularly expansive (6.3 – 21%). **6.0-5.9 ka**: ^{18}O-depleted mollusk (-6.274 vpdb) and highest $CaCO_3$ (54%) **6.9 – 6.4 ka**: high molar C:N and organics; suppressed CHARs and $CaCO_3$ deposition, TCT expansion **7.1 – 6.5 ka**: pollen zone 3, *Pinus* decreased and shrub, herb, aquatic plant expanded **7.1 – 6.9 ka**: increased CHARs and Ti **7.16 ka**: low *Pinus* (41.4%) and unusually high expansion of Rhamnaceae (33.6%) **7.2 – 7.1 ka**: littoral mollusks present; $\delta^{18}O$ of *Valvata* moderate (-4.046 to -3.425 vpdb)	**4.4 ka**: no change in other proxy data to support cause of enhanced wildfire **6.4 – 4 ka**: relatively stable landscape, with low-energy deposition and infrequent low severity wildfire **6.0 ka**: Ca-saturated lake with relatively warm lake temperatures **6.9 – 6.4 ka**: vegetation and wildfire response to PE-IV ambiguous **7.1 – 6.9 ka**: high-energy deposition **7.2 – 7.1 ka**: lower, relatively warmer lake	**4.5 – 4 ka**: enhanced sedimentation in Dry Lake (Bird et al., 2010) **5.5 ka**: precipitation began to increase in Sierra Nevada (Street et al., 2012); lake lowstand at Dry Lake (Bird et al., 2010) **6.9 – 4.3 ka**: Owens Lake lowstand (Bacon et al., 2006) **7.2 – 2 ka**: no charcoal deposition in Dry Lake (Bird et al., 2010) **7.5 – 6.0 ka**: western Sierra Nevada aridity (Swamp Lake, Street et al., 2012) **7.8 – 4.0 ka:** aridity in Mojave Desert (Silver Lake and Mojave River headwaters, Kirby et al., 2015) **8.0 – 3.0 ka**: eastern Sierra Nevada aridity (Kirman Lake, MacDonald et al., 2016)

Table 5.2 *cont.*

Sedimentological, Geochemical, and Paleoecological Evidence	Paleoenvironmental Interpretation	Regional Records
Early Holocene (10 – 7.5 ka)		
8.1 – 6.9 ka: low organic, Ca, and charcoal deposition; bulk $CaCO_3$ >40% **8.6 ka**: *Pinus* reached highest values in core (86%), declined to ~71% by **8.1 ka** while grasses, shrubs, and aquatic plants expanded **9.2 – 8.6 ka**: sand deposition, high Ca and CHARs, second-highest concentration of herb + shrub pollen (36.8% at 9.1 ka) while *Pinus* declined and TCT increased.	**8.1 – 6.9 ka**: low-energy deposition prevailed **8.6 ka**: Expansive forest present by this time produced from prior wet years, and wildfire clearing understory **9.2 – 8.6 ka**: High-energy deposition during PE-V with frequent wildfire, supported by more open vegetation cover and available fine fuels. Vegetation assemblage more xerix; *Artemisia* expanded its range into western part of Valley.	**8 ka**: onset of Sierra Nevada aridity (Swamp Lake, Street et al., 2012; Kirman Lake, MacDonald et al., 2016) **10 – 9 ka**: summer insolation highs of 518 – 515 W/m^2 at 34˚N (Laskar, 2004) **11 ka:** arrival of C_4 grasses to Mojave Desert due to expanded North American Monsoon (Holmgren et al., 2010) **11.6 – 7.8 ka:** enhanced moisture in Mojave Desert (Silver Lake, Kirby et al., 2015)

indeed a period of enhanced moisture from the Pacific, it would be an anomalous response for California sites: Owens lake reached a ~1.6 kyr lowstand at 6.9 ka (Bacon et al., 2006), and sedimentation slowed in the SBM at Dry Lake (Bird et al., 2010).

Mollusk $\delta^{18}O$ data became available at the onset of the Middle Holocene. This proxy can potentially capture numerous environmental processes occurring in lacustrine sites; analysis of modern fauna can provide insight to most-important factors, and is not available for this study. Generally, these data are interpreted as a measure of temperature or the precipitation-evaporation ratio at the site, with more-enriched values indicating higher temperatures and greater evaporation (Leng and Marshall, 2004). At Lower Bear Lake, 6.0 ka was least-enriched, suggesting the lowest evaporation regime of the record at a time when other proxies and regional records signal widespread aridity. From 6.4 - 4 ka, deposition slowed again and physcial and geochemical proxies resembled those of the second half of the Early Holocene, though with more apparent small-order variability (Figure 5.2). Enhanced moisture in the Sierra Nevada at 5.5 ka (Street et al., 2012; MacDonald et al., 2016) apparently did not affect the SBM, as Dry Lake's lowstand occurred at this time (Bird et al., 2010), and Silver Lake, a basin fed by waters originating in the SBM, was persistently dry during the Middle Holocene (Kirby et al., 2015). Upland herbs and shrubs, including Amaranthaceae, maintained relatively high levels during this time. At 4.5 - 4.3 ka, changes occurred at Southern California lakes: a brief highstand at Owens Lake was detected 4.3 ka (Bacon et al., 2006), and CHARs increased at Lower Bear Lake, though all other proxy data remain remain static. Sedimentation increased at Dry Lake 4.5 - 4.0 ka (Bird et al., 2010),

Low-organic and high-carbonate deposition into Lower Bear Lake and a stable vegetation cover of *Pinus* and shrub+herb cover continued into the first part of the Late Holocene, 4.0 - 3.5

ka. PE-III was designated at 3.3 - 3.0 ka, and *Abies* and Cyperaceae expanded. Aquatic vegetation expanded in the millennium afterwards, with *Typha latifolia* disappearing from the record as *Myriophyllum* expanded in apparently quiet waters from 3.0 - 2.1 ka. CHARs deposition was particularly reduced 2.8 - 2.2 ka. This evidence shows that the Late Holocene Dry Period, first documented in the southern Great Basin from 2.8 - 1.85 ka (Mensing et al., 2013), expanded its influence to coastal California. Already documented at Zaca Lake from 2.7 - 2.0 ka (Dingemans et al., 2014), the Lower Bear Lake record shows that alpine Southern California also experienced extended aridity until as late as 1.5 ka, a horizon where the second-most enriched $\delta^{18}O$ *Valvata* were sampled, suggesting higher evaporation rates. At this time, sedimentation increases at Dry Lake (Bird et al., 2010), and declining $\delta^{18}O$ values from 1.5 - 1.3 ka support reduced evaporation, and a possible return to cool and wet conditions. Conifer taxa are abundant and wildfire dynamic, with charcoal deposition occurring at levels not observed since the Early Holocene. Lower Bear Lake's response to the Medieval Climate Anomaly was not clear. While the MCA was consistently dry in the Sierra Nevada from 1.0 - 0.7 ka (Street et al., 2012; MacDonald et al., 2016), the Zaca Lake record showed a more complex hydroclimatic history, with reversed (i.e. wet) conditions from 0.9 - 0.7 ka, perhaps due to its more coastal location (Dingemans et al., 2014). In addition, Lower Bear pollen data are coarser-resolution for the Late Holocene, which obscured centennial-to-decadal scale changes. PE-II spans 0.83 - 0.75 ka in the midst of MCA detected elsewhere, although the fine resolution of this event is difficult to compare to other datasets. Only CHARs show rapid reversal to near-zero values during this hypothetically wet time.

The finer-resolution data that are available for Lower Bear Lake do show that the Late Holocene was a time of high-amplitude, rapid change. In particular, the CHARs record over the

last 2 ka shows a dynamism not observed in other parts of the sequence. This may be due to shorter-term, higher-amplitude hydroclimatic variability induced by a more variable El Niño Southern Oscillation after 3 ka (Conroy et al., 2008). The Serrano tribe also occupied Big Bear Valley seasonally during the Late Holocene (Chong, 2003), and harvested *Pinus monophylla* seeds employing fire (Benedict, 1924). Throughout the U.S. Southwest, *Juniperus* was a preferred fuel for Native American cooking fires, as it is a slow burning wood (Lanner and Lanner, 1981). Eastward in Big Bear Valley towards the Baldwin Lake basin, the co-occurrence of *P. monophylla* and *J. occidentalis* would have provided this food-fuel combination to Native Americans, and potentially been an important source of charcoal production.

5.7 Conclusions

Existing and new data from Lower Bear Lake show Holocene record that had a dynamic response both to regional climate trends observed at other sites, and the Pacific-derived pluvial episodes proposed by Kirby et al. (2012) that range from 655 – 14 years in duration. The following research questions have been addressed:

1) What was Holocene vegetation and wildfire response at a semi-arid montane site during the Holocene?

Coniferous forests, largely comprised of *Pinus*, persisted in the Big Bear Valley during the Holocene. Significant terrestrial vegetation shifts and excursions tend to be short-lived (<400 years, often coeval with pluvial events. Increases in shrubs and herbs occurred during the Middle Holocene, evidence that supports an arid state in the SBM for most of the Middle Holocene. Wildfire activity was evident from CHARs c. 9.1 ka, then followed by relatively slow deposition during the Middle Holocene. The higher-amplitude, shorter-lived shifts in CHARs during the

Late Holocene, particularly since 1.6 ka, attest to a greater variability in wildfire occurrence and extent.

2) Do new data support the current hydroclimatic interpretation for the SBM, which is a series of Holocene pluvial events?

Pluvial events were identified with positive excursions towards more organic matter and molar C:N, caused by enhanced water availability, runoff, and deposition into the basin. The vegetation and wildfire response reported here were not consistent for all pluvials. Early and Middle Holocene pluvial events involved declines in *Pinus,* while other conifers (TCT, Taxaceae-Cupressaceae-Taxodiaceae) expanded. Higher concentrations of shrubs and herbs were also detected during pluvials, suggesting these too expanded and created a more open landscape. Enhanced charcoal deposition occurred at the onset of Early Holocene and Late Holocene events, but not all. Late Holocene events coincide with apparent expansion of *Abies,* though fossil pollen data was collected at coarser intervals. While the landscape response was inconsistent across events, it is key to remember that these varied in duration, and each occurred at times when different climatic drivers may have been impactful (e.g. enhanced summer insolation during the Early Holocene).

3) Is the Lower Bear Lake record sensitive to wet and arid episodes documented throughout Southern California, the U.S. Southwest, and Great Basin?

Lower Bear Lake experienced several well-known events documented during the Holocene. These include wet conditions during the Early Holocene from 9.2 – 8.6 ka, the onset of dry conditions c. 8.0 ka that lasted into the Middle Holocene and became drier c. 6.0 ka. Greater hydroclimatic variability persisted through the Late Holocene, with wet conditions 3.3 – 3.0 ka, dry conditions 3.0 – 2.1 ka correlating with the Great Basin Late Holocene Dry Period,

and cool and wet conditions 1.5 – 1.2 ka. Overprinted on these widespread events, there was an apparent site-specific hydroclimatic variability and complexity, evidenced by the repeated pluvials, and the complexity of the Medieval Climate Anomaly. This may be due to the SBM's proximity to a marine moisture source, though determining the precise origin and mechanism for enhanced storm delivery from the Pacific remains to be investigated.

6. Dissertation Conclusions

Over the past 125,000 years in alpine southern California, its climate and landscape have undergone significant change, as evidenced from a pair of lake cores in the Big Bear Valley of the San Bernardino Mountains (SBM). The first general research question of the dissertation asked: how can temperature and available moisture changes in the SBM inform our understanding of climate phenomena that affected southern California? Evidence from these sites demonstrated that millennial-scale fluctuations in local insolation, and shifts in eastern Pacific Ocean sea surface temperatures (SSTs), were key phenomena that drove climate change in the region. Summer insolation was the primary influence on lake level and primary productivity changes in Baldwin Lake during Marine Isotope Stages 5e - 5a (c. 125 - 71 ka). During the penultimate glacial, shifts in summer and winter insolation became lower-amplitude and less divergent. This allowed wet conditions to prevail for ~35 kyr until the onset of the last glacial c. 29 ka. Two millennia of aridity marked the onset of the last glacial, with subsequent rapid return of focused moisture to the region by 24-23 ka. These events showed Southern California's proclivity for hydroclimatic extremes, even at times when cold temperatures were present and summer insolation was minimal.

The influence of the Pacific Ocean on these terrestrial climate changes was constant over the past 125 kyr, though it manifested in various ways. Like the coupled insolation and moisture shifts in the SBM during MIS 5, marine records of offshore California are synchronous with summer insolation and the globally-averaged isotopic shifts that demarcate glacial and interglacial periods. This association was less robust during the last glacial; early onset of SST warming during MIS 2 by 5-10 kyr was well-documented along the California margin, and attributed to a weaker California Current. The closest marine record to Southern California

exhibited this decoupling earlier, during the prior glacial MIS 4. This provides a possible cause for the rapid hydroclimatic changed observed c. 71 ka in the SBM. While broadly wet conditions followed during MIS 3, rapid warm excursions in the Santa Barbara Basin are paced with Dansgaard-Oeschger SST increases in the North Atlantic, and caused comparable warm excursions at Baldwin Lake. A dry response at terrestrial sites to these ~1.48 kyr events was widespread throughout California and the U.S. Southwest.

The second broad research question this dissertation addressed was: how has vegetation changed over time, and what role does wildfire play in past ecosystem dynamics? The most pronounced landscape response to temperature and moisture shifts was the expansion and contraction of forests; reduced trees allowed a more open cover of shrubs and perennials. During MIS 5, conifer expansion followed rising insolation, and shrubland increased with summer insolation. This slower, orbitally-paced pattern of change suggests that insolation shifts were the primary influence on the prevailing hydroclimate regime. This vegetation-insolation association changed suddenly 71 ka, shifting toward a hydroclimate subject to high amplitude changes during glacials that had potential to be relatively shorter (i.e. 2-5 kyr, compared to a 10+ kyr insolation cycle), with rapid onset (<1 kyr). Vegetation response to aridity continued to be forest canopy loss and shrubland/steppe expansion, though dry states after MIS 5 were never as long nor pronounced, and moderate-to-high forest density was maintained through the Holocene. Evidence from both lake records showed that wildfire was particularly active in two scenarios: 1) during vegetation shifts from forest-to-shrubland as summer solar radiation increased to values above ~480 W/m^2, and 2) during times of high-amplitude hydroclimatic variability and forest cover, such as MIS 3 and the last ~1.6 ka of the Late Holocene.

Despite differences in duration and timing of Pacific SST changes off the California margin over the past 125 ka, local marine dynamics consistently transmitted climatic change to alpine Southern California. Local increases in SSTs (i.e., within and southward of the Santa Barbara Basin) in particular seem to be the harbinger of dry terrestrial conditions prior to the Last Glacial Maximum, though *how* atmospheric circulation may have changed to accommodate moisture differences between the land and sea is beyond the scope of this project. Still, a sensitivity localized to southern California seems apparent, with past examples of hydroclimatic extremes demonstrating that high-amplitude climate change can manifest rapidly in the area. Coupled with projections that southern California will be warmer and drier for the remainder of the 21st century as greenhouse gas emissions enhance radiative forcing, this is a precarious situation for an already populous and water-stressed region.

7. References

Adam, D.P., 1985. Quaternary pollen records from California, in: Pollen Records of Late-Quaternary North American Sediments. American Association of Stratigraphic Palynologists Foundation, Austin, TX, pp. 125–140.

Adam, D.P., Robinson, S.W., 1988. Palynology of two upper quaternary cores from Clear Lake, County, California [WWW Document]. URL http://www.getcited.org/pub/102754991 (accessed 2.13.12).

Adam, D.P., Sarna-Wojcicki, A.M., Rieck, H.J., Bradbury, J.P., Dean, W.E., Forester, R.M., 1989. Tulelake, California: The last 3 million years. Palaeogeogr. Palaeoclimatol. Palaeoecol. 72, 89–103. doi:10.1016/0031-0182(89)90134-X

Adam, D.P., Sims, J.D., Throckmorton, C.K., 1981. 130,000-yr continuous pollen record from Clear Lake, Lake County, California. Geology 9, 373. doi:10.1130/0091-7613(1981)9<373:YCPRFC>2.0.CO;2

Adam, D.P., West, G.J., 1983. Temperature and Precipitation Estimates Through the Last Glacial Cycle from Clear Lake, California, Pollen Data. Science 219, 168–170. doi:10.1126/science.219.4581.168

Adams, D.K., Comrie, A.C., 1997. The North American Monsoon. Bull. Am. Meteorol. Soc. 78, 2197–2213. doi:10.1175/1520-0477(1997)078<2197:TNAM>2.0.CO;2

Anderson, R.S., 2003. Paleoenvironment of the Owens Lake Area during the late Quaternary., in: Lacustrine Lifestyles Along Owens Lake. ASM Affiliates, pp. 475–488.

Anderson, R.S., 1990a. Holocene Forest Development and Paleoclimates Within the Central Sierra Nevada, California. J. Ecol. 78, 470–489.

Anderson, R.S., 1990b. Holocene Forest Development and Paleoclimates Within the Central Sierra Nevada, California. J. Ecol. 78, 470–489.

Anderson, R.S., 1987. Late-Quaternary environments of the Sierra Nevada, California. University of Arizona, Tucson, AZ.

Anderson, R.S., Betancourt, J.L., Mead, J.I., Hevly, R.H., Adam, D.P., 2000. Middle- and late-Wisconsin paleobotanic and paleoclimatic records from the southern Colorado Plateau, USA. Palaeogeogr. Palaeoclimatol. Palaeoecol. 155, 31–57. doi:10.1016/S0031-0182(99)00093-0

Anderson, R.S., Byrd, B.F., 1988. Late-Holocene Vegetation Changes from the Las Flores Creek Coastal Lowlands, San Diego County, California. Madroño 45, 171–182.

Anderson, R.S., Power, M.J., Smith, S.J., Springer, K., Scott, E., 2002. Paleoecology of a Middle Wisconsin Deposit from Southern California. Quat. Res. 58, 310–317. doi:10.1006/qres.2002.2388

Anderson, R.S., Smith, S.J., Jass, R.B., Geoffrey Spaulding, W., 2008. A Late Holocene Record of Vegetation and Climate from a Small Wetland in Shasta County, California. Madroño 55, 15–25. doi:10.3120/0024-9637(2008)55[15:ALHROV]2.0.CO;2

Anderson, R.S., Starratt, S., Jass, R.M.B., Pinter, N., 2009. Fire and vegetation history on Santa Rosa Island, Channel Islands, and long-term environmental change in southern California. J. Quat. Sci. 25, 782–797. doi:10.1002/jqs.1358

Asmerom, Y., Polyak, V.J., Burns, S.J., 2010. Variable winter moisture in the southwestern United States linked to rapid glacial climate shifts. Nat. Geosci. 3, 114–117. doi:10.1038/ngeo754

Bacon, S.N., Burke, R.M., Pezzopane, S.K., Jayko, A.S., 2006. Last glacial maximum and Holocene lake levels of Owens Lake, eastern California, USA. Quat. Sci. Rev. 25, 1264–1282. doi:10.1016/j.quascirev.2005.10.014

Bailey, R.G., 2009. Ecosystem geography: from ecoregions to sites, 2nd ed. ed. Springer, New York.

Balch, D.P., Cohen, A.S., Schnurrenberger, D.W., Haskell, B.J., Valero Garces, B.L., Beck, J.W., Cheng, H., Edwards, R.L., 2005. Ecosystem and paleohydrological response to Quaternary climate change in the Bonneville Basin, Utah. Palaeogeogr. Palaeoclimatol. Palaeoecol. 221, 99–122. doi:10.1016/j.palaeo.2005.01.013

Baldwin, B.G., 2002. The Jepson desert manual: vascular plants of southeastern California. University of California Press, Berkeley, Calif.; London.

Ballard, J.P., 2009. A Lateglacial Paleofire Record for East-central Michigan. University of Cincinnati, Cincinnati, OH.

Barron, J.A., Anderson, L., 2011. Enhanced Late Holocene ENSO/PDO expression along the margins of the eastern North Pacific. Quat. Int. 235, 3–12. doi:10.1016/j.quaint.2010.02.026

Barron, J.A., Heusser, L., Herbert, T., Lyle, M., 2003. High-resolution climatic evolution of coastal northern California during the past 16,000 years. Paleoceanography 18, n/a-n/a. doi:10.1029/2002PA000768

Batchelder, G.L., 1970. Postglacial ecology at Black Lake, Mono County, California. University of Arizona, Tempe.

Behl, R.J., Kennett, J.P., 1996. Brief interstadial events in the Santa Barbara basin, NE Pacific, during the past 60 kyr. Nature 379, 243–246. doi:10.1038/379243a0

Benedict, R.F., 1924. A Brief Sketch of Serrano Culture. Am. Anthropol. 26, 366–392.

Bennett, K.D., Willis, K.J., 2001. Pollen, in: Smol, J.P., Birks, H.J.B., Last, W.M., Bradley, R.S., Alverson, K. (Eds.), Tracking Environmental Change Using Lake Sediments. Kluwer Academic Publishers, Dordrecht, pp. 5–32.

Benson, L., 1999. Records of millennial-scale climate change from the Great Basin of the Western United States, in: Clark, U., Webb, S., Keigwin, D. (Eds.), Geophysical Monograph Series. American Geophysical Union, Washington, D. C., pp. 203–225.

Benson, L., Lund, S., Negrini, R., Linsley, B., Zic, M., 2003. Response of North American Great Basin Lakes to Dansgaard–Oeschger oscillations. Quat. Sci. Rev. 22, 2239–2251. doi:10.1016/S0277-3791(03)00210-5

Benson, L.V., Burdett, J.W., Kashgarian, M., Lund, S.P., Phillips, F.M., Rye, R.O., 1996. Climatic and Hydrologic Oscillations in the Owens Lake Basin and Adjacent Sierra Nevada, California. Science 274, 746–749. doi:10.1126/science.274.5288.746

Benson, L.V., Kashgarian, M., Rye, R.O., Lund, S.P., Paillet, F., Smoot, J.P., Kester, C., Mensing, S.A., Meko, D.M., Lindström, S., 2002. Holocene Multidecadal and Multicentennial Droughts Affecting Northern California and Nevada. Quat. Sci. Rev. 21, 659–682.

Benson, L.V., Lund, S.P., Smoot, J.P., Rhode, D.E., Spencer, R.J., Verosub, K.L., Louderback, L.A., Johnson, C.A., Rye, R.O., Negrini, R.M., 2011. The rise and fall of Lake Bonneville between 45 and 10.5 ka. Quat. Int. 235, 57–69. doi:10.1016/j.quaint.2010.12.014

Benson, L.V., Smoot, J.P., Lund, S.P., Mensing, S.A., Foit, F.F., Rye, R.O., 2013. Insights from a synthesis of old and new climate-proxy data from the Pyramid and Winnemucca lake basins for the period 48 to 11.5 cal ka. Quat. Int. 310, 62–82. doi:10.1016/j.quaint.2012.02.040

Big Bear Lake TMDL Task Force [WWW Document], 2012. URL http://www.sawpa.org/collaboration/past-projects/big-bear-lake-tmdl-taskforce/ (accessed 6.18.14).

Bird, B.W., Kirby, M.E., 2006. An Alpine Lacustrine Record of Early Holocene North American Monsoon Dynamics from Dry Lake, Southern California (USA). J. Paleolimnol. 35, 179–192. doi:10.1007/s10933-005-8514-3

Bird, B.W., Kirby, M.E., Howat, I.M., Tulaczyk, S., 2010. Geophysical evidence for Holocene lake-level change in southern California (Dry Lake). Boreas 39, 131–144. doi:10.1111/j.1502-3885.2009.00114.x

Birks, H.J.B., Heiri, O., Seppä, H., Bjune, A.E., 2010. Strengths and Weaknesses of Quantitative Climate Reconstructions Based on Late-Quaternary Biological Proxies. Open Ecol. J. 3, 68–110.

Blaauw, M., Christen, J.A., 2011. Flexible Paleoclimate Age-Depth Models Using an Autoregressive Gamma Process. Bayesian Anal. 6, 457–474. doi:10.1214/11-BA618

Blass, A., Bigler, C., Grosjean, M., Sturm, M., 2007. Decadal-scale autumn temperature reconstruction back to AD 1580 inferred from the varved sediments of Lake Silvaplana (southeastern Swiss Alps). Quat. Res. 68, 184–195. doi:10.1016/j.yqres.2007.05.004

Blazevic, M.A., Kirby, M.E., Woods, A.D., Browne, B.L., Bowman, D.D., 2009. A sedimentary facies model for glacial-age sediments in Baldwin Lake, Southern California. Sediment. Geol. 219, 151–168. doi:10.1016/j.sedgeo.2009.05.003

Booth, M.S., Caldwell, M.M., Stark, J.M., 2003. Overlapping resource use in three Great Basin species: implications for community invasibility and vegetation dynamics. J. Ecol. 91, 36–48. doi:10.1046/j.1365-2745.2003.00739.x

Brenner, M., Whitmore, T.J., Curtis, J.H., Hodell, D.A., Schelske, C.L., 1999. Stable isotope (δ13C and δ15N) signatures of sedimented organic matter as indicators of historic lake trophic state. J. Paleolimnol. 22, 205–221.

Briles, C.E., Whitlock, C., Bartlein, P.J., 2005. Postglacial vegetation, fire, and climate history of the Siskiyou Mountains, Oregon, USA. Quat. Res. 64, 44–56. doi:10.1016/j.yqres.2005.03.001

Briles, C.E., Whitlock, C., Bartlein, P.J., Higuera, P., 2008. Regional and local controls on postglacial vegetation and fire in the Siskiyou Mountains, northern California, USA. Palaeogeogr. Palaeoclimatol. Palaeoecol. 265, 159–169. doi:10.1016/j.palaeo.2008.05.007

Briles, C.E., Whitlock, C., Skinner, C.N., Mohr, J., 2011. Holocene forest development and maintenance on different substrates in the Klamath Mountains, northern California, USA. Ecology 92, 590–601. doi:10.1890/09-1772.1

Brook, G.A., Ellwood, B.B., Railsback, L.B., Cowart, J.B., 2006. A 164 ka record of environmental change in the American Southwest from a Carlsbad Cavern speleothem. Palaeogeogr. Palaeoclimatol. Palaeoecol. 237, 483–507. doi:10.1016/j.palaeo.2006.01.001

Brooks, M.L., Matchett, J.R., 2006. Spatial and temporal patterns of wildfires in the Mojave Desert, 1980–2004. J. Arid Environ. 67, 148–164. doi:10.1016/j.jaridenv.2006.09.027

Brooks, M.L., Minnich, R.A., 2006. Southeastern Deserts Bioregion, in: Fire in California's Ecosystems. The University of California Press, Berkeley, CA, pp. 391–414.

Brunelle, A., Anderson, R.S., 2003. Sedimentary charcoal as an indicator of late-Holocene drought in the Sierra Nevada, California, and its relevance to the future. The Holocene 13, 21–28. doi:10.1191/0959683603hl591rp

Burch, J.B., 1982. Freshwater snails (Mollusca: Gastropoda) of North America (No. EPA-600/3-82-026). United States Environmental Protection Agency.

Buylaert, J.P., Murray, A.S., Thomsen, K.J., Jain, M., 2009. Testing the potential of an elevated temperature IRSL signal from K-feldspar. Radiat. Meas. 44, 560–565. doi:10.1016/j.radmeas.2009.02.007

Cacho, I., Grimalt, J.O., Pelejero, C., Canals, M., Sierro, F.J., Flores, J.A., Shackleton, N., 1999. Dansgaard-Oeschger and Heinrich event imprints in Alboran Sea paleotemperatures. Paleoceanography 14, 698–705. doi:10.1029/1999PA900044

Calsbeek, R., Thompson, J.N., Richardson, J.E., 2003. Patterns of molecular evolution and diversification in a biodiversity hotspot: the California Floristic Province. Mol. Ecol. 12, 1021–1029. doi:10.1046/j.1365-294X.2003.01794.x

Cayan, D.R., Das, T., Pierce, D.W., Barnett, T.P., Tyree, M., Gershunov, A., 2010. Future dryness in the southwest US and the hydrology of the early 21st century drought. Proc. Natl. Acad. Sci. 107, 21271–21276. doi:10.1073/pnas.0912391107

Cayan, D.R., Peterson, D.H., 1989. The influence of North Pacific atmospheric circulation on streamflow in the west., in: Aspects of Climate Variability in the Pacific and the Western Americas. American Geophysical Union, pp. 375–397.

Chong, J.-R., 2003. Wildfires Lead to Peek at Serrano Indian History. Los Angel. Times.

Ciano, L.M., 1984. Pebble Plain Communities as Islands: Test of Island Biogeography Theory, Ecological Genetics of Island Species. University of California - Riverside, Riverside, CA.

Clark, P.U., Dyke, A.S., Shakun, J.D., Carlson, A.E., Clark, J., Wohlfarth, B., Mitrovica, J.X., Hostetler, S.W., McCabe, A.M., 2009. The Last Glacial Maximum. Science 325, 710–714. doi:10.1126/science.1172873

Cole, K.L., Liu, G.-W., 1994. Holocene Paleoecology of an Estuary on Santa Rosa Island, California. Quat. Res. 41, 326–335. doi:10.1006/qres.1994.1037

Cole, K.L., Wahl, E., 2000. A Late Holocene Paleoecological Record from Torrey Pines State Reserve, California. Quat. Res. 53, 341–351. doi:10.1006/qres.1999.2121

Collins, B.J., 1976. Key to Trees and Shrubs of the Deserts of Southern California. California State University Foundation, Northridge, CA.

Colman, S.M., Peck, J.A., Karabanov, E.B., Carter, S.J., Bradbury, J.P., King, J.W., Williams, D.F., 1995. Continental climate response to orbital forcing from biogenic silica records in Lake Baikal. Nature 378, 769–771. doi:10.1038/378769a0

Colman, S.M., Platt Bradbury, J., Rosenbaum, J.G., 2004. Paleolimnology and Paleoclimate Studies in Upper Klamath Lake, Oregon. J. Paleolimnol. 31, 129–138. doi:10.1023/B:JOPL.0000019235.72107.92

Conedera, M., Tinner, W., Neff, C., Meurer, M., Dickens, A.F., Krebs, P., 2009. Reconstructing past fire regimes: methods, applications, and relevance to fire management and conservation. Quat. Sci. Rev. 28, 555–576. doi:10.1016/j.quascirev.2008.11.005

Conley, D.J., Schelske, C.L., 2002. Biogenic Silica, in: Smol, J.P., Birks, H.J.B., Last, W.M., Bradley, R.S., Alverson, K. (Eds.), Tracking Environmental Change Using Lake Sediments. Kluwer Academic Publishers, Dordrecht, pp. 281–293.

Conroy, J.L., Overpeck, J.T., Cole, J.E., Shanahan, T.M., Steinitz-Kannan, M., 2008. Holocene changes in eastern tropical Pacific climate inferred from a Galápagos lake sediment record. Quat. Sci. Rev. 27, 1166–1180. doi:10.1016/j.quascirev.2008.02.015

Crawford, J.N., Mensing, S.A., Lake, F.K., Zimmerman, S.R., 2015. Late Holocene fire and vegetation reconstruction from the western Klamath Mountains, California, USA: A multi-disciplinary approach for examining potential human land-use impacts. The Holocene 25, 1341–1357. doi:10.1177/0959683615584205

Daniels, M.L., Anderson, R.S., Whitlock, C., 2005. Vegetation and fire history since the Late Pleistocene from the Trinity Mountains, northwestern California, USA. The Holocene 15, 1062–1071. doi:10.1191/0959683605hl878ra

Dansgaard, W., Johnsen, S.J., Clausen, H.B., Dahl-Jensen, D., Gundestrup, N.S., Hammer, C.U., Hvidberg, C.S., Steffensen, N.S., Sceinbjörnsdottir, A.E., Jouzel, J., Bond, G., 1993. Climate instability during the last interglacial period recorded in the GRIP ice core. Nature 364, 203–207. doi:10.1038/364203a0

Davis, O.K., 1999a. Pollen analysis of Tulare Lake, California: Great Basin-like vegetation in Central California during the full-glacial and early Holocene. Rev. Palaeobot. Palynol. 107, 249–257. doi:10.1016/S0034-6667(99)00020-2

Davis, O.K., 1999b. Pollen Analysis of a Late-Glacial and Holocene Sediment Core from Mono Lake, Mono Couty, California. Quat. Res. 52, 243–249.

Davis, O.K., 1992. Rapid climatic change in coastal southern California inferred from pollen analysis of San Joaquin Marsh. Quat. Res. 37, 89–100. doi:10.1016/0033-5894(92)90008-7

Davis, O.K., Moratto, M.J., 1988. Evidence for a warm dry early Holocene in the western Sierra Nevada of California: pollen and plant macrofossil analysis of Dinkey and Exchequer Meadows. 35, 132–149.

Davis, O.K., Scott Anderson, R., Fall, P.L., O'Rourke, M.K., Thompson, R.S., 1985. Palynological evidence for early Holocene aridity in the southern Sierra Nevada, California. Quat. Res. 24, 322–332. doi:10.1016/0033-5894(85)90054-7

Dean, W.E., 2010. Recent advances in global lake coring hold promise for global change research in paleolimnology. J. Paleolimnol. 44, 741–743. doi:10.1007/s10933-010-9430-8

Dean, W.E., 1974. Determination of Carbonate and Organic Matter in Calcareous Sediments and Sedimentary Rocks by Loss on Ignition: Comparison With Other Methods. SEPM J. Sediment. Res. Vol. 44. doi:10.1306/74D729D2-2B21-11D7-8648000102C1865D

Dean, W.E., Gorham, E., 1998. Magnitude and significance of carbon burial in lakes, reservoirs, and peatlands. Geology 26, 535. doi:10.1130/0091-7613(1998)026<0535:MASOCB>2.3.CO;2

Dearing, J., 1999. Environmental Magnetic Susceptibility: Using the Bartington MS2 System, 2nd ed. Chi Publishing, Kenilworth, England.

DellaSala, D.A., Alaback, P., Spribille, T., Wehrden, H., Nauman, R.S., 2011. Just What Are Temperate and Boreal Rainforests?, in: Temperate and Boreal Rainforests of the World: Ecology and Conservation. Island Press/Center for Resource Economics, Washington, DC, pp. 1–41.

DeLucia, E.H., Schlesinger, W.H., Billings, W.D., 1989. Edaphic limitations to growth and photosynthesis in Sierran and Great Basin vegetation. Oecologia 78, 184–190. doi:10.1007/BF00377154

Denniston, R.F., Asmerom, Y., Polyak, V., Dorale, J.A., Carpenter, S.J., Trodick, C., Hoye, B., González, L.A., 2007. Synchronous millennial-scale climatic changes in the Great Basin and the North Atlantic during the last interglacial. Geology 35, 619. doi:10.1130/G23445A.1

Dettinger, M.D., 2013. Atmospheric Rivers as Drought Busters on the U.S. West Coast. J. Hydrometeorol. 14, 1721–1732. doi:10.1175/JHM-D-13-02.1

Dietz, S.A., Hildebrandt, W.R., Jones, T., 1988. Archaeological investigations at Elkhorn Slough: CA-MNT-229 A Middle Period site on the central California coast., Papers in Northern California Anthropology. Northern California Anthropological Group, Berkeley, CA.

Diffenbaugh, N.S., Swain, D.L., Touma, D., 2015. Anthropogenic warming has increased drought risk in California. Proc. Natl. Acad. Sci. 112, 3931–3936. doi:10.1073/pnas.1422385112

Dingemans, T., Mensing, S.A., Feakins, S.J., Kirby, M.E., Zimmerman, S.R.H., 2014. 3000 years of environmental change at Zaca Lake, California, USA. Front. Ecol. Evol. 2. doi:10.3389/fevo.2014.00034

Edlund, E.G., 1996. Late Quaternary environmental history of montane forests of the Sierra Nevada. Doctoral dissertation. (Doctoral dissertation). University of California - Berkeley, Berkeley, CA.

Elliot, M., Labeyrie, L., Duplessy, J.-C., 2002. Changes in North Atlantic deep-water formation associated with the Dansgaard–Oeschger temperature oscillations (60–10ka). Quat. Sci. Rev. 21, 1153–1165. doi:10.1016/S0277-3791(01)00137-8

Faegri, K., Kaland, P.E., Krzywinski, K., 1989. Textbook of pollen analysis, 4th ed. ed. Wiley, Chichester [England] ; New York.

Flint, L.E., Martin, P., 2012. Geohydrology of Big Bear Valley, California: Phase 1—Geologic Framework, Recharge, and Preliminary Assessment of the Source and Age of Groundwater (Scientific Investigations No. 2012–5100). U. S. Geological Survey.

Forester, R.M., Lowenstein, T.K., Spencer, R.J., 2005. An ostracode based paleolimnologic and paleohydrologic history of Death Valley: 200 to 0 ka. Geol. Soc. Am. Bull. 117, 1379. doi:10.1130/B25637.1

Garcia, A.L., Knott, J.R., Mahan, S.A., Bright, J., 2014. Geochronology and paleoenvironment of pluvial Harper Lake, Mojave Desert, California, USA. Quat. Res. 81, 305–317. doi:10.1016/j.yqres.2013.10.008

Georgescu, M., Moustaoui, M., Mahalov, A., Dudhia, J., 2012. Summer-time climate impacts of projected megapolitan expansion in Arizona. Nat. Clim. Change 3, 37–41. doi:10.1038/nclimate1656

Glover, K.C., MacDonald, G.M., Kirby, M.E., Rhodes, E.J., Stevens, L., Silveira, E.I., Whitaker, A., submitted. Insolation and North Atlantic Climate Forcing in alpine Southern California since 125 ka.

Goring, S., Dawson, A., Simpson, G.L., Ram, K., Graham, R.W., Grimm, E.C., Williams, J.W., 2015. neotoma: A Programmatic Interface to the Neotoma Paleoecological Database. Open Quat. 1. doi:10.5334/oq.ab

Gottschalk, J., Skinner, L.C., Misra, S., Waelbroeck, C., Menviel, L., Timmermann, A., 2015. Abrupt changes in the southern extent of North Atlantic Deep Water during Dansgaard–Oeschger events. Nat. Geosci. 8, 950–954. doi:10.1038/ngeo2558

Grimm, E.C., 2008. Neotoma: an ecosystem database for the Pliocene, Pleistocene, and Holocene. (No. 1), Scientific Papers E Series. Illinois State Museum.

Grimm, E.C., Bradshaw, R.H.W., Brewer, S., Flantua, S., Giesecke, T., Lézine, A.-M., Takahara, H., Williams, J.E., 2013. Databases and their Application, in: Elias, S.A., Mock, C.J. (Eds.), Encyclopedia of Quaternary Science. Elsevier, Amsterdam, pp. 831–838.

Groot, M.H.M., van der Plicht, J., Hooghiemstra, H., Lourens, L.J., Rowe, H.D., 2014. Age modelling for Pleistocene lake sediments: A comparison of methods from the Andean Fúquene Basin (Colombia) case study. Quat. Geochronol. 22, 144–154. doi:10.1016/j.quageo.2014.01.002

Grootes, P.M., Stuiver, M., White, J.W.C., Johnsen, S., Jouzel, J., 1993. Comparison of oxygen isotope records from the GISP2 and GRIP Greenland ice cores. Nature 366, 552–554. doi:10.1038/366552a0

Guerin, E., 2016. Why fighting wildfires in California costs more than other states. South. Calif. Public Radio News.

Hahn, A., Kliem, P., Ohlendorf, C., Zolitschka, B., Rosén, P., 2013. Climate induced changes as registered in inorganic and organic sediment components from Laguna Potrok Aike (Argentina) during the past 51 ka. Quat. Sci. Rev. 71, 154–166. doi:10.1016/j.quascirev.2012.09.015

Hakala, K.J., Adam, D.P., 2004. Late Pleistocene Vegetation and Climate in the Southern Cascade Range and the Modoc Plateau Region. J. Paleolimnol. 31, 189–215. doi:10.1023/B:JOPL.0000019231.58234.fb

Hallett, D.J., Anderson, R.S., 2010. Paleofire reconstruction for high-elevation forests in the Sierra Nevada, California, with implications for wildfire synchrony and climate variability in the late Holocene. Quat. Res. 73, 180–190. doi:10.1016/j.yqres.2009.11.008

Hanak, E., Mount, J., Chappelle, C., Lund, J., Medellín-Azuara, J., Moyle, P., 2015. What If California's Drought Continues? Public Policy Institute of California, San Francisco, CA.

Heiri, O., Lotter, A.F., Lemcke, G., 2001. Loss on ignition as a method for estimating organic and carbonate content in sediments: reproducibility and comparability of results. J. Paleolimnol. 25, 101–110.

Hemming, S.R., 2004. Heinrich events: Massive late Pleistocene detritus layers of the North Atlantic and their global climate imprint. Rev. Geophys. 42. doi:10.1029/2003RG000128

Hendy, I.L., Dunn, L., Schimmelmann, A., Pak, D.K., 2012. Resolving varve and radiocarbon chronology differences during the last 2000 years in the Santa Barbara Basin sedimentary record, California. Quat. Int. doi:10.1016/j.quaint.2012.09.006

Hendy, I.L., Kennett, J.P., 2000. Dansgaard-Oeschger Cycles and the California Current System: Planktonic foraminiferal response to rapid climate change in Santa Barbara Basin, Ocean Drilling Program Hole 893A. Paleoceanography 15, 30. doi:10.1029/1999PA000413

Hendy, I.L., Kennett, J.P., 2000. Stable isotope stratigraphy and paleoceanography of the last 170 ky: Site 1014, Tanner Basin, California., in: Proceedings of the Ocean Drilling Program, Scientific Results. pp. 129–140.

Hendy, I.L., Pedersen, T.F., 2005. Is pore water oxygen content decoupled from productivity on the California Margin? Trace element results from Ocean Drilling Program Hole 1017E, San Lucia slope, California: PRODUCTIVITY-PORE WATER OXYGEN DECOUPLING. Paleoceanography 20, n/a-n/a. doi:10.1029/2004PA001123

Hendy, I.L., Pedersen, T.F., Kennett, J.P., Tada, R., 2004. Intermittent existence of a southern Californian upwelling cell during submillennial climate change of the last 60 kyr. Paleoceanography 19, n/a-n/a. doi:10.1029/2003PA000965

Herbert, T.D., Schuffert, J.., Andreasen, D., Heusser, L.E., Lyle, M., Mix, A., Ravelo, A.C., Stott, L.D., Herguera, J.C., 2001. Collapse of the California Current During Glacial Maxima Linked to Climate Change on Land. Science 293, 71–76. doi:10.1126/science.1059209

Heusser, C.J., 1972. Palynology and Phytogeographical Significance of a Late-Pleistocene Refugium Near Kalalock, Washington. Quat. Res. 2, 189–201.

Heusser, L., 1998. Direct correlation of millennial-scale changes in western North American vegetation and climate with changes in the California Current System over the past ~60 kyr. Paleoceanography 13, 252–262. doi:10.1029/98PA00670

Heusser, L.E., 2000. Rapid oscillations in western North America vegetation and climate during oxygen isotope stage 5 inferred from pollen data from Santa Barbara Basin (Hole 893A). Palaeogeogr. Palaeoclimatol. Palaeoecol. 161, 407–421. doi:10.1016/S0031-0182(00)00096-1

Heusser, L.E., 1992. POLLEN STRATIGRAPHY AND PALEOECOLOGIC INTERPRETATION OF THE 160-KY RECORD FROM SANTA BARBARA BASIN, HOLE 893A1, in: In Proceedings of the Ocean Drilling Program, Scientific Results.

Heusser, L.E., Basalm, W.L., 1977. Pollen Distribution in the Northeast Pacific Ocean. Quat. Res. 7, 45–62.

Heusser, L.E., King, J.E., 1988. North America, in: Huntley, B., Webb, T. (Eds.), Vegetation History. Springer Netherlands, Dordrecht, pp. 193–236.

Heusser, L.E., Kirby, M.E., Nichols, J.E., 2015. Pollen-based evidence of extreme drought during the last Glacial (32.6–9.0 ka) in coastal southern California. Quat. Sci. Rev. 126, 242–253. doi:10.1016/j.quascirev.2015.08.029

Heusser, L.E., Shackleton, N.J., 1979. Direct Marine-Continental Correlation: 150,000-Year Oxygen Isotope--Pollen Record from the North Pacific. Science 204, 837–839. doi:10.1126/science.204.4395.837

Hicks, S., Hyvärinen, H., 1999. Pollen influx values measured in different sedimentary environments and their palaeoecological implications. Grana 38, 228–242. doi:10.1080/001731300750044618

Hildebrandt, W.R., Hayes, J.F., 1983. Archaeological investigations on Pilot Ridge Six Rivers National Forest (U.S. Forest Service Contract 53-9JHA-2-140). Anthropological Studies Center Sonoma State University and Center for Anthropological Research San Jose State University, San Jose, CA.

Hiltzik, M., 2016. No, California's drought isn't over. Here's why easing the drought rules would be a big mistake. Los Angel. Times.

Holmgren, C.A., Betancourt, J.L., Rylander, K.A., 2010. A long-term vegetation history of the Mojave-Colorado desert ecotone at Joshua Tree National Park. J. Quat. Sci. 25, 222–236. doi:10.1002/jqs.1313

Hooghiemstra, H., Lézine, A.-M., Leroy, S.A.G., Dupont, L., Marret, F., 2006. Late Quaternary palynology in marine sediments: A synthesis of the understanding of pollen distribution patterns in the NW African setting. Quat. Int. 148, 29–44. doi:10.1016/j.quaint.2005.11.005

Hu, F.S., Kaufman, D.S., Yoneji, S., Nelson, D., Shemesh, A., Huang, Y., Tian, J., Bond, G., Clegg, B., Brown, T., 2003. Cyclic Variation and Solar Forcing of Holocene Climate in the Alaskan Subarctic. Science 301, 1890–1893. doi:10.1126/science.1088568

Hughes, P.D., Gibbard, P.L., Ehlers, J., 2013. Timing of glaciation during the last glacial cycle: Evaluating the concept of a global "Last Glacial Maximum" (LGM). Earth-Sci. Rev. doi:10.1016/j.earscirev.2013.07.003

Imbrie, J., Hays, J.D., Martinson, D.G., McIntyre, A., Mix, A.C., Morley, J.J., Pisias, N.., Prell, W.L., Shackleton, N.J., 1984. The orbital theory of Pleistocene climate: Support from a revised chronology of the marine delta18O record., in: Ilankovitch and Climate: Understanding the Response to Astronomical Forcing. p. 269.

IPCC, 2013. Climate Change 2013: The Physical Science Basis. Contribution of Working Group I to the Fifth Assessment Report of the Intergovernmental Panel on Climate Change. Cambridge University Press, Cambridge, United Kingdom and New York, NY, USA.

Jiménez-Moreno, G., Anderson, R.S., Desprat, S., Grigg, L.D., Grimm, E.C., Heusser, L.E., Jacobs, B.F., López-Martínez, C., Whitlock, C.L., Willard, D.A., 2010. Millennial-scale variability during the last glacial in vegetation records from North America. Quat. Sci. Rev. 29, 2865–2881. doi:10.1016/j.quascirev.2009.12.013

Johnsen, S.J., Clausen, H.B., Dansgaard, W., Fuhrer, K., Gundestrup, N., Hammer, C.U., Iversen, P., Jouzel, J., Stauffer, B., steffensen, J.P., 1992. Irregular glacial interstadials recorded in a new Greenland ice core. Nature 359, 311–313. doi:10.1038/359311a0

Kaplan, M.R., Wolfe, A.P., Miller, G.H., 2002. Holocene Environmental Variability in Southern Greenland Inferred from Lake Sediments. Quat. Res. 58, 149–159. doi:10.1006/qres.2002.2352

Keeley, J.E., Bond, W.J., Bradstock, R.A., Pausas, J., Rundel, P.W., 2012. Fire in Mediterranean ecosystems: ecology, evolution and management. Cambridge University Press, Cambridge, UK ; New York.

Kennett, D., Kennett, J., West, G., Erlandson, J., Johnson, J., Hendy, I., West, A., Culleton, B., Jones, T., Staffordjr, T., 2008. Wildfire and abrupt ecosystem disruption on California's

Northern Channel Islands at the Ållerød–Younger Dryas boundary (13.0–12.9ka). Quat. Sci. Rev. 27, 2530–2545. doi:10.1016/j.quascirev.2008.09.006

Kirby, M.E., Feakins, S.J., Bonuso, N., Fantozzi, J.M., Hiner, C.A., 2013. Latest Pleistocene to Holocene hydroclimates from Lake Elsinore, California. Quat. Sci. Rev. 76, 1–15. doi:10.1016/j.quascirev.2013.05.023

Kirby, M.E., Feakins, S.J., Hiner, C.A., Fantozzi, J., Zimmerman, S.R.H., Dingemans, T., Mensing, S.A., 2014. Tropical Pacific forcing of Late-Holocene hydrologic variability in the coastal southwest United States. Quat. Sci. Rev. 102, 27–38. doi:10.1016/j.quascirev.2014.08.005

Kirby, M.E., Knell, E.J., Anderson, W.T., Lachniet, M.S., Palermo, J., Eeg, H., Lucero, R., Murrieta, R., Arevalo, A., Silveira, E., Hiner, C.A., 2015. Evidence for insolation and Pacific forcing of late glacial through Holocene climate in the Central Mojave Desert (Silver Lake, CA). Quat. Res. 84, 174–186. doi:10.1016/j.yqres.2015.07.003

Kirby, M.E., Lund, S.P., Anderson, M.A., Bird, B.W., 2007. Insolation forcing of Holocene climate change in Southern California: a sediment study from Lake Elsinore. J. Paleolimnol. 38, 395–417. doi:10.1007/s10933-006-9085-7

Kirby, M.E., Lund, S.P., Bird, B.W., 2006. Mid-Wisconsin sediment record from Baldwin Lake reveals hemispheric climate dynamics (Southern CA, USA). Palaeogeogr. Palaeoclimatol. Palaeoecol. 241, 267–283. doi:10.1016/j.palaeo.2006.03.043

Kirby, M.E., Zimmerman, S.R.H., Patterson, W.P., Rivera, J.J., 2012. A 9170-year record of decadal-to-multi-centennial scale pluvial episodes from the coastal Southwest United States: a role for atmospheric rivers? Quat. Sci. Rev. 46, 57–65. doi:10.1016/j.quascirev.2012.05.008

Koehler, P.A., Anderson, R.S., 1995. Thirty Thousand Years of Vegetation Changes in the Alabama Hills, Owens Valley, California. Quat. Res. 43, 238–248. doi:10.1006/qres.1995.1024

Koehler, P.A., Scott Anderson, R., 1994. The paleoecology and stratigraphy of Nichols Meadow, Sierra National Forest, California, USA. Palaeogeogr. Palaeoclimatol. Palaeoecol. 112, 1–17. doi:10.1016/0031-0182(94)90132-5

Krantz, T., 1990. A Guide to the Rare and Unusual Wildflowers of the Big Bear Valley Preserve. Friends of Big Bear Valley Preserve, Big Bear City, CA.

Krantz, T., 1983. The Pebble Plains of Baldwin Lake. Fremontia 10, 9–13.

Kukla, G.J., Bender, M.L., de Beaulieu, J.-L., Bond, G., Broecker, W.S., Cleveringa, P., Gavin, J.E., Herbert, T.D., Imbrie, J., Jouzel, J., Keigwin, L.D., Knudsen, K.-L., McManus, J.F., Merkt, J., Muhs, D.R., Müller, H., Poore, R.Z., Porter, S.C., Seret, G., Shackleton, N.J., Turner, C., Tzedakis, P.C., Winograd, I.J., 2002. Last Interglacial Climates. Quat. Res. 58, 2–13. doi:10.1006/qres.2001.2316

Kylander, M.E., Ampel, L., Wohlfarth, B., Veres, D., 2011. High-resolution X-ray fluorescence core scanning analysis of Les Echets (France) sedimentary sequence: new insights from chemical proxies. J. Quat. Sci. 26, 109–117. doi:10.1002/jqs.1438

Lachniet, M.S., Denniston, R.F., Asmerom, Y., Polyak, V.J., 2014. Orbital control of western North America atmospheric circulation and climate over two glacial cycles. Nat. Commun. 5. doi:10.1038/ncomms4805

Lami, A., Niessen, F., Guilizzoni, P., Masaferro, J., Belis, C.A., 1994. Palaeolimnological studies of the eutrophication of volcanic Lake Albano (Central Italy). J. Paleolimnol. 10, 181–197. doi:10.1007/BF00684032

Lanner, R.M., Lanner, H., 1981. The Piñon Pine: A Natural and Cultural History. University of Nevada Press, Reno, NV.

Laskar, J., Robutel, P., Joutel, F., Gastineau, M., Correia, A.C.M., Levrard, B., 2004. A long-term numerical solution for the insolation quantities of the Earth. Astron. Astrophys. 428, 261–285. doi:10.1051/0004-6361:20041335

Lawson, M.J., Roder, B.J., Stang, D.M., Rhodes, E.J., 2012. OSL and IRSL characteristics of quartz and feldspar from southern California, USA. Radiat. Meas. 47, 830–836. doi:10.1016/j.radmeas.2012.03.025

Leduc, G., Schneider, R., Kim, J.-H., Lohmann, G., 2010. Holocene and Eemian sea surface temperature trends as revealed by alkenone and Mg/Ca paleothermometry. Quat. Sci. Rev. 29, 989–1004. doi:10.1016/j.quascirev.2010.01.004

Leidy, R., 2006. Prehistoric and Historic Environmental Conditions in Bear Valley, San Bernardino County, California. Sacramento, CA.

Leng, M.J., Marshall, J.D., 2004. Palaeoclimate interpretation of stable isotope data from lake sediment archives. Quat. Sci. Rev. 23, 811–831. doi:10.1016/j.quascirev.2003.06.012

Li, J., Lowenstein, T.K., Brown, C.B., Ku, T.-L., Luo, S., 1996. A 100 ka record of water tables and paleoclimates from salt cores, Death Valley, California. Palaeogeogr. Palaeoclimatol. Palaeoecol. 123, 179–203. doi:10.1016/0031-0182(95)00123-9

Lin, J.C., Broecker, W.S., Hemming, S.R., Hajdas, I., Anderson, R.F., Smith, G.I., Kelley, M., Bonani, G., 1998. A Reassessment of U-Th and14C Ages for Late-Glacial High-Frequency Hydrological Events at Searles Lake, California. Quat. Res. 49, 11–23. doi:10.1006/qres.1997.1949

Lisiecki, L.E., Raymo, M.E., 2005. A Pliocene-Pleistocene stack of 57 globally distributed benthic δ^{18}O records: PLIOCENE-PLEISTOCENE BENTHIC STACK. Paleoceanography 20, n/a-n/a. doi:10.1029/2004PA001071

Litwin, R.J., Adam, D.P., Frederiksen, N.O., Woolfenden, W.B., 1997. An 800,000-year pollen record from Owens Lake, California; preliminary analyses, in: Special Paper 317: An

800,000-Year Paleoclimatic Record from Core OL-92, Owens Lake, Southeast California. Geological Society of America, pp. 127–142.

Litwin, R.J., Smoot, J.P., Durika, N.J., Smith, G.I., 1999. Calibrating Late Quaternary terrestrial climate signals: radiometrically dated pollen evidence. Quat. Sci. Rev. 18, 1151–1171.

Lund, D.C., Mix, A.C., 1998. Millennial-scale deep water oscillations: Reflections of the North Atlantic in the deep Pacific from 10 to 60 ka. Paleoceanography 13, 10–19. doi:10.1029/97PA02984

Lyle, M., Heusser, L., Ravelo, C., Andreasen, D., Olivarez Lyle, A., Diffenbaugh, N., 2010. Pleistocene water cycle and eastern boundary current processes along the California continental margin. Paleoceanography 25. doi:10.1029/2009PA001836

Lyle, M., Heusser, L., Ravelo, C., Yamamoto, M., Barron, J., Diffenbaugh, N.S., Herbert, T., Andreasen, D., 2012. Out of the Tropics: The Pacific, Great Basin Lakes, and Late Pleistocene Water Cycle in the Western United States. Science 337, 1629–1633. doi:10.1126/science.1218390

MacDonald, G.M., Case, R.A., 2005. Variations in the Pacific Decadal Oscillation over the past millennium. Geophys. Res. Lett. 32. doi:10.1029/2005GL022478

MacDonald, G.M., Larsen, C.P.S., Szeicz, J.M., Moser, K.A., 1991. The reconstruction of boreal forest fire history from lake sediments: A comparison of charcoal, pollen, sedimentological, and geochemical indices. Quat. Sci. Rev. 10, 53–71. doi:10.1016/0277-3791(91)90030-X

MacDonald, G.M., Moser, K.A., Bloom, A.M., Porinchu, D.F., Potito, A.P., Wolfe, B.B., Edwards, T.W.D., Petel, A., Orme, A.R., Orme, A.J., 2008a. Evidence of temperature depression and hydrological variations in the eastern Sierra Nevada during the Younger Dryas stade. Quat. Res. 70, 131–140. doi:10.1016/j.yqres.2008.04.005

MacDonald, G.M., Moser, K.A., Bloom, A.M., Potito, A.P., Porinchu, D.F., Holmquist, J.R., Hughes, J., Kremenetski, K.V., 2016. Prolonged California aridity linked to climate warming and Pacific sea surface temperature. Sci. Rep. 6, 33325. doi:10.1038/srep33325

MacDonald, G.M., Stahle, D.W., Diaz, J.V., Beer, N., Busby, S.J., Cerano-Paredes, J., Cole, J.E., Cook, E.R., Endfield, G., Gutierrez-Garcia, G., Hall, B., Magan, V., Meko, D.M., Méndez-Pérez, M., Sauchyn, D.J., Watson, E., Woodhouse, C.A., 2008b. Climate Warming and 21st-Century Drought in Southwestern North America. Eos Trans. Am. Geophys. Union 89, 82–82. doi:10.1029/2008EO090003

Mahan, S.A., Gray, H.J., Pigati, J.S., Wilson, J., Lifton, N.A., Paces, J.B., Blaauw, M., 2014. A geochronologic framework for the Ziegler Reservoir fossil site, Snowmass Village, Colorado. Quat. Res. 82, 490–503. doi:10.1016/j.yqres.2014.03.004

Maher, K., Ibarra, D.E., Oster, J.L., Miller, D.M., Redwine, J.L., Reheis, M.C., Harden, J.W., 2014. Uranium isotopes in soils as a proxy for past infiltration and precipitation across the western United States. Am. J. Sci. 314, 821–857. doi:10.2475/04.2014.01

Malamud-Roam, F., Lynn Ingram, B., 2004. Late Holocene δ13C and pollen records of paleosalinity from tidal marshes in the San Francisco Bay estuary, California. Quat. Res. 62, 134–145. doi:10.1016/j.yqres.2004.02.011

Mann, M.E., Gleick, P.H., 2015. Climate change and California drought in the 21st century: Fig. 1. Proc. Natl. Acad. Sci. 112, 3858–3859. doi:10.1073/pnas.1503667112

Marty, J., Myrbo, A., 2014. Radiocarbon dating suitability of aquatic plant macrofossils. J. Paleolimnol. 52, 435–443. doi:10.1007/s10933-014-9796-0

Maslin, M., Sarnthein, M., Knaack, J.-J., Grootes, P., Tzedakis, C., 1998. Intra-interglacial cold events: an Eemian-Holocene comparison. Geol. Soc. Lond. Spec. Publ. 131, 91–99. doi:10.1144/GSL.SP.1998.131.01.07

Maurer, E., n.d. Gridded Observed Meteorological Data [WWW Document]. URL http://www.engr.scu.edu/~emaurer/data.shtml

May, M.D., 1999. Vegetation and salinity changes over the last 2000 years at two islands in the northern San Francisco Estuary, California. (Masters Thesis). University of California - Berkeley, Berkeley, CA.

McKay, N.P., Kaufman, D.S., Michelutti, N., 2008. Biogenic silica concentration as a high-resolution, quantitative temperature proxy at Hallet Lake, south-central Alaska. Geophys. Res. Lett. 35. doi:10.1029/2007GL032876

Melles, M., Brigham-Grette, J., Glushkova, O.Y., Minyuk, P.S., Nowaczyk, N.R., Hubberten, H.-W., 2006. Sedimentary geochemistry of core PG1351 from Lake El'gygytgyn—a sensitive record of climate variability in the East Siberian Arctic during the past three glacial–interglacial cycles. J. Paleolimnol. 37, 89–104. doi:10.1007/s10933-006-9025-6

Mensing, S.A., Benson, L.V., Kashgarian, M., Lund, S., 2004. A Holocene pollen record of persistent droughts from Pyramid Lake, Nevada, USA. Quat. Res. 62, 29–38. doi:10.1016/j.yqres.2004.04.002

Mensing, S.A., Sharpe, S.E., Tunno, I., Sada, D.W., Thomas, J.M., Starratt, S., Smith, J., 2013. The Late Holocene Dry Period: multiproxy evidence for an extended drought between 2800 and 1850 cal yr BP across the central Great Basin, USA. Quat. Sci. Rev. 78, 266–282. doi:10.1016/j.quascirev.2013.08.010

Metcalfe, S.E., Barron, J.A., Davies, S.J., 2015. The Holocene history of the North American Monsoon: "known knowns" and "known unknowns" in understanding its spatial and temporal complexity. Quat. Sci. Rev. 120, 1–27. doi:10.1016/j.quascirev.2015.04.004

Michelutti, N., Wolfe, A.P., Vinebrooke, R.D., Rivard, B., Briner, J.P., 2005. Recent primary production increases in arctic lakes: PRODUCTION INCREASES IN ARCTIC LAKES. Geophys. Res. Lett. 32, n/a-n/a. doi:10.1029/2005GL023693

Minckley, T.A., Whitlock, C., Bartlein, P.J., 2007. Vegetation, fire, and climate history of the northwestern Great Basin during the last 14,000 years. Quat. Sci. Rev. 26, 2167–2184. doi:10.1016/j.quascirev.2007.04.009

Minnich, R.A., 1984. Snow Drifting and Timberline Dynamics on Mount San Gorgonio, California, U.S.A. Arct. Alp. Res. 16, 395. doi:10.2307/1550901

Minnich, R.A., 1976. Vegetation of the San Bernardino Mountains, in: Symposium Proceedings: Plant Communities of Southern California; 1974 May 4; Fullerton, CA. California Native Plant Society, Berkeley, CA, pp. 99–124.

Minnich, R.A., Barbour, M.G., Burk, J.H., Fernau, R.F., 1995. Sixty Years of Change in Californian Conifer Forests of the San Bernardino Mountains. Conserv. Biol. 9, 902–914. doi:10.1046/j.1523-1739.1995.09040902.x

Mittermeier, R.A., Cemex, S.A. de C.V, Agrupación Sierra Madre, Conservation International, 1999. Hotspots: earth's biologically richest and most endangered terrestrial ecoregions, 1st English ed. ed. CEMEX, Mexico City.

Mohr, J.A., Whitlock, C., Skinner, C.N., 2000. Postglacial vegetation and fire history, eastern Klamath Mountains, California, USA. The Holocene 10, 587–601. doi:10.1191/095968300675837671

Montade, V., Nebout, N.C., Kissel, C., Mulsow, S., 2011. Pollen distribution in marine surface sediments from Chilean Patagonia. Mar. Geol. 282, 161–168. doi:10.1016/j.margeo.2011.02.001

Mooney, H.A., Dunn, E.L., 1970. Convergent Evolution of Mediterranean-Climate Evergreen Sclerophyll Shrubs. Evolution 24, 292–303.

Morton, D.M., Miller, F.K., 2006. Geologic map of the San Bernardino and Santa Ana 30' x 60' quadrangles, California (Open-File No. 2006–1217). U. S. Geological Survey.

Moseley, G.E., Edwards, R.L., Wendt, K.A., Cheng, H., Dublyansky, Y., Lu, Y., Boch, R., Spotl, C., 2016. Reconciliation of the Devils Hole climate record with orbital forcing. Science 351, 165–168. doi:10.1126/science.aad4132

Mudie, P.J., McCarthy, F.M.G., 2006. Marine palynology: potentials for onshore—offshore correlation of Pleistocene—Holocene records. Trans. R. Soc. South Afr. 61, 139–157. doi:10.1080/00359190609519964

Muhs, D.R., Simmons, K.R., Schumann, R.R., Groves, L.T., Mitrovica, J.X., Laurel, D., 2012. Sea-level history during the Last Interglacial complex on San Nicolas Island, California:

implications for glacial isostatic adjustment processes, paleozoogeography and tectonics. Quat. Sci. Rev. 37, 1–25. doi:10.1016/j.quascirev.2012.01.010

Myrbo, A., 2015. Pulling on the Long Tail with Flyover Country, a Mobile App to Expose, Visualize, Discover, and Explore Open Geoscience Data. Presented at the American Geophysical Union Annual Fall Meeting, San Francisco.

Myrbo, A., Lynch, B., Curran, S., 2005. Limnological Research Center Core Facility SOP Series charcoal-sieve.pdf.

Naumburg, E., Mata-gonzalez, R., Hunter, R.G., Mclendon, T., Martin, D.W., 2005. Phreatophytic Vegetation and Groundwater Fluctuations: A Review of Current Research and Application of Ecosystem Response Modeling with an Emphasis on Great Basin Vegetation. Environ. Manage. 35, 726–740. doi:10.1007/s00267-004-0194-7

Nowaczyk, N.R., Melles, M., Minyuk, P., 2006. A revised age model for core PG1351 from Lake El'gygytgyn, Chukotka, based on magnetic susceptibility variations tuned to northern hemisphere insolation variations. J. Paleolimnol. 37, 65–76. doi:10.1007/s10933-006-9023-8

Nussbaumer, S.U., Steinhilber, F., Trachsel, M., Breitenmoser, P., Beer, J., Blass, A., Grosjean, M., Hafner, A., Holzhauser, H., Wanner, H., Zumbühl, H.J., 2011. Alpine climate during the Holocene: a comparison between records of glaciers, lake sediments and solar activity. J. Quat. Sci. 26, 703–713. doi:10.1002/jqs.1495

Oster, J.L., Ibarra, D.E., Winnick, M.J., Maher, K., 2015. Steering of westerly storms over western North America at the Last Glacial Maximum. Nat. Geosci. 8, 201–205. doi:10.1038/ngeo2365

Oster, J.L., Montañez, I.P., Mertz-Kraus, R., Sharp, W.D., Stock, G.M., Spero, H.J., Tinsley, J., Zachos, J.C., 2014. Millennial-scale variations in western Sierra Nevada precipitation during the last glacial cycle MIS 4/3 transition. Quat. Res. 82, 236–248. doi:10.1016/j.yqres.2014.04.010

Overpeck, J., Garfin, G., Jardine, A., Busch, D.E., Cayan, D., Dettinger, M., Fleishman, E., Gershunov, A., MacDonald, G., Redmond, K.T., Travis, W.R., Udall, B., 2013. Summary for Decision Makers, in: Garfin, G., Jardine, A., Merideth, R., Black, M., LeRoy, S. (Eds.), Assessment of Climate Change in the Southwest United States. Island Press/Center for Resource Economics, Washington, DC, pp. 1–20.

Overpeck, J., Udall, B., 2010. Dry Times Ahead. Science 328, 1642–1643. doi:10.1126/science.1186591

Owen, L.A., Clemmens, S.J., Finkel, R.C., Gray, H., 2014. Late Quaternary alluvial fans at the eastern end of the San Bernardino Mountains, Southern California. Quat. Sci. Rev. 87, 114–134. doi:10.1016/j.quascirev.2014.01.003

Owen, L.A., Finkel, R.C., Minnich, R.A., Perez, A.E., 2003. Extreme southwestern margin of late Quaternary glaciation in North America: Timing and controls. Geology 31, 729. doi:10.1130/G19561.1

Pak, D.K., Lea, D.W., Kennett, J.P., 2012. Millennial scale changes in sea surface temperature and ocean circulation in the northeast Pacific, 10-60 kyr BP: CA MARGIN MILLENNIAL SCALE EVENTS. Paleoceanography 27, n/a-n/a. doi:10.1029/2011PA002238

Paladino, L., 2008. A vegetation reconstruction of Big Bear Lake: local changes and inferred regional climatology. UCLA, Los Angeles.

Parisien, M.-A., Moritz, M.A., 2009. Environmental Controls on the Distribution of Wildfire at Multiple Spatial Scales. Ecol. Monogr. 79, 127–154.

Phillips, F.M., Zreda, M.G., Benson, L.V., Plummer, M.A., Elmore, D., Sharma, P., 1996. Chronology for Fluctuations in Late Pleistocene Sierra Nevada Glaciers and Lakes. Science 274, 749–751. doi:10.1126/science.274.5288.749

Pigati, J.S., Bright, J.E., Shanahan, T.M., Mahan, S.A., 2009. Late Pleistocene paleohydrology near the boundary of the Sonoran and Chihuahuan Deserts, southeastern Arizona, USA. Quat. Sci. Rev. 28, 286–300. doi:10.1016/j.quascirev.2008.09.022

Pigati, J.S., Miller, D.M., Bright, J.E., Mahan, S.A., Nekola, J.C., Paces, J.B., 2011. Chronology, sedimentology, and microfauna of groundwater discharge deposits in the central Mojave Desert, Valley Wells, California. Geol. Soc. Am. Bull. 123, 2224–2239. doi:10.1130/B30357.1

Pisias, N.., Mix, A.., Heusser, L., 2001. Millennial scale climate variability of the northeast Pacific Ocean and northwest North America based on radiolaria and pollen. Quat. Sci. Rev. 20, 1561–1576. doi:10.1016/S0277-3791(01)00018-X

Poore, R.Z., Dowsett, H.J., Barron, J.A., Heusser, L.E., Ravelo, C., Mix, A., 2000. Multiproxy record of the last interglacial (MIS 5e) off central and northern California, U.S.A., from Ocean Drilling Program sites 1018 and 1020 (USGS Numbered Series No. 1632). U. S. Geological Survey, Menlo Park, CA.

Pospelova, V., Price, A.M., Pedersen, T.F., 2015. Palynological evidence for late Quaternary climate and marine primary productivity changes along the California margin: CLIMATE AND PRIMARY PRODUCTIVITY ON CM. Paleoceanography 30, 877–894. doi:10.1002/2014PA002728

Price, A.M., Mertens, K.N., Pospelova, V., Pedersen, T.F., Ganeshram, R.S., 2013. Late Quaternary climatic and oceanographic changes in the Northeast Pacific as recorded by dinoflagellate cysts from Guaymas Basin, Gulf of California (Mexico): DINOFLAGELLATE CYSTS FROM GUAYMAS BASIN. Paleoceanography 28, 200–212. doi:10.1002/palo.20019

Prokopenko, A.A., Hinnov, L.A., Williams, D.F., Kuzmin, M.I., 2006. Orbital forcing of continental climate during the Pleistocene: a complete astronomically tuned climatic record from Lake Baikal, SE Siberia. Quat. Sci. Rev. 25, 3431–3457. doi:10.1016/j.quascirev.2006.10.002

Pyne, S.J., Andrews, P.L., Laven, R.D., 1996. Introduction to wildland fire, 2nd ed. ed. Wiley, New York.

Quinn, R.D., 2006. Introduction to California chaparral, California natural history guides. University of California Press, Berkeley, Calif.

Rack, F.R., Heise, E.A., Stein, R., 1995. MAGNETIC SUSCEPTIBILITY AND PHYSICAL PROPERTIES OF SEDIMENT CORES FROM SITE 893, SANTA BARBARA BASIN: RECORDS OF SEDIMENT DIAGENESIS OR OF PALEOCLIMATIC AND PALEOCEANOGRAPHIC CHANGE?., in: In Proceedings of the Ocean Drilling Program, Scientific Results.

Rasmussen, S.O., Bigler, M., Blockley, S.P., Blunier, T., Buchardt, S.L., Clausen, H.B., Cvijanovic, I., Dahl-Jensen, D., Johnsen, S.J., Fischer, H., Gkinis, V., Guillevic, M., Hoek, W.Z., Lowe, J.J., Pedro, J.B., Popp, T., Seierstad, I.K., Steffensen, J.P., Svensson, A.M., Vallelonga, P., Vinther, B.M., Walker, M.J.C., Wheatley, J.J., Winstrup, M., 2014. A stratigraphic framework for abrupt climatic changes during the Last Glacial period based on three synchronized Greenland ice-core records: refining and extending the INTIMATE event stratigraphy. Quat. Sci. Rev. 106, 14–28. doi:10.1016/j.quascirev.2014.09.007

Redmond, K.T., 2009. Historic Climate Variability in the Mojave Desert, in: Webb, R.H., Fenstermaker, L.F., Heaton, J.S., Hughson, D.L., McDonald, E.V., Miller, D.M. (Eds.), The Mojave Desert: Ecosystem Processes and Sustainability. University of Nevada Press, Reno.

Reheis, M.C., Miller, D.M., McGeehin, J.P., Redwine, J.R., Oviatt, C.G., Bright, J., 2015. Directly dated MIS 3 lake-level record from Lake Manix, Mojave Desert, California, USA. Quat. Res. 83, 187–203. doi:10.1016/j.yqres.2014.11.003

Reimer, P., 2013. IntCal13 and Marine13 Radiocarbon Age Calibration Curves 0–50,000 Years cal BP. Radiocarbon 55, 1869–1887. doi:10.2458/azu_js_rc.55.16947

Retelle, M., Child, J., 1996. Suspended sediment transport and deposition in a high arctic meromictic lake. J. Paleolimnol. 16. doi:10.1007/BF00176933

Rhodes, E.J., 2015. Dating sediments using potassium feldspar single-grain IRSL: Initial methodological considerations. Quat. Int. 362, 14–22. doi:10.1016/j.quaint.2014.12.012

Rood, D.H., Burbank, D.W., Finkel, R.C., 2011. Chronology of glaciations in the Sierra Nevada, California, from 10Be surface exposure dating. Quat. Sci. Rev. 30, 646–661. doi:10.1016/j.quascirev.2010.12.001

Roy, P.D., Quiroz-Jiménez, J.D., Pérez-Cruz, L.L., Lozano-García, S., Metcalfe, S.E., Lozano-Santacruz, R., López-Balbiaux, N., Sánchez-Zavala, J.L., Romero, F.M., 2013. Late Quaternary paleohydrological conditions in the drylands of northern Mexico: a summer precipitation proxy record of the last 80 cal ka BP. Quat. Sci. Rev. 78, 342–354. doi:10.1016/j.quascirev.2012.11.020

Sancetta, C., Lyle, M., Heusser, L., Zahn, R., Bradbury, J.P., 1992. Late-glacial to holocene changes in winds, upwelling, and seasonal production of the northern California current system. Quat. Res. 38, 359–370. doi:10.1016/0033-5894(92)90044-J

Sánchez Goñi, M.F., Turon, J.-L., Eynaud, F., Shackleton, N.J., Cayre, O., 2000. Direct land/sea correlation of the Eemian, and its comparison with the Holocene: a high-resolution palynological record off the Iberian margin. Neth. J. Geosci. 79, 345–354. doi:10.1017/S0016774600023702

Schnurrenberger, D., Russell, J., Kelts, K., 2003. Classification of lacustrine sediments based on sedimentary components. J. Paleolimnol. 29, 141–154. doi:10.1023/A:1023270324800

Scott Anderson, R., Ejarque, A., Rice, J., Smith, S.J., Lebow, C.G., 2015. Historic and Holocene environmental change in the San Antonio Creek Basin, mid-coastal California. Quat. Res. 83, 273–286. doi:10.1016/j.yqres.2014.11.005

Scott Anderson, R., Koehler, P.A., 2003. Modern pollen and vegetation relationships in the mountains of southern California, USA. Grana 42, 129–146. doi:10.1080/00173130310009949

Seki, O., Ishiwatari, R., Matsumoto, K., 2002. Millennial climate oscillations in NE Pacific surface waters over the last 82 kyr: New evidence from alkenones: ALKENONE SEA SURFACE TEMPERATURE IN CALIFORNIA MARGIN. Geophys. Res. Lett. 29, 59-1-59–4. doi:10.1029/2002GL015200

Sheppard, P., Comrie, A., Packin, G., Angersbach, K., Hughes, M., 2002. The climate of the US Southwest. Clim. Res. 21, 219–238. doi:10.3354/cr021219

Silveira, E.I., 2014. Reconstructing hydrologic change over the past 96,000 years using sediments from Baldwin Lake, San Bernardino County, California (B.A. Thesis). CSU-Fullerton, Fullerton, CA.

Smith, S.J., 1989. Pollen and microscopic charcoal analysis of a sediment core from Swamp Lake, Yosemite National Park, California. Northern Arizona University, Flagstaff, AZ.

Smith, S.J., Anderson, R.S., 1992. Late Wisconsin paleoecologic record from Swamp Lake, Yosemite National Park, California. Quat. Res. 38, 91–102. doi:10.1016/0033-5894(92)90032-E

Sofiev, M., Belmonte, J., Gehrig, R., Izquierdo, R., Smith, M., Dahl, Å., Siljamo, P., 2013. Airborne Pollen Transport, in: Sofiev, M., Bergmann, K.-C. (Eds.), Allergenic Pollen. Springer Netherlands, Dordrecht, pp. 127–159.

Springer, K.B., Manker, C.R., Pigati, J.S., 2015. Dynamic response of desert wetlands to abrupt climate change. Proc. Natl. Acad. Sci. 112, 14522–14526. doi:10.1073/pnas.1513352112

Stephenson, J.R., Calcarone, G.M., 1999. Southern California Mountains and Foothills Assessment: habitat and species conservation issues (General Technical Report No. GTR-PSW-175). Pacific Southwest Forest Research Station, Forest Service, Albany, CA.

Stine, S., 1994. Extreme and persistent drought in California and Patagonia during mediaeval time. Nature 369, 546–549. doi:10.1038/369546a0

Stout, M.L., 1976. Geologic Guide to the San Bernardino Mountains, Southern California: Annual Spring Field Trip.

Street, J.H., Anderson, R.S., Paytan, A., 2012. An organic geochemical record of Sierra Nevada climate since the LGM from Swamp Lake, Yosemite. Quat. Sci. Rev. 40, 89–106. doi:10.1016/j.quascirev.2012.02.017

Sugita, S., 1994. Pollen representation of vegetation in Quaternary sediments: theory and method in patchy vegetation. J. Ecol. 82, 881–897.

Taylor, R.J., Douglas, G.W., 1995. Mountain plants of the Pacific Northwest: a field guide to Washington, western British Columbia, and southeastern Alaska. Mountain Press, Missoula, Mont.

Thackray, G.D., Owen, L.A., Yi, C., 2008. Timing and nature of late Quaternary mountain glaciation. J. Quat. Sci. 23, 503–508. doi:10.1002/jqs.1225

Theuerkauf, M., Kuparinen, A., Joosten, H., 2012. Pollen productivity estimates strongly depend on assumed pollen dispersal. The Holocene 23, 14–24. doi:10.1177/0959683612450194

Thompson, R.S., Shafer, S.L., Anderson, K.H., Strickland, L.E., Pelltier, R.T., Bartlein, P.J., Kerwin, M.W., 2005. Topographic, Bioclimatic, and Vegetation Characteristics of Three Ecoregion Classification Systems in North America: Comparisons Along Continent-wide Transects. Environ. Manage. 34, S125–S148. doi:10.1007/s00267-003-7200-3

Tubbs, A.M., 1972. Summer Thunderstorms Over Southern California. Mon. Weather Rev. 100, 799–807. doi:10.1175/1520-0493(1972)100<0799:STOSC>2.3.CO;2

Tzedakis, P.C., 2004. The Duration of Forest Stages in Southern Europe and Interglacial Climate Variability. Science 306, 2231–2235. doi:10.1126/science.1102398

Tzedakis, P.C., Andrieu, V., de Beaulieu, J.-L., Birks, H.J.B., Crowhurst, S., Follieri, M., Hooghiemstra, H., Magri, D., Reille, M., Sadori, L., Shackleton, N.J., Wijmstra, T.A., 2001. Establishing a terrestrial chronological framework as a basis for biostratigraphical comparisons. Quat. Sci. Rev. 20, 1583–1592. doi:10.1016/S0277-3791(01)00025-7

U.S. Climate Data [WWW Document], 2016. . US Clim. Data Big Bear Lake - Calif. URL http://www.usclimatedata.com/climate/big-bear-lake/california/united-states/usca0094 (accessed 8.8.16).

van Mantgem, P.J., Stephenson, N.L., Byrne, J.C., Daniels, L.D., Franklin, J.F., Fule, P.Z., Harmon, M.E., Larson, A.J., Smith, J.M., Taylor, A.H., Veblen, T.T., 2009. Widespread Increase of Tree Mortality Rates in the Western United States. Science 323, 521–524. doi:10.1126/science.1165000

Vera, C., Higgins, W., Amador, J., Ambrizzi, T., Garreaud, R., Gochis, D., Gutzler, D., Lettenmaier, D., Marengo, J., Mechoso, C.R., Nogues-Paegle, J., Dias, P.L.S., Zhang, C., 2006. Toward a Unified View of the American Monsoon Systems. J. Clim. 19, 4977–5000. doi:10.1175/JCLI3896.1

Vogel, H., Meyer-Jacob, C., Melles, M., Brigham-Grette, J., Andreev, A.A., Wennrich, V., Tarasov, P.E., Rosén, P., 2013. Detailed insight into Arctic climatic variability during MIS 11c at Lake El'gygytgyn, NE Russia. Clim. Past 9, 1467–1479. doi:10.5194/cp-9-1467-2013

Wagner, J.D.M., Cole, J.E., Beck, J.W., Patchett, P.J., Henderson, G.M., Barnett, H.R., 2010. Moisture variability in the southwestern United States linked to abrupt glacial climate change. Nat. Geosci. 3, 110–113. doi:10.1038/ngeo707

Wahl, E.R., 2002. Paleoecology and testing of paleoclimate hypotheses in southern California during the Holocene. University of Minnesota, Minneapolis, Minnesota, USA.

West, G.J., 2003. A late Pleistocene-Holocene pollen record of vegetation change from Little Willow Lake, Lassen Volcanic National Park, California., in: Pacific Climate Conference Procedings. pp. 65–80.

West, G.J., 1993. The late Pleistocene-Holocene pollen record and prehistory of California's North Coast Ranges, in: White, G., Mikkelsen, W.R., Hildebrandt, W.R., Basgall (Eds.), There Grows a Green Tree: Papers in Honor of David A Fredrickson. Center for Archaeological Research, Davis, California, pp. 219–235.

West, G.J., 1989. Late Pleistocene/Holocene vegetation and climate., in: Prehistory of the Sacramento River Canyon, Shasta County, California. Davis, California, USA., Center for Archaeological Research at Davis.

West, G.J., McGuire, K.R., 2000. 9,500 years of burning recorded in a high desert marsh., in: Proceedings of the Springfed Wetlands: Important Scientific and Cultural Resources of the Intermountain Region.

Westerling, A.L., 2006. Warming and Earlier Spring Increase Western U.S. Forest Wildfire Activity. Science 313, 940–943. doi:10.1126/science.1128834

Whelan, R.J., 1995. The ecology of fire. Cambridge University Press, Cambridge; New York.

Whitlock, C., Larsen, C., 2001. Charcoal as a Fire Proxy, in: Smol, J.P., Birks, H.J.B., Last, W.M., Bradley, R.S., Alverson, K. (Eds.), Tracking Environmental Change Using Lake Sediments. Kluwer Academic Publishers, Dordrecht, pp. 75–97.

Willis, K.J., MacDonald, G.M., 2011. Long-Term Ecological Records and Their Relevance to Climate Change Predictions for a Warmer World. Annu. Rev. Ecol. Evol. Syst. 42, 267–287. doi:10.1146/annurev-ecolsys-102209-144704

Winograd, I.J., Landwehr, J.M., Coplen, T.B., Sharp, W.D., Riggs, A.C., Ludwig, K.R., Kolesar, P.T., 2006. Devils Hole, Nevada, δ18O record extended to the mid-Holocene. Quat. Res. 66, 202–212. doi:10.1016/j.yqres.2006.06.003

Wise, E.K., 2010. Spatiotemporal variability of the precipitation dipole transition zone in the western United States: PRECIPITATION DIPOLE TRANSITION ZONE. Geophys. Res. Lett. 37, n/a-n/a. doi:10.1029/2009GL042193

Woodhouse, C.A., Meko, D.M., MacDonald, G.M., Stahle, D.W., Cook, E.R., 2010a. A 1,200-year perspective of 21st century drought in southwestern North America. Proc. Natl. Acad. Sci. 107, 21283–21288. doi:10.1073/pnas.0911197107

Woodhouse, C.A., Meko, D.M., MacDonald, G.M., Stahle, D.W., Cook, E.R., 2010b. A 1,200-year perspective of 21st century drought in southwestern North America. Proc. Natl. Acad. Sci. 107, 21283–21288. doi:10.1073/pnas.0911197107

Woolfenden, W.B., 2003. A 180,000-year pollen record from Owens Lake, CA: terrestrial vegetation change on orbital scales. Quat. Res. 59, 430–444. doi:10.1016/S0033-5894(03)00033-4

Woolfenden, W.B., 1996. Late Quaternary vegetation history of the southern Owens Valley region, Inyo County, California. University of Arizona, Tucson, AZ.

Wu, F., Fang, X., An, C., Herrmann, M., Zhao, Y., Miao, Y., 2013. Over-representation of Picea pollen induced by water transport in arid regions. Quat. Int. 298, 134–140. doi:10.1016/j.quaint.2012.11.026

Yamamoto, M., Yamamuro, M., Tanaka, Y., 2007. The California current system during the last 136,000 years: response of the North Pacific High to precessional forcing. Quat. Sci. Rev. 26, 405–414. doi:10.1016/j.quascirev.2006.07.014

Zimmerman, S.H., Myrbo, A., 2015. Lacustrine Environments (14 C)., in: Encyclopedia of Scientific Dating Methods. pp. 365–371.

Zimmerman, S.R.H., Pearl, C., Hemming, S.R., Tamulonis, K., Hemming, N.G., Searle, S.Y., 2011. Freshwater control of ice-rafted debris in the last glacial period at Mono Lake, California, USA. Quat. Res. 76, 264–271. doi:10.1016/j.yqres.2011.06.003